STUDIES OF SOME ACTIVE CIRCUITS FOR APPLICATION IN INSTRUMENTATION, COMMUNICATION AND INDUSTRIAL CONTROL SYSTEMS

THESIS SUBMITTED FOR THE DEGREE OF
DOCTOR OF PHILOSOPHY (ENGINEERING)
OF THE
UNIVERSITY OF NORTH BENGAL

SAKTI BRATO ROY, M. E. Tel. E.

MAY, 1982

STOCK TAKING - 2011

PREFACE

This thesis embodies the results of studies made on some active circuits for application in instrumentation, communication and industrial control systems.

The work was carried out by the author in the Department of Electronics & Telecommunication Engineering, Jadavpur University.

The author wishes to record his indebtedness and gratitude to Dr.D.C.Patranabis, Professor, Department of Electronics and Telecommunication Engineering, Jadavpur University and Professor N.Majumdar, Head of Electrical Engineering Department, Jalpaiguri Government Engineering College, University of North Bengal for their invaluable advice and guidance in conducting the work. The author wishes to thank Dr.D.Ghosh Dastidar of Electronics and Telecommunication Engineering Department, Jadavpur University for his help in writing the computer programmes and Mr.D.Ghosh of the same department for his constant encouragement and help in the way of discussions.

The author wishes to thank Prof.J.S.Chatterjee, Prof. P.Kundu, Prof.A.R.Saha and Prof.P.C.Sen and also Mr.A.K. Chakraborty and Mr.D.Dey of Jadavpur University.

He also wishes to convey his thanks to the authorities of University of North Bengal and in particular to Mr.B.K.Bajpai, Registrar for the kind co-operation.

Also he thanks Mr.A.K.Ghosh of Macneill & Magor for helping to make the Xerox Copies of the thesis.

Lastly the author wishes to convey his gratitude to his sisters Buri and Chote for going through the typed manuscript with pain.

Sakti Brato Roy

(SAKTI BRATO ROY)

Jadavpur University
Department of Electronics
and Telecommunication Engineering
Calcutta-700032

and

University of North Bengal
Jalpaiguri Government
Engineering College
Jalpaiguri-735102

May 1982.

CONTENTS

CHAPTER-III

CHAPTER-IV

CHAPTER-V

CHAPTER-VI

CHAPTER-VII

CHAPTER-I

INTRODUCTION

1.1 MOTIVATION

With the introduction of transistor as a basic active device[1] in the fifties, active circuits have shot into prominence and found wide-scale application in various areas of Instrumentation, Communication and Industrial Control. Previous to this, vacuum triodes and pentodes have often been used but they have certain obvious limitations. Transistor brought the age of the solid state, the technology of which is growing in a pace large enough to push today's marvels into tomorrow's oblivion. However the basic transistor which had been in use as a discrete active block alone till mid-sixties is now being used in the integrated form[2] in a very large scale side by side with its older form. The growth of the integration process for the passive components like resistance and capacitance[3] has extended additional charm to the design of active circuits in miniature and microminiature 'Chips'. Earlier to this, for reasons of cost, size, powerloss and parasitic enhancement it was argued that inductor do not conform to the requirement of an acceptably good passive component particularly if the frequency range is quite low, as required in Instrumentation and Industrial control areas. Attention of the researchers, circuit theorists in particular, turned towards the development of active RC circuits and a bulk of literatures are now available[4-8] to prove that real inductors can be totally dispensed with when proper active insertion is permitted in the design of signal processing networks, signal

generators, control circuits and a variety of others where high selectivity or high Q was previously obtained through LC-tuning. The pursuit on this track, for the development of (i) simulated inductance for direct application as a component,(ii) filters of all types or (iii) circuits of autonomous nature, that are economically viable, have superior performance and are amenable to generalization in design procedure and integration more conveniently, should, therefore be more worthwhile than apparently appears.

1.2 ACTIVE NETWORKS

For the Instrumentation, Communication and Industrial Control Systems, the system design is of very basic importance. Particularly in the network front a design, with RC elements and active blocks only, is attractive for its compactness and economy. The characteristic function realized by passive RC network has many restrictions compared to that of LCR networks. To overcome these, active elements have been inserted in the passive structure in a proper manner for the desired purpose[9].

1.3 ACTIVE NETWORK ELEMENTS

Transistor, Transistor Differential Pair : Transistor is the basic solid state active building element which can be used singly or in conglomeration coupled with an appropriate set of connected resistors to form other blocks. Through continued research towards achieving perfection in its performance, it has now been possible to produce transistors of near ideal nature represented by the model shown in figure 1.1. However the limitation in the operating frequency and other imperfections call for

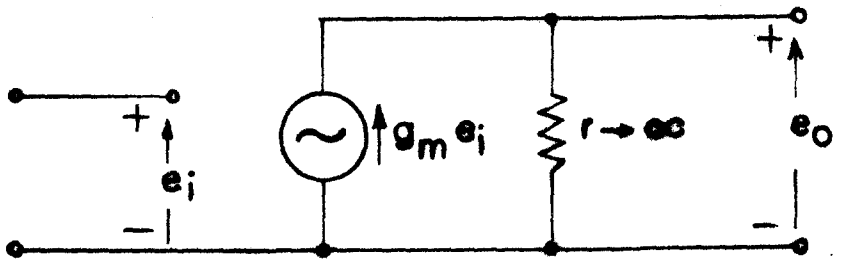

Fig.1.1 Transistor Model

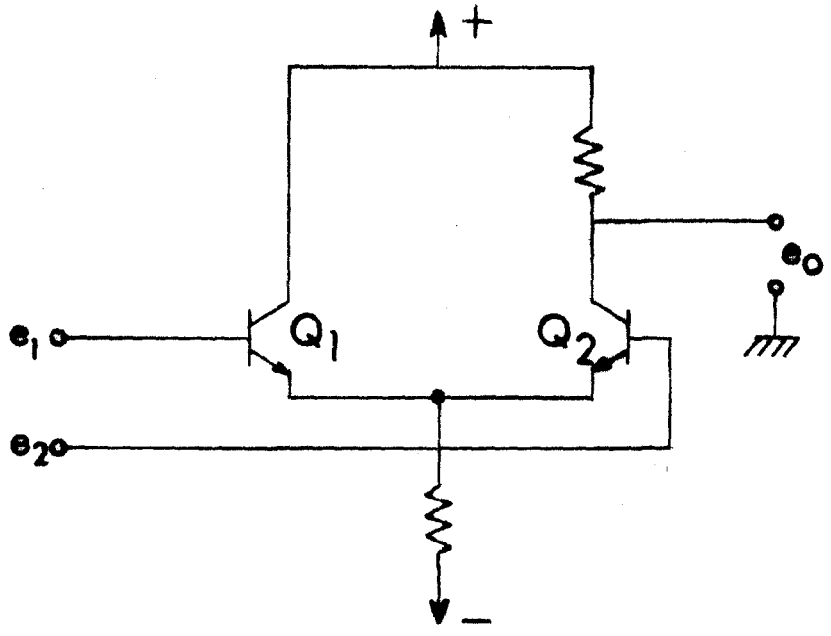

Fig.1.2 Emitter coupled differential pair(ECDP)

a more complex model for circuit synthesis purpose. Transistor being the basic active element, any kind of active circuit can be generated by the use of it.

A very important active building block that is obtained through a pair of transistors is the Emitter Coupled Differential Pair[10] (ECDP) shown in figure 1.2. It can be used with both e_1 and e_2 effective or with e_1 effective and e_2 at a.c. ground potential or vice-versa. The common emitter coupling provides a degenerative feedback in the individual transistors due to which the effect of the changes in the transistor parameter is minimized, the current variation due to supply potential or temperature change in individual transistor tends to cancel, distortion is reduced, input impedance is increased, flow of base current is restricted, bandwidth is increased and the overall stability improves. This, thus provides an overall improvement in performance in the realization of active building block. It has naturally been accepted as the starting phase of what is known as the operational amplifier.

Operational Amplifiers (OA) : The operational amplifier is the most popular active network element now-a-days and is extensively used in active network synthesis. The OA is a direct coupled high gain amplifier, and with applied feedback its performance characteristic is controllable. It is capable of amplifying, controlling or generating any waveform of frequencies from d.c. to several megahertz. All the classical computation functions are easily performed by this. The output of an OA is controlled by its two inputs, inverting and non-inverting. An input to the inverting

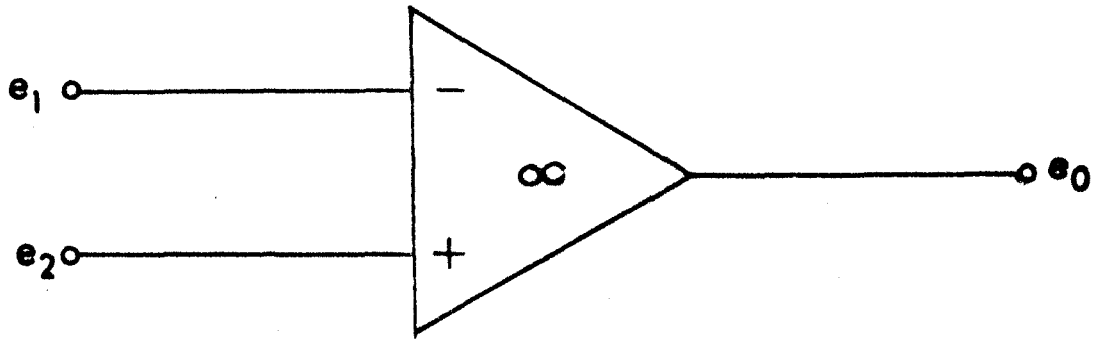

(a)

Operatianal amplifier representation

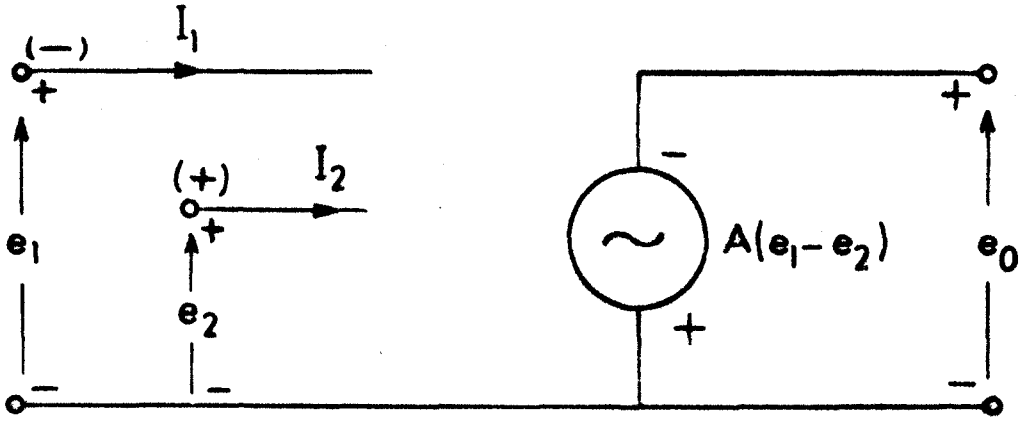

(b)

Fig.1.3 Controlled-source model of Fig. 1.3 (a)

input terminal gives phase-reversed output whereas an input to the non-inverting terminal gives in-phase output.

The OA can be represented by a voltage source which is controlled by two floating terminals as shown in figure 1.3. The OA has high voltage gain for differential signals effective between two inputs and has very low gain for the same signal applied to both the inputs simultaneously. These are called differential mode and common-mode input signals respectively. The synthesis techniques with OA already galore in literature out of which a few are exemplary[11-14]. However its applicability remains to be exploited fully as yet. Operational Amplifier can be considered to be an idealized version of a transistor with very high gain and is thus useful in obtaining many other active elements such as

i) Generalized Immitance Converter (GIC)[15].

ii) Controlled Sources[16]

   a) Voltage Controlled Voltage Source (VCVS).

   b) Current Controlled Current Source (CCCS).

   c) Voltage Controlled Current Source (VCCS).

   d) Current Controlled Voltage Source (CCVS).

iii) Gyrator[17].

iv) Frequency Dependent Negative Resistance[18].

1.4 INDUCTOR REALIZATION

Active RC networks have to be basically active because the replacement of real inductor is to be done with a simulated one. The simulation is in terms of R, C and one or more active blocks.

There has been a considerable effort in recent years for an appropriate simulation of an inductor. Depending on the types of realization such as linear, bilinear, ideal etc., on the port orientation such as grounded or floating or on the use of type of the active blocks different categorization of the realization technique is possible. The basic aim remains, however, to realize an ideal grounded or floating inductor with (i) low parameter sensitivity, (ii) the use of acceptable active blocks and (iii) low count components. Further, grounded capacitor realization adds to the convenience of micro-circuit adaptability[19] of the design. Realized inductors have also been successfully tried in the design of signal processing networks[20], oscillators[21], and various other areas of interest.

1.5 FILTERS

Although simulated inductor can be well adopted for circuit realization of a desired system such as a filter, direct realization of it appears to be more convenient and rather straightforward[22]. This is commonly known in the literature as inductorless filter. The essence of such a scheme lies in the inherent elimination of any real inductor through active RC synthesis. Although literature abounds in such realization techniques[23-29], the final word about it is still to be told. Here again insertion of an acceptable active block in low count with versatility in easy convertibility of the filter for the desired response characteristics receives major attention. Superior performance and high selectivity are other features to consider.

For active blocks, one major aspect to look upon is the dependence of the realization on the gain bandwidth product which affects the operational frequency range as also the Q-factor. Compensation techniques are lately being investigated to increase the gain bandwidth to improve the performance, but very often these increase the complexity in the realization[30,31]. The limited range with uncompensated schemes is, however, sufficient for application in Instrumentation and Industrial Control systems. In any case, this is an inherent limitation of the device and it creeps in during the integration stage of the solid state block. Further development towards its improvement is likely to compensate for this deficiency in a simpler manner.

1.6 OSCILLATORS

Inductor simulation or inductorless filter realization are realization of functions of nonautonomous nature. Often in the application areas mentioned, conservative autonomous functions are of great importance. All practical oscillators come under this category. The autonomous conservative networks are basically regenerative in nature. In quite a few such cases, multifrequency oscillations are generated. It is however possible to design an electrical network to obtain single frequency oscillation. The analytical representation of such a system is quite simple and is given as

$$\ddot{x}^2 + \omega_o^2 x = 0 \qquad (1.1)$$

The quantities characterising such oscillations are (1) amplitude, (2) frequency and (3) phase. The frequency is determined by the system parameters only. In classical mechanics, analyses of all

the nature of a linear system have been made and successfully applied to mechanical, electrical and other types of oscillatory systems. The energy relation in such a system determines its period of oscillation. In electrical types evidently the system should have an inductance and capacitance in the ciruit. The oscillation condition has been enunciated from the principle of feedback and is given as

$$\bar{A}.\bar{B} = 1 \qquad (1.2)$$

where $\bar{A}$ = gain of the active block in the circuit
and $\bar{B}$ = amount of back coupling.

Analysis of the linear systems of oscillations can be made with the help of conventional linear techniques. The added advantage is that many nonlinear techniques can be applied with appropriate limiting conditions to derive the solutions.

1.6.1 THE SINEWAVE GENERATORS

Active devices coupled with passive networks are capable of generating sinewave oscillations with the appropriate conditions specified. The passive circuit parameters are generally the determining factors of the system frequency.

Low frequency sinewave generation is inconvenient with an LC network because of their large values. RC networks are more advantageous in that respect. An oscillator with a 3-section CR phase shifting network and a vacuum tube was described by Ginzton and Hollingsworth[32]. The transistorised version of this circuit is due to Nichols[33]. Continued efforts in this line have produced

different RC oscillators with special types of networks like Wienbridge, Bridge-T, Twin-T etc.[34-38].

The main consideration in sinewave generation is to obtain oscillations of good frequency and amplitude stability and also frequency variability. All the requirements are rarely met by any individual circuit suggested so far.

Active RC filter may be convenient in so far as the choice of the frequency selective networks are considered. The basic limitations are conceivable in terms of the drifts in the active parts. But now it is known that the drifts with time and temperature in active devices which are amenable to compensation (compensated active devices) are no worse than that of passive elements. Variation of the function of an active element such as the gain of a closed loop operational amplifier, may be used with advantage in a variable frequency oscillator. With special active blocks such as the differential transistor pair with a high CMRR the drift problem can be reduced as well.

Irrespective of the types of the circuits used, the derivation of the equation, pertinent to the analysis of harmonic oscillations is made, following a suitable technique dependent on the system alone. Usually the frequency and the starting conditions are determined from the conventional loop or nodal analysis of the circuit.

1.6.2 NON-LINEAR SYSTEMS

Majority of the problems relating to real physical systems are possibly investigated mathematically involving solution of

differention equations - ordinary linear, nonlinear and partial.

For the solution of the nonlinear problems the mathematics involved is, in the present day state-of-the-art, referred to as nonlinear mathematics. The analytical treatment of the nonlinear problems are hindered due to insufficient mathematical development in this area. The engineers however have the complementing tools in computer for the analysis of the dynamic behaviour of the physical system. In fact, the highly nonlinear problems which occur in practice, have been successfully solved when the analytical approach is coupled with the aid of computers.

1.6.3 THE PERIODIC SOLUTION

Attempting to solve the autonomous and nonautonomous oscillatory system, the primary interest grows around the steady state oscillations i.e., existence of a periodic solution, ensuring the stability. Ponicaré[39] was the first to present a suitable analytical approach for obtaining the periodic solution. The basic principle is the parameter (μ, say) dependence of certain term of the nonautonomous differential equation. The major difficulty in Ponicaré method is in finding the characteristic exponents required for the solution. Minorsky's strobscopic method[40,41] solves this difficulty by replacing the original nonautonomous differential equation by another autonomous one, such that the existence and the stability of its singular points is a criterion of the existence and stability of the periodic solution of the original problem.

The classical van der Pol[42] equation describes many of the operating features of the oscillator. The equation is quite simple

but the small parameter approximation method is not applicable for a large value of the parameter (μ or ϵ) associated with the first derivative term. A study of van der Pol equation for both small and large value of ϵ has led to the appropriate understanding of the operation of self-oscillations. Van der Pol's original method of solution was graphical and was presented in the form of an integral curve in the phase plane. The latter efforts for an analytical solution[43,44] of the equation acquired little significance although it was demonstrated that for larger and larger values of ϵ the system tends to oscillate in relaxation mode.

1.6.4 RELAXATION OSCILLATION

Relaxation oscillations differ considerably from sinusoidal or quasi-sinusoidal oscillations. Relaxation oscillations are rich in harmonics which can attain very high order.

In practical relaxation oscillations, pulse generation for example, effectively there is a single reactive element capable of storing energy. The energy can be stored only in one part of the period. In the other part this energy is dissipated in a resistance. Naturally the exciting device should supply an amount of energy equal to that stored or dissipated in the period. In an autonomous system, the exciting device is formed in the system which is required to supply the energy and this often is a negative resistance device or a generator[40-42]. The presence of the negative resistance in the circuit of the oscillatory system may be considered in two general ways. First an actual negative resistance is used for circuit synthesis; secondly a feedback is applied in such

a way as to produce an effective negative resistance in the system during the part energy is supplied.

It was due to the study of van der Pol[45] that a method obtaining a continuous transition from the sinusoidal to relaxation oscillation is known. Physically this is interpreted as in an LRC circuit one of the reactive elements is gradually reduced to zero and the system being beyond the 'limit' state, the oscillation that occurs may be considered as a kind of jumping from one state of equilibrium to another. The period of oscillation in such circuits is generally controlled by the alteration of the passive elements which simultaneously affect the performance of the multivibrator or pulse generator. Synthesis of multivibrator circuit whose time period can be linearly altered by varying a single circuit parameter other than the formal frequency determining network element without affecting the operating characteristics of the generator can be a welcome addition to the list of the range of the multivibrators.

1.7 SCOPE OF THE WORK

Of late nonautonomous and autonomous function realization have gained tremendous importance in the areas of Communication, Instrumentation and Industrial Control. Active RC filters have consequently been receiving attention in a generalized way[46-48] or in a discreet manner[49]. The generalized studies have been directed to evaluate the realizability criteria such that the filters received adequate mathematical description. Individual design has to have more of down to earth and practical approach. Since the recent approach based on various counts of superior

performance requirements; convenience in tuning, I.C. implementation; sensitivity minimization and others is to develop second order building blocks, at the most, for the system design, major attention has been given to the design of such blocks with more versatility. These blocks themselves may be developed through an integrated approach or through the replacement of the inductors in the existing models by these active RC simulations.

The present study begins with the simulation of inductors of different types with RC and a very general active block i.e. the operational amplifier. The grounded inductor realization is presented in Chapter-II. The method is a little deviated from the now conventional approach of using a single capacitor. However the method presented shows that in it a number of type of inductors can be realized including an ideal one having very large inductance values. The application of the inductor in obtaining a variable frequency sinewave oscillator has also been demonstrated.

Not all filters are realizable with a grounded inductor. In modern practice filters with floating inductors are modelled with different types of simulated elements[50-51]. The direct approach, however is to simulate floating inductors and use them in such a realization. The scheme of a floating ideal inductor with three operational amplifiers and a grounded capacitor has been presented in Chapter-III and a filter realization scheme has also been given with experimental results.

Chapter-IV presents a generalized approach of active RC filter realization with a single operational amplifier. The presentation has been motivated to obtain the important communication

filter, the all pass filter, through a generalized approach. Subsequently through various examples realizability of all other types of filters has also been demonstrated.

Single resistive element control sinewave generators have acquired importance in data telemetering and other industrial control. Such types have been produced of late through individual trials[52-56] and with some constraints. In Chapter-V a systematic development of systems to provide the desired facility has been presented. The waiver of some critical restrictions has even allowed the system to be adopted as a voltage controlled oscillator.

Single stage emitter coupled transistor differential pair has been exploited here as a very convenient active block. As mentioned, it is a highly stable controlled source and can be made effective in a wide variety of purpose. A very stable sinewave generator has been produced through it which is minimally sensitive to temperature and supply voltage as well. The system has been presented in Chapter-VI.

Interestingly, the basic scheme with the emitter coupled transistor differential pair presented in Chapter-VI turns out to be a van der Pol generator whose operation may be continuously controlled from single frequency harmonic to relaxation mode by simple parameter control. Chapter-VII presents this van der Pol generator and shows that the long standing discrepancy between the practically obtained waveform and the theoretical one, either through graphical or approximated analytical approach[57,58], exists only because of inaccurate modelling of the active block. The

antisymmetric transfer characteristics of the differential pair has been suggested to be of hyperbolic tangent type and the transcendental characteristic equation has been solved in the computer for various timing ranges. The results have been compared to show that the suggestion is apt. This system can be seen to be a very convenient waveform generator. The system can be adapted quite easily as a voltage controlled oscillator. This adaptation has also been included in this chapter with sufficient details.

Specifically the relaxation mode oscillation deserves special mention because of its versatile utility. It has further been improved to suit wide scale practical applications. This has been presented in Chapter-VIII by adapting the scheme as a single resistive element controlled linear pulse generator which has been simultaneously made minimally sensitive to variable operating conditions. The emitter coupling helps to attain this insensitivity to a great extent. The extent of coupling is important for this purpose.

Finally in Chapter-IX concluding remarks with necessary critical discussions are made.

REFERENCES

1. Shockley,W. : 'The theory of p-n junctions in semiconductors and p-n junction transistors'; Bell Syst. Tech. J., Vol.28, pp.435-489, July 1949.

2. Moschytz,G.S. : 'Miniaturised filter building blocks using frequency emphasizing networks'; Proc. Nat. Electronics Conf., Vol.23, pp.364-369, 1967.

3. Moschytz,G.S. : 'Linear Integrated Networks : Fundamentals'; New York : Van Nostrand Reinhold, 1974.

4. Mitra,S.K. : 'Active Inductorless Filters'; New York : IEEE Press, 1971.

5. Sen,P.C. and Patranabis,D. : 'An active RC filter exhibiting selective, all-pass and notch characteristics'; Int. J. Electron., Vol.33, pp.583-591, 1972.

6. Sedra,A. and Brackett; 'Filter Theory and Design : Active and Passive'; Portland : Matrix,1978.

7. Akerberg,D. and Mossberg,K. : 'A versatile RC building block with inherent compensation for the finite bandwidth of the amplifier'; IEEE Trans. Circuits and Systems, Vol.CAS-21, pp.75-78, 1974.

8. Daniels,R.W. : 'Approximation Methods for Electronic Filter Design'; New York : McGraw-Hill, 1975.

9. Linvill,J.G. : 'RC active filters'; Proc. IRE, Vol.42, pp.555-564, March 1954.

10. Kundu,P. and Roy,S.B. : 'A temperature stable RC transistor oscillator'; Proc. IEEE, Vol.57, pp.356-357, March 1969.

11. Thomas,L.C. : 'The biquad : Part-I - Some practical design considerations'; IEEE Trans. Circuit Theory, Vol.CT-18, pp.350-357, 1971.

12. Girling,F.E.T., and Good,E.F. : 'Active filters 7 and 8, the two integrator loops'; Wireless World, Vol.76, pp.117-119, and pp.134-139, 1970.

13. Friend,J.J. Harris,C.A. and Hilberman,D. : 'STAR : An active biquadratic filter-section'; IEEE Trans. Circuits and Systems, Vol.CAS-22, pp.115-121, 1975.

14. Patranabis,D. Roy,S.B. and Tripathi,M.P. : 'Generalization of active RC all-pass schemes'; Proc. IEEE, Vol.66, pp.354-356, 1978.

15. Bruton,L.T. : 'Filter Synthesis Using Generalized Impedance Converters'; Proc. NATO Advanced Inst. of Signal and Network Theory, London : Peter Perigrinus, 1973.

16. Huelsman,L.P. : 'Theory and Design of Active RC Circuits'; New York : McGraw-Hill, 1968.

17. Riordan,R.H.S. : 'Simulated inductors using differential amplifiers'; Electron. Lett., Vol.3, pp.50-51, 1967.

18. Bruton,L.T. : 'Network transfer function using the concept of frequency dependent negative resistance'; IEEE Trans. Circuit Theory, Vol.CT-16, pp.406-408, Aug.1969.

19. Lessor,A.I. Maissel,L.I. and Their,R.E. : 'Thin film circuit technology : Part-I - Thin film networks'; IEEE Spectrum, Vol.1, pp.72-80, April 1960.

20. Paul,A.N. : 'On the studies of Active RC Network Functions for Nonautonomous and Autonomous Systems'; Ph.D. Thesis, Jadavpur University, India, December 1981.

21. Sen,P.C. and Patranabis,D. : 'A sinewave oscillator'; Int. J.Electron, Vol.29, pp.441-447, 1969.

22. Mitra,S.K. : 'Analysis and Synthesis of Linear Active Networks'; New York : Wiley,1969.

23. Holt,A.G.J. and Linggard,R. : 'RC active synthesis procedure for polynomial filters'; Proc. IEEE, Vol.113, pp.777-782, May 1966.

24. Dutta Roy,S.C. : 'RC active all-pass networks using a differential input operational amplifier'; Proc. IEEE, Vol.57, pp.2055-2056, Nov.1969.

25. Vloschytz,G.S. : 'The operational amplifier in linear active networks'; IEEE Spectrum, Vol.7, pp.42-50, Jan.1970.

26. Tow,J. : 'A step-by-step active filter design'; IEEE Spectrum, Vol.6, pp.64-68, Dec.1969.

27. Kerwin,W.J. : 'Active RC network Synthesis using voltage amplifier : in Active Filter : Lumped, Distributed, Integrated, Digital and Parametric'; Edited by Huelsman, L.P.; New York : McGraw-Hill, 1970.

28. Patranabis,D. : 'Synthesis of RC all-pass networks'; Int. J. Electron., Vol.27, pp.337-347, 1969.

29. Laker,K.R. Schaumann,R. and Ghausi,M.S. : 'Multiloop feedback topologies for the design of low sensitivity active filters'; IEEE Trans. Circuits and Systems, Vol.CAS-26, pp.1-21, Jan. 1979.

30. Wilson,G. : 'Compensation of some operational amplifier based RC active networks'; IEEE Trans. Circuits and Systems, Vol.CAS-23, pp.443-446, July 1976.

31. Budak,A. Wullink,G. and Geiger,R.L. : 'Active filters with zero transfer function sensitivity with respect to the time constants of operational amplifiers'; IEEE Trans. Circuits and Systems, Vol.CAS-27, pp.849-854, Oct.1980.

32. Ginzton,E.L. and Hollingsworth,L.M. : 'Phase-shift oscillators'; Proc. IRE. Vol.29, pp.43-49, 1941 and Vol.32, p.641, 1944.

33. Nichols,K.G. : 'The use of transfer matrices in the analysis of condition of oscillation'; The Radio and Electronic Engineer, The J. of Brit. IRE. Vol.25, pp.41-48, Jan.1963.

34. Taeger,W. : 'The Wienbridge as phaseshift element for RC oscillator'; Funk.u.Ton., Vol.4, pp.569-575, Nov.1950.

35. Hickman,D.E.D. : 'Wien bridge oscillators - theoretical analysis and practical design'; Wireless World, Vol.65, pp.550-555, Dec.1959.

36. Clifford,F.G. : 'A bridge stabilized RC oscillator'; Electron. Engg., Vol.7, p.560, 1945.

37. Davidson,J.A.B. : 'Variable frequency RC oscillator'; Electron. Engg., Vol.6, pp.316-319, 1944.

38. Patranabis,D. : 'On the study of oscillations in Active Filters Systems'; Ph.D.Thesis, Calcutta University, India, 1971.

39. Poincaré,H. : Translation of 'Sur le probleme de trois corps et les equations de la dynamique'; Acta Math., Vol.13, 1890.

40. Minorsky,N. : 'Introduction to Nonlinear Mechanics'; Ann Abor : Edward, 1947.

41. Minorsky,N. : 'Nonlinear Oscillations'; New York : Van Nostrand, 1962.

42. van der Pol,B. : 'Nonlinear theory of electric oscillations'; Proc. IRE, Vol.22, pp.1051-1082, Sept.1934.

43. Cesari,L. and Hale,J.K. : 'A new sufficient condition for the periodic solutions of nonlinear differential equations'; Proc. Amer. Math, Soc., Vol.8, p.757, 1957.

44. Bogoliuboff,N.N. and Mitropolski,Y.A. : 'Asymptotic Methods in Nonlinear oscillations'; New York : Gordon and Breach, 1962.

45. van der Pol,B. : 'On relaxation oscillations'; Phil. Mag., Ser.7, Vol.2, pp.978-992, 1926.

46. Szentirmai,G. : 'Synthesis of multiple-feedback active filters'; Bell Syst. Tech. J., Vol.52, pp.527-555, April 1973.

47. Dubois,D. and Niernyck,J. : 'General synthesis methods for FLF active filters'; Proc. 1976 European Conf. on Circuit Theory Design, (Genoa, Italy); pp.565-571, Sept.1976.

48. Bruton,L.T. : 'Multiple amplifier RC active filter design with emphasis on GIC realizations'; IEEE Trans. Circuits and Systems, Vol.CAS-25, pp.830-844, Oct.1978.

49. Mackay,R. and Sedra,A.S. : 'Generation of low-sensitivity state space active filters'; IEEE Trans. Circuits and Systems, Vol.CAS-27, pp.863-870, Oct.1980.

50. Bruton,L.T. : 'Topological equivalence of inductorless ladder structures using integrators'; IEEE Trans. Circuit Theory, Vol.CT-20, pp.434-437, July 1973.

51. Antoniou,A. : 'Bandpass transformations and realization using frequency dependent negative resistance elements'; IEEE Trans.Circuit Theory, Vol.CT-18, pp.297-299, March 1971.

52. Hribsek,M. and Newcomb,R.W. : 'VCO controlled by one variable resistor'; IEEE Trans. Circuits and Systems, Vol.CAS-23, pp.166-169, March 1976.

53. Patranabis,D. : 'Sinusoidal oscillations in active RC filters'; Int.J.Electron., Vol.29, pp.93-99, 1970.

54. Dutta Roy,S.C. : 'Variable frequency RC oscillator with single resistance control'; Proc. IEEE, Vol.64, pp.1016-1017, June 1976.

55. Sundarmurthy,M. Bhattacharyya,B.B. and Swamy,M.N.S. : 'A single voltage-controlled oscillator with grounded capacitors'; Proc. IEEE, Vol.65, pp.1612-1614, Nov.1977.

56. Senani,R. : 'New canonic sinusoidal oscillator with independent frequency control through a single grounded resistor'; Proc. IEEE, Vol.67, pp.691-692, April 1979.

57. Scott,P.R. : 'Large-amplitude operation of the nonlinear oscillator'; Proc. IEEE, Vol.56, pp.2182-2183, Dec.1968.

58. Roy,S.B. and Patranabis,D. : 'Non-linear oscillations using antisymmetric transfer characteristics of a differential pair'; Int. J. Electron., Vol.42, pp.19-32, 1977.

CHAPTER-II

ACTIVE RC REALIZATION OF GROUNDED INDUCTOR WITH OPERATIONAL AMPLIFIERS

2.1 INTRODUCTION

Inductor simulation in active RC schemes has been of considerable significance for designing analogue signal processing network of special types and sinewave oscillators for use in the areas of instrumentation, communication and control. Considerable number of literatures are now available on realization of specific type of inductors such as linear, bilinear, ideal etc[1-4]. These schemes use different types of active blocks for the realization. A single scheme realizing the different forms of inductors through minor modification in passive or active parameters should however be a welcome addition to the simulation method. Such a scheme becomes not only very versatile, its usefulness is also widened to a large extent. Such a scheme is presented here which uses two operational amplifiers, one used as an integrating amplifier of low closed loop gain and the other as a negative immittance converter (n.i.c). The proposed circuit has been analysed to yield linear, bilinear inductor and also ideal inductor of arbitrarily large inductance value. The presence of an n.i.c. in an appropriate position allows the circuit to behave as an oscillator with a suitable capacitor at the input port of the scheme thus demonstrating the usefulness of the realized inductor scheme. The experimental results have fully corroborated the theoretical calculations for the scheme as an inductor or as an oscillator.

2.2 THE RL IMPEDANCE[5*]

The basic circuit of the proposed scheme is shown in figure 2.1.

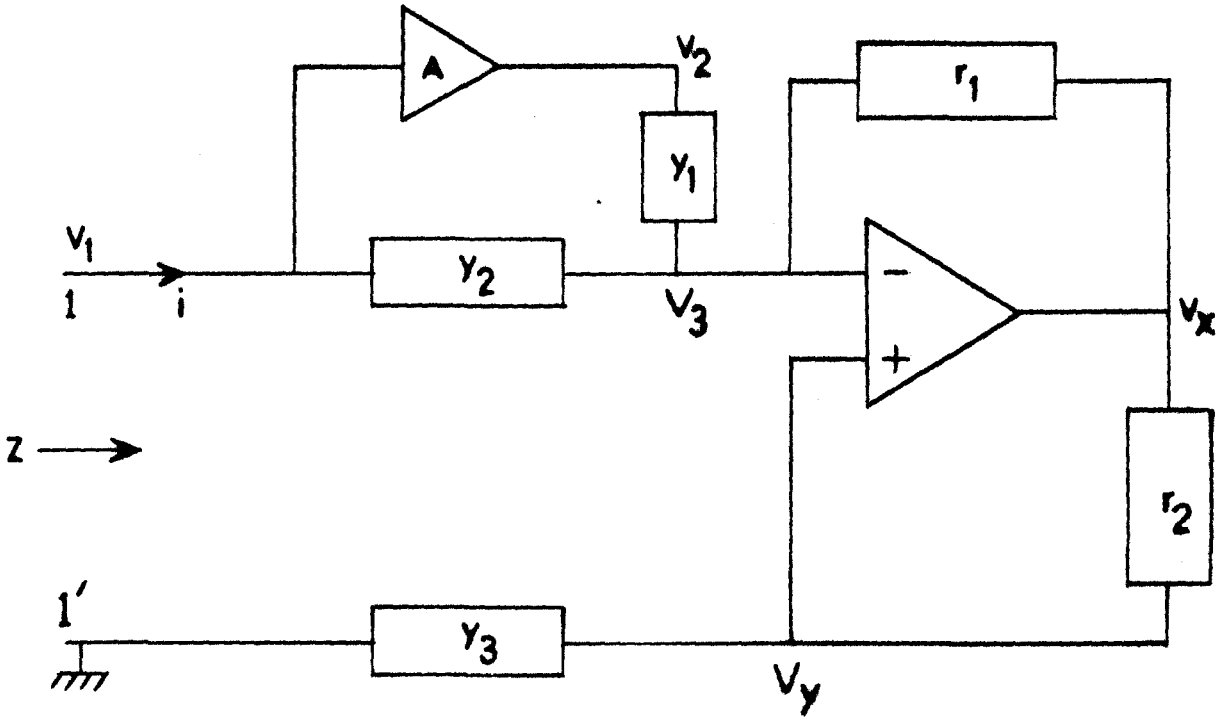

Fig. 2.1 The schematic circuit

Following equation are obtained from this circuit,

$$i = (V_1 - V_3)y_2 \tag{2.1a}$$

$$(V_1 - V_3)y_2 + (V_2 - V_3)y_1 = (V_3 - V_x)\frac{1}{r_1} \tag{2.1b}$$

$$(V_x - V_y)\frac{1}{r_2} = V_3 y_3 \tag{2.1c}$$

and

$$V_2 = AV_1 \tag{2.2}$$

Since $V_y = V_3$ from equation (2.1c) one may write

$$V_x = V_3(y_3 r_2 + 1) \tag{2.3}$$

Substituting V_2 and V_x from equation (2.2) and (2.3) into equation (2.1b) one obtains

$$V_3 = \frac{y_2 + Ay_1}{y_1 + y_2 - \frac{r_2}{r_1} y_3} V_1 \tag{2.4}$$

Finally with this V_3, equation (2.1a) changes to

$$i = V_1 \left[\frac{y_1 y_2 (1-A) - \frac{r_2}{r_1} y_2 y_3}{y_1 + y_2 - \frac{r_2}{r_1} y_3} \right]$$

Such that the input impedance Z is given by

$$Z = \frac{V_1}{I} = \frac{y_1 + y_2 - \frac{r_2}{r_1} y_3}{y_2 \left\{ y_1(1-A) - \frac{r_2}{r_1} y_3 \right\}} \tag{2.5}$$

If the admittances y_1, y_2 and y_3 are of the form

$$\left.\begin{aligned} y_i &= a_i s + b_i \\ a_i &= C_i \\ b_i &= \frac{1}{R_i} \end{aligned}\right\} \quad i = 1, 2 \text{ and } 3 \tag{2.6}$$

and $(1-A) = m \gg 1$, equation (2.5) may be rewritten as

$$Z = \frac{(a_1 + a_2 - \frac{r_2}{r_1} a_3)s + (b_1 + b_2 - \frac{r_2}{r_1} b_3)}{(a_2 s + b_2)\left\{(ma_1 - \frac{r_2}{r_1} a_3)s + (mb_1 - \frac{r_2}{r_1} b_3)\right\}} \qquad (2.7)$$

2.2.1 THE BILINEAR RL IMPEDANCE

For a bilinear inductive impedance function Z can be represented as

$$Z = \frac{Bs + D}{Hs + G} \qquad (2.8)$$

with a constraint $\frac{D}{B} < \frac{G}{H}$.

Comparing equations (2.7) and (2.8) the following identifications can be made

$$\left.\begin{aligned} (a_1 - \frac{r_2}{r_1} a_3) &= B \\ (b_1 + b_2 - \frac{r_2}{r_1} b_3) &= D \\ b_2(ma_1 - \frac{r_2}{r_1} a_3) &= H \\ b_2(mb_1 - \frac{r_2}{r_1} b_3) &= G \end{aligned}\right\} \qquad (2.9)$$

and

$$a_2 = 0$$

It may be noted here that for equation (2.7) to represent bilinear impedance function, either a_2 may be made zero or $(ma_1 - \frac{r_2}{r_1} a_3)$ may be made zero. When a_2 is made zero there is reduction in circuit components and no rigid constraint is put on m, r_2, r_1, a_1 and a_3. This obviously is an advantage from the point of view of realization.

Where as for the other alternative $(ma_1 - \frac{r_2}{r_1} a_3) = 0$ and $a_2 > 0$, to make the denominator of equation (2.7) compatible, generally leads to extra complexity and this may not always be advisable for a stable driving point impedance function realization.

Combining equations (2.6) and (2.9) the impedance function Z is obtained in terms of the circuit parameters. Thus

$$Z = \frac{R_1R_2R_3(C_1 - \frac{r_2}{r_1} C_3)s + R_3(R_1 + R_2) - \frac{r_2}{r_1} R_1R_2}{R_1R_3(mC_1 - \frac{r_2}{r_1} C_3)s + mR_3 - \frac{r_2}{r_1} R_1} \qquad (2.10)$$

Choosing now,

$$\left.\begin{aligned} R &= \frac{R_1}{\beta} = \frac{R_2}{\gamma} = R_3 \\ \text{and} \qquad C &= \frac{C_1}{\delta} = C_3 \end{aligned}\right\} \qquad (2.11)$$

equation (2.10) may be rewritten as

$$Z = R \frac{\frac{r_2}{r_1}\beta\gamma - (\beta+\gamma) + s\beta\gamma RC(\frac{r_2}{r_1} - \delta)}{\frac{r_2}{r_1}\beta - m + s\beta RC(\frac{r_2}{r_1} - m\delta)} \qquad (2.12)$$

which may be factored into real and imaginary parts as

$$Z = R \frac{\left\{\frac{r_2}{r_1}\beta\gamma - (\beta+\gamma)\right\}(\frac{r_2}{r_1}\beta - m) + \omega^2\beta^2\gamma R^2C^2(\frac{r_2}{r_1} - \delta)(\frac{r_2}{r_1} - m\delta)}{(\frac{r_2}{r_1}\beta - m)^2 + \omega^2\beta^2R^2C^2(\frac{r_2}{r_1} - m\delta)^2}$$

$$+ j\omega CR^2 \frac{\beta\gamma(\frac{r_2}{r_1} - \delta)(\frac{r_2}{r_1}\beta - m) - \beta(\frac{r_2}{r_1} - m\delta)\left\{\frac{r_2}{r_1}\beta\gamma - (\beta+\gamma)\right\}}{(\frac{r_2}{r_1}\beta - m)^2 + \omega^2\beta^2R^2C^2(\frac{r_2}{r_1} - m\delta)^2}$$

$$= R_b + j\omega L_b \qquad (2.13)$$

From equation (2.13) the resistive and inductive components are obtained as

$$R_b = R\,\frac{\left\{\frac{r_2}{r_1}\beta\gamma - (\beta+\gamma)\right\}\left(\frac{r_2}{r_1}\beta - m\right) + \omega^2\beta^2\gamma R^2C^2\left(\frac{r_2}{r_1} - \delta\right)\left(\frac{r_2}{r_1} - m\delta\right)}{\left(\frac{r_2}{r_1}\beta - m\right)^2 + \omega^2\beta^2R^2C^2\left(\frac{r_2}{r_1} - m\delta\right)^2} \qquad (2.14a)$$

and

$$L_b = CR^2\,\frac{\beta\gamma\left(\frac{r_2}{r_1} - \delta\right)\left(\frac{r_2}{r_1}\beta - m\right) - \beta\left(\frac{r_2}{r_1} - m\delta\right)\left\{\frac{r_2}{r_1}\beta\gamma - (\beta+\gamma)\right\}}{\left(\frac{r_2}{r_1}\beta - m\right)^2 + \omega^2\beta^2R^2C^2\left(\frac{r_2}{r_1} - m\delta\right)^2} \qquad (2.14b)$$

Both R_b and L_b the resistance and inductance of the impedance Z are frequency dependent. It can be shown that suitable sets of m, β, γ, δ and $\frac{r_2}{r_1}$ may be found for stable bilinear RL impedance function Z. Figure 2.2 shows R_b - frequency and L_b - frequency curver as obtained from equation (2.14a) and (2.14b) for an identical set of the parameters m, β, γ, δ and two values of $\frac{r_2}{r_1}$; and R = 5K ohms and C = 0.094μF.

The Q factor of this impedance Z is given by

$$Q_b = \omega CR\,\frac{\beta\gamma\left(\frac{r_2}{r_1} - \delta\right)\left(\frac{r_2}{r_1}\beta - m\right) - \beta\left(\frac{r_2}{r_1} - m\delta\right)\left\{\frac{r_2}{r_1}\beta\gamma - (\beta+\gamma)\right\}}{\left\{\frac{r_2}{r_1}\beta\gamma - (\beta+\gamma)\right\}\left(\frac{r_2}{r_1}\beta - m\right) + \omega^2\beta^2\gamma R^2C^2\left(\frac{r_2}{r_1} - \delta\right)\left(\frac{r_2}{r_1} - m\delta\right)} \qquad (2.15)$$

Q_b may be increased by adjusting $\frac{r_2}{r_1}$, m, β, γ and δ maintaining the condition indicated by equation (2.8). For specific parameters $\frac{r_2}{r_1}$, m, β, γ and δ , Q_b is maximum at an angular frequency

$$\omega_{b_{max}} = \frac{1}{CR}\sqrt{\frac{\left\{\frac{r_2}{r_1}\beta\gamma - (\beta+\gamma)\right\}\left(\frac{r_2}{r_1}\beta - m\right)}{\beta^2\gamma\left(\frac{r_2}{r_1} - \delta\right)\left(\frac{r_2}{r_1} - m\delta\right)}} \qquad (2.16)$$

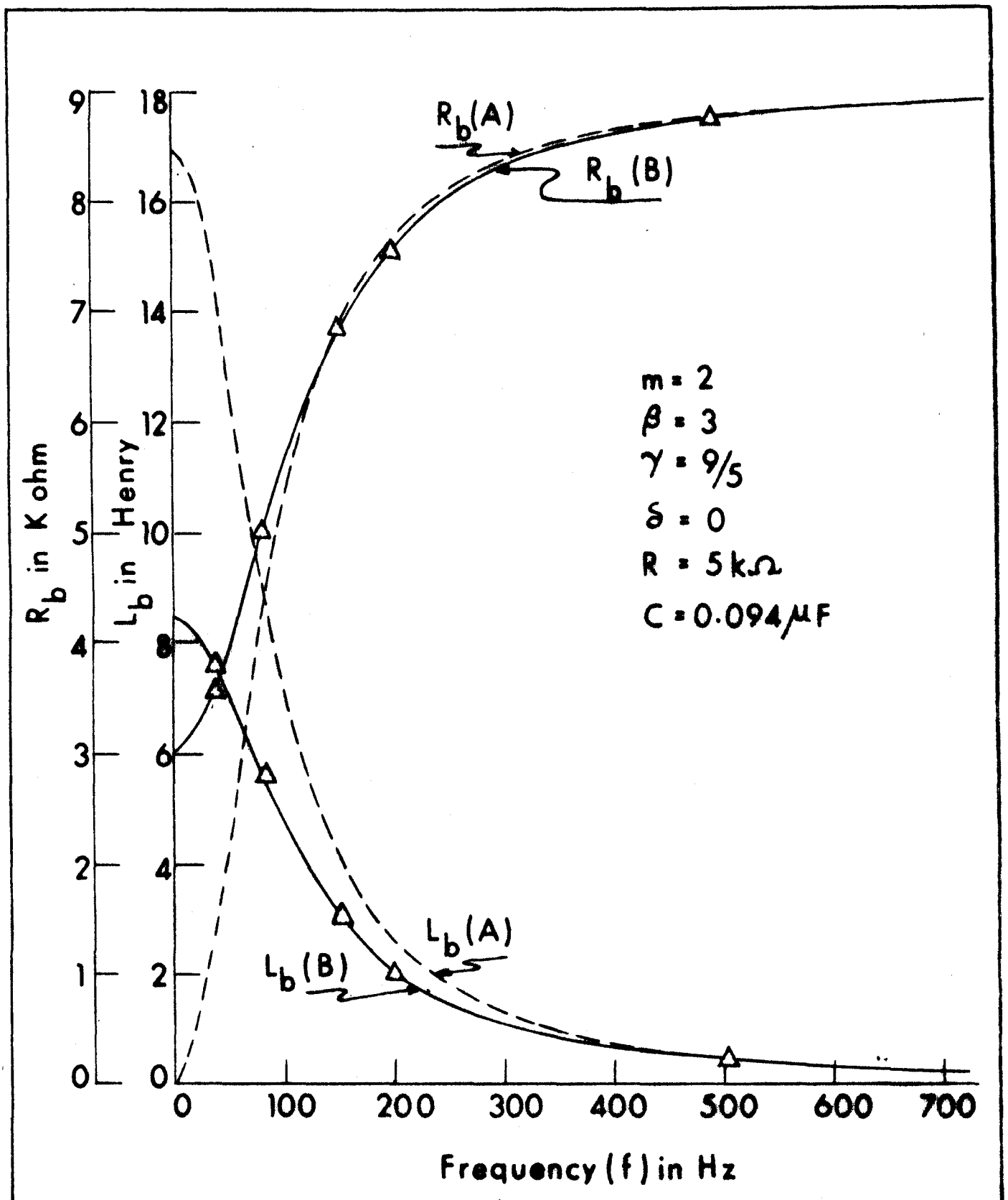

Fig.2.2. The R_b - Frequency and L_b - Frequency curves for bilinear case: (A) $r_2/r_1 = \frac{24}{27}$ (B) $r_2/r_1 = 1$

and the corresponding $Q_{b_{max}}$ is given by

$$Q_{b_{max}} = \frac{1}{2} \frac{\gamma(\frac{r_2}{r_1} - \delta)(\frac{r_2}{r_1}\beta - m) - (\frac{r_2}{r_1} - m\delta)\left\{\frac{r_2}{r_1}\beta\gamma - (\beta+\gamma)\right\}}{\sqrt{\gamma(\frac{r_2}{r_1} - \delta)(\frac{r_2}{r_1} - m\delta)(\frac{r_2}{r_1}\beta - m)\left\{\frac{r_2}{r_1}\beta\gamma - (\beta+\gamma)\right\}}} \tag{2.17}$$

2.2.2 THE LINEAR RL IMPEDANCE

It is seen from equation (2.12) that if the capacitance C_1 is adjusted such that

$$\delta = \frac{r_2}{r_1 m} \tag{2.18}$$

the impedance Z is given by

$$Z = R\delta \frac{\beta\gamma - \frac{r_1}{r_2}(\beta+\gamma)}{(\beta\delta - 1)} + sCR^2 \frac{\beta\gamma\delta \frac{r_1}{r_2}(\frac{r_2}{r_1} - \delta)}{(\beta\delta - 1)} \tag{2.19}$$

Equation (2.19) is linear in R and L and the resistance and inductance values are then given respectively by

$$R_1 = R\delta \frac{\beta\gamma - \frac{r_1}{r_2}(\beta+\gamma)}{(\beta\delta - 1)} \tag{2.20a}$$

and

$$L_1 = CR^2 \frac{\beta\gamma\delta \frac{r_1}{r_2}(\frac{r_2}{r_1} - \delta)}{(\beta\delta - 1)} \tag{2.20b}$$

The Q factor of the realized inductor is therefore

$$Q_1 = CR \frac{\omega\beta\gamma \frac{r_1}{r_2}(\frac{r_2}{r_1} - \delta)}{\beta\gamma - \frac{r_1}{r_2}(\beta+\gamma)} \tag{2.21}$$

Q_1 is a linear function of frequency and is therefore maximum at $\omega = \infty$. However both R_1 and L_1 are independent of frequency and the simulated inductor has the characteristics of real inductors. Adjusting the parameters β and γ and maintaining $\beta\delta > 1$ the resistive part of the inductor can be made arbitrarily small and the Q factor at any frequency may be made arbitrarily large. Condition (2.18) can be realized by varying the phase inverter gain, keeping C_1 constant.

2.2.3 THE IDEAL INDUCTOR

From equation (2.19) it may be observed that if,

$$\left(\frac{1}{\beta} + \frac{1}{\gamma}\right) = \frac{r_2}{r_1} \tag{2.22}$$

the simulated inductor is ideal with its inductance value

$$L_i = CR^2 \frac{\beta^2 \left(\frac{r_1}{r_2}\right)^2 \left(\frac{r_2}{r_1} - \delta\right)}{\left(\beta - \frac{1}{\delta}\right)\left(\beta - \frac{r_1}{r_2}\right)} \tag{2.23}$$

The ideal inductor has infinite Q-factor at all frequencies. However its inductance value can be altered by suitable choice of parameters. It is interesting to note that the inductance can have very large value including infinity for reasonable values of the parameters.

Figure 2.3 shows the L_i-β curves for three different values of δ and $\frac{r_2}{r_1} = 1$. The parameters β, γ and δ can be adjusted within reasonable limits to realize a very large value of L_i.

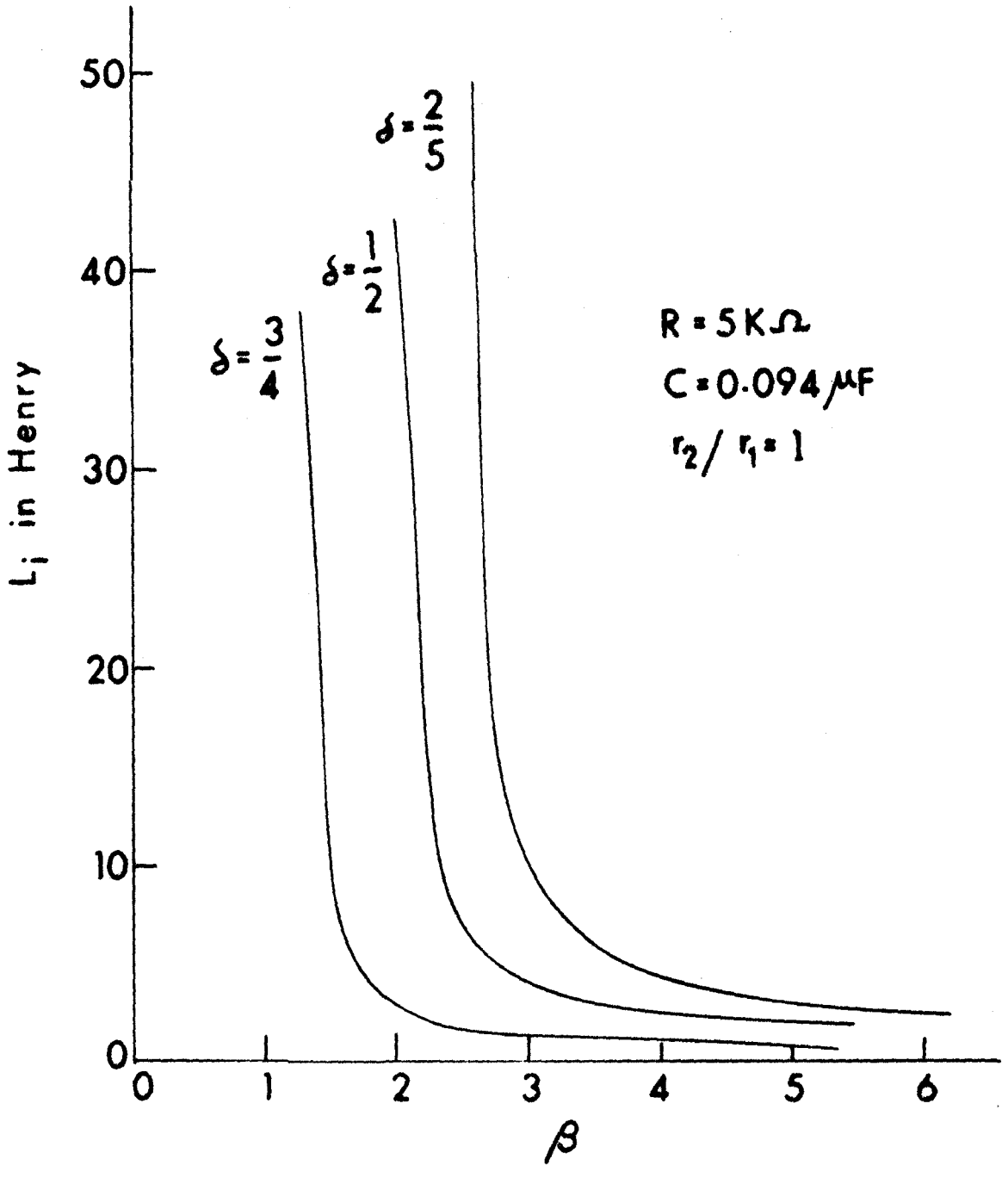

Fig.2.3. The $L_i - \beta$ curves for three different δ.

2.2.4 SENSITIVITY

The sensitivity study of the realized inductor becomes very important as the usefulness the inductor depends much on this sensitivity. For brevity the sensitivity of the ideal inductor is only considered. Instead of calculating the sensitivities to different active and passive parameters, the parasitic concept is introduced[6] to obtain the rationalized deviation of the impedance when ideal inductor realization constraints are tolerated. From equations (2.12) and (2.22) the constraints are,

$$\left.\begin{aligned} \frac{r_2}{r_1} &= m\delta \\ \text{and} \\ \frac{r_2}{r_1} &= \frac{1}{\beta} + \frac{1}{\gamma} \end{aligned}\right\} \qquad (2.24)$$

for an ideal inductor of value

$$L_i = CR^2 \frac{\beta\gamma\left(\frac{r_2}{r_1} - \delta\right)}{\frac{r_2}{r_1}\beta - m} \qquad (2.25)$$

We now introduce the parasitics

$$\left.\begin{aligned} \epsilon_1 &= \frac{r_2}{r_1} - m\delta \\ \text{and} \\ \epsilon_2 &= \frac{r_2}{r_1} - \left(\frac{1}{\beta} + \frac{1}{\gamma}\right) \end{aligned}\right\} \qquad (2.26)$$

so that

$$Z = R \frac{\epsilon_2 + s\beta\gamma CR\left(\frac{r_2}{r_1} - \delta\right)}{\frac{r_2}{r_1}\beta - m + s\beta CR\,\epsilon_1}$$

$$= R \frac{\epsilon_2 + j\gamma\omega_o \left(\frac{r_2}{r_1} - \delta\right)}{\frac{r_2}{r_1}\beta - m + j\omega_o \epsilon_1} \qquad (2.27)$$

where $\omega\beta CR = \omega_o$

Ideally ϵ_1 and ϵ_2 are nonexistent (i.e.zero). For their tolerance, the inductor becomes bilinear. Following the definition of the magnitude sensitivity function

$$MS_{\epsilon}^{f(\epsilon)} = \frac{\partial f(\epsilon)}{\partial \epsilon} \cdot \frac{\epsilon}{f(\epsilon)} \qquad (2.28)$$

one gets

$$MS_{\epsilon_1}^{Z(\epsilon_1)} \Big|_{\epsilon_2 = 0} = \frac{\omega_o \epsilon_1}{\omega_o^2 \epsilon_1^2 + \left(\frac{r_2}{r_1}\beta - m\right)^2} \qquad (2.29)$$

which has a maximum value of unity with $\omega_o \to \infty$ and

$$MS_{\epsilon_2}^{Z(\epsilon_2)} \Big|_{\epsilon_1 = 0} = \frac{\epsilon_2}{\sqrt{\epsilon_2^2 + \omega_o^2 \gamma^2 \left(\frac{r_2}{r_1} - \delta\right)^2}} \qquad (2.30)$$

which has a maximum value of unity with $\omega_o \longrightarrow 0$. This indicate that the sensitivity of the scheme is only nominal. It is interesting to note that the sensitivity of the inductance value L_i is given by

$$MS_{\epsilon_{1,2}}^{L_i(\epsilon_{1,2})} = \frac{2\omega_o^2 \epsilon_1^2}{\left(\frac{r_2}{r_1}\beta - m\right)^2 + \omega_o^2 \epsilon_1^2} \qquad (2.31)$$

So that, with $\omega_o^2 \epsilon_1^2 \ll \left(\frac{r_2}{r_1}\beta - m\right)^2$, MS^{L_i} is quite small. The

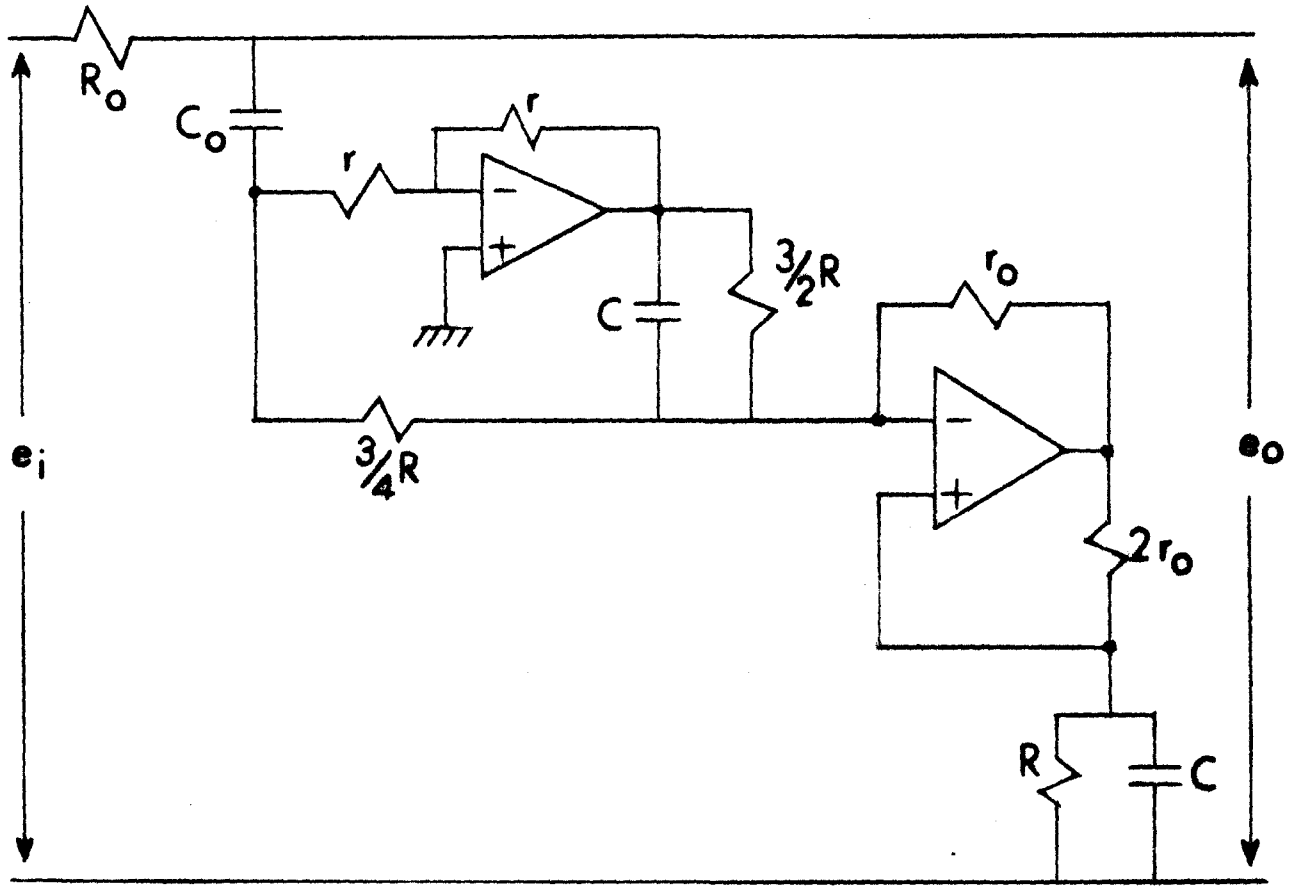

Fig. 2.4 A notch filter

maximum value of MS^{L_i} is 2 when $\omega \to \infty$.

2.3 FILTER REALIZATION

To demonstrate the application of the simulated inductor a notch filter is realized as shown in figure 2.4.

The transfer function is easily calculated as

$$\frac{V_o}{V_i}(s) = \frac{s^2 \frac{9}{4} CC_oR^2 + 1}{s^2 \frac{9}{4} CC_oR^2 + sC_oR_o + 1} \tag{2.32}$$

such that the notch frequency and the selectivity Q are given respectively by

$$\omega_n = \frac{2}{3R} \frac{1}{\sqrt{CC_o}} \tag{2.33}$$

and

$$Q = \frac{3}{2} \frac{R}{R_o}\sqrt{\frac{C}{C_o}} \tag{2.34}$$

It is interesting to note that the Q of such a filter is controlable independent of ω_n by adjusting R_o.

2.4 THE OSCILLATOR

When the realized inductor is ideal ($Q = \infty$) and has a sufficiently large value, a capacitor C' connected across port 1-1' (figure 2.1) would lead to realization of low frequency oscillator with a frequency of oscillation,

$$f = \frac{1}{2\pi\sqrt{L_i C'}}$$

$$= \frac{1}{2\pi\beta\frac{r_1}{r_2}R}\sqrt{\frac{(\beta - \frac{1}{\delta})(\beta - \frac{r_1}{r_2})}{(\frac{r_2}{r_1} - \delta)CC'}} \tag{2.35}$$

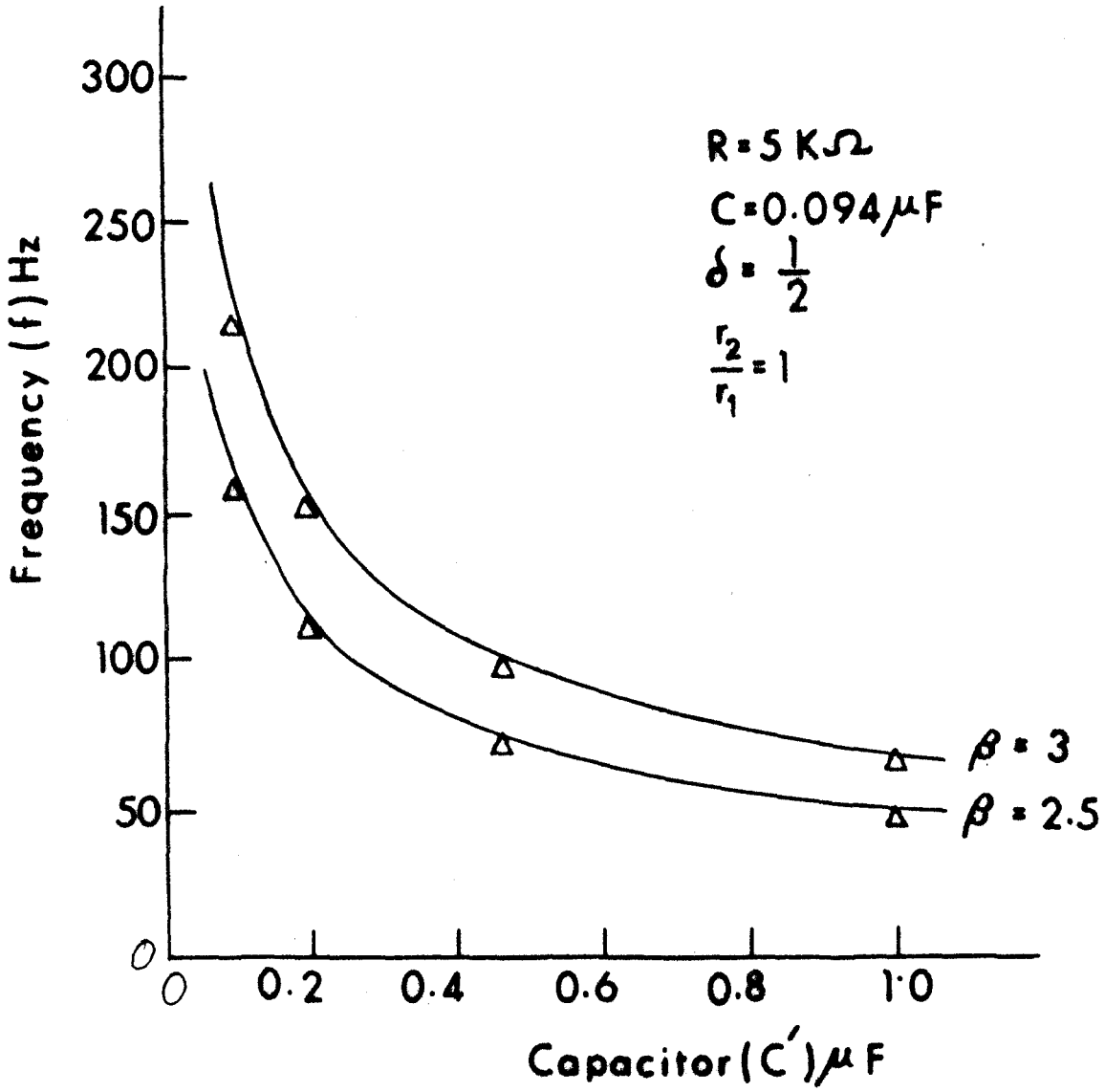

Fig.2.5. The f-C′ curves for two different β
(Experimental points: Δ)

A separate active device is not necessary but it is necessary that the passive parameters adapted in the circuit should lead to the condition of oscillation in terms of the circuit stability. This however is not difficult to realize in practice and in fact is obtained by interchanging the input terminals of the operational amplifier used as n.i.c.(cf. figure 2.4). The f-C' curves for two different values of β are shown in figure 2.5.

2.5 RESULTS

The measured values of L_b and R_b with varying f, for the bilinear case are shown by triangles in figure 2.2 for different parameter values along with the theoretical curves.

With the simulated ideal inductor an oscillator was set-up by connecting capacitor C' of different values across port 1-1' (figure 2.1). The measured frequencies indicated by triangles are plotted in the f-C' coordinates along with the theoretical curves in figure 2.5 for two different values of β. The results plotted in the curves show good agreement with the calculated values.

2.6 CONCLUSION

The proposed circuit is a very generalized scheme of inductor realization as may be seen that with passive parameter adjustment it is possible to realize bilinear, linear and ideal inductor. In the case of ideal inductor it is seen that it is possible to simulate inductance of any value including infinity. Besides, realizing typical filters with the simulated inductor, a variable

low frequency sine-wave oscillator very often required in instrumentation system can also be conveniently constructed with it. The tolerance in adjustment and matching of components needed, is also shown by the sensitivity analysis to be not very high. The circuit is well adaptable for integrated circuit form, with only a few external components required to adjust the operation in the desired mode.

The grounded inductor, non-ideal or ideal is not suitable to realize an arbitrary filter for signal processing purposes. Floating inductor is much more versatile in this respect. A method of realizing a low loss floating inductor is described in the next chapter.

REFERENCES

1. Patranabis,D. : 'Inductor realization with a negative impedance converter'; Electron . Lett., Vol.6, No.13, pp.415-417, June 1970.

2. Patranabis,D. : 'Grounded inductor simulation with a differential amplifier'; Int.J.Electron., Vol.28, No.5, pp.481-483, 1970.

3. Berndt,D.F. and Dutta Roy,S.C. : 'Inductor simulation using a single unity gain amplifier'; IEEE J.Solid State Circuits, Vol.SC-4, pp.161-162, 1969.

4. Sipress,J.M. : 'Synthesis of active RC networks'; IRE Trans. Circuit Theory, Vol.CT-8, pp.260-269, Sept.1961.

*5. Patranabis,D. and Roy,S.B. : 'Active RC realization of bilinear and linear RL impedances'; Int.J.Electron., Vol.33, No.6, pp.681-687, 1972.

6. Moschytz,G.S. : 'On the analysis of sensitivity of parasitic effects'; Electron. Circuits and Systems, Vol.13, pp.232-238, 1979.

---

* Chapter-II is based mainly on this publication

CHAPTER-III

A LOSSLESS FLOATING INDUCTOR REALIZATION : TWO NEW APPROACHES

3.1 INTRODUCTION

Although active RC grounded ideal inductors are now easily realizable in practice in some applications, such as a type of filters, they are unsuitable. Floating ideal inductor realization with RC elements then started receiving attention. Lately, there has been some efforts to realize a floating lossless inductor with RC elements and operational amplifiers or other active devices, which are in turn realizable by operational amplifiers. Rollett[1] obtained a floating inductance from a floating capacitance via an active 3-port circulator. Reddy[2] developed an approach to realize a floating inductance from a floating capacitance starting from a type of two operational amplifier grounded-inductor-realization scheme using the complementing properties of input and ground in active filters[3]. Sewell[4] developed Rollett's approach further to produce ungrounded inductance from two grounded capacitances. Holt and Taylor[5] suggested a scheme with two ideal gyrators and a grounded capacitance. A circuit with one grounded capacitance was also proposed by Deboo[6] in a somewhat arbitrary manner. In this chapter two new systematic approaches to realize an ideal floating inductor with a single grounded capacitance and three operational amplifiers are presented. The operational amplifiers are connected as Current type negative immittance converter (INIC). It has also been shown that the non-unity gains may be allowed in the INIC's which then are required to be compensated by controlling the conductance parameter of the circuit.

3.2 REALIZATION APPROACHES[7*]

One approach follows from the 3-port gyrator model proposed by Sewell[8]. The nodal equations are first written from his block schematic and these equations are then expanded. The expanded equations lead straight right to the implementation of the proposed scheme.

The second approach is through a step by step process starting from a five-element ladder section. From the admittance matrix of such a ladder the elements that are to be negative for the desired realization are first listed. The possibility of obtaining these negative parameters through minimal actual passive and active elements is then explored. Both the approaches are discussed in brief in the following.

3.2.1 APPROACH FROM THE 3-PORT GYRATOR MODEL

The block schematic of the proposed scheme is shown in figure 3.1. From this figure and the admittance matrix

$$\begin{bmatrix} Y \end{bmatrix} = \begin{bmatrix} 0 & 0 & g \\ 0 & 0 & -g \\ -g & g & 0 \end{bmatrix} \tag{3.1}$$

of the 3-port gyrator (Sewell[8]), the nodal equations are easily written as

$$I_1 = gE_3 \tag{3.2a}$$

$$I_2 = -gE_3 \tag{3.2b}$$

$$I_3 = -gE_1 + gE_2 \tag{3.2c}$$

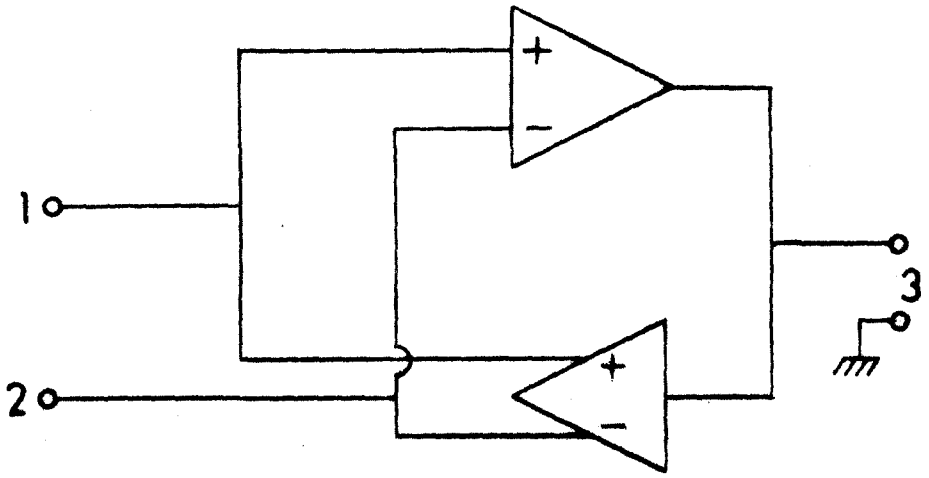

Fig.3.1 Block of a gyrator

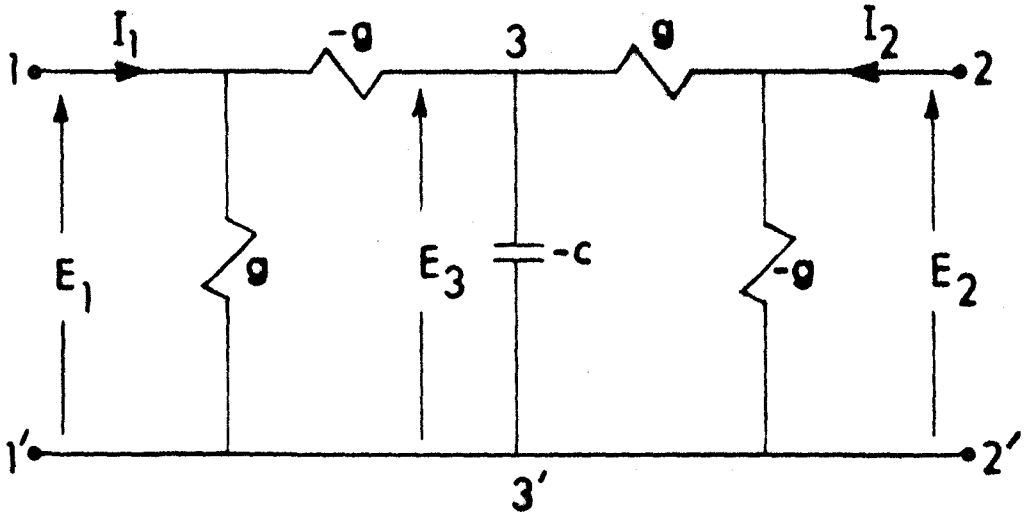

Fig.3.2 Circuit schematic of the gyrator with capacitive termination

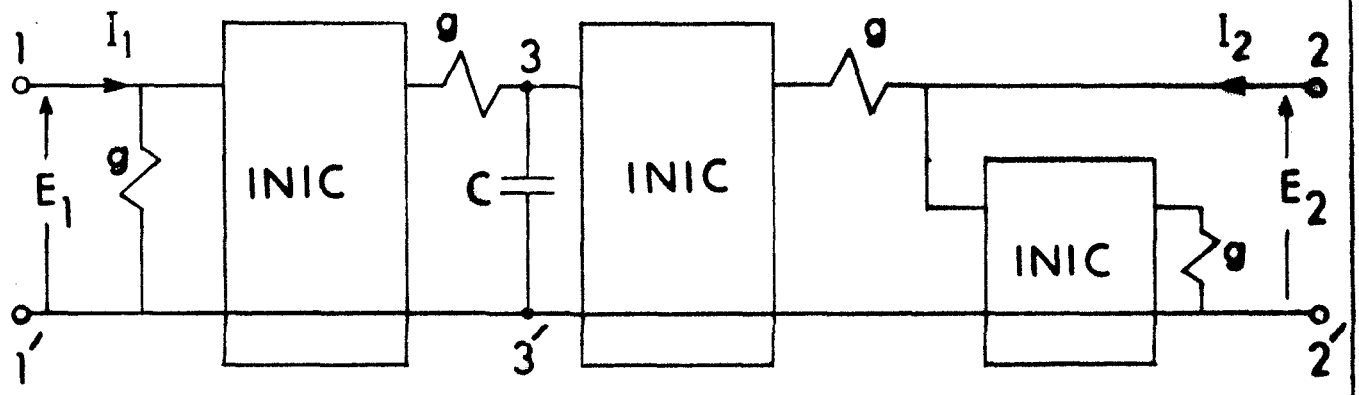

Fig. 3.3 Realization scheme of the circuit of Fig. 3.2

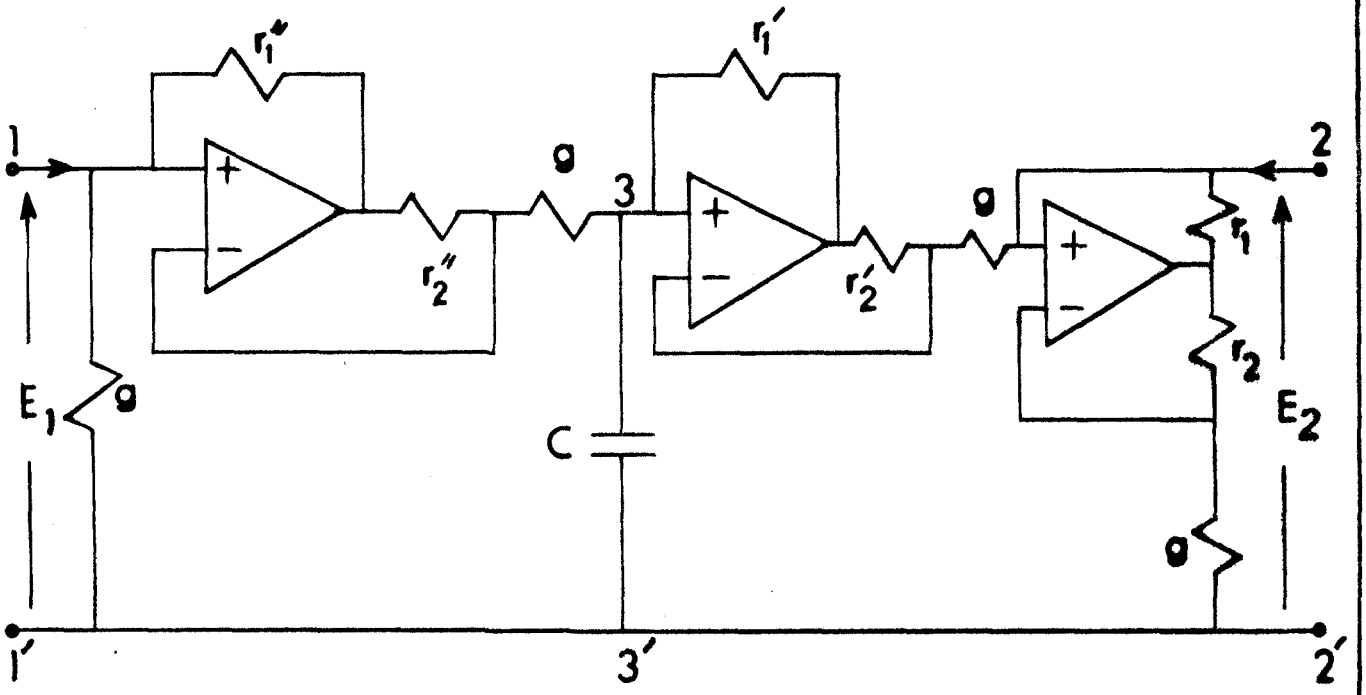

Fig. 3.4 The OA version of Fig. 3.3

Without affecting the gyrator admittance matrix, equations (3.2) may be expanded as

$$I_1 = (-g)\ (E_1 - E_3) + gE_1 \qquad (3.3a)$$

$$I_2 = g\ (E_2 - E_3) + (-g)\ E_2 \qquad (3.3b)$$

$$I_3 = (-g)\ (E_1 - E_3) + g(E_2 - E_3) \qquad (3.3c)$$

For circuit implementation of equations (3.3), voltage differences in the right hand side of the third one of equations (3.3) should appear as $(E_3 - E_1)$ and $(E_3 - E_2)$. The changes made are however taken care of, in the floating ideal inductor realization, by terminating port 3 with a negative capacitance. Then from equations (3.3) one easily obtains the circuit scheme as shown in figure 3.2. The presence of the negative conductance at port 2 make this circuit realizable by three INIC's as shown in figure 3.3. The operational amplifier version of figure 3.3 is shown in figure 3.4.

3.2.2 APPROACH FROM THE LADDER NETWORK

The five element ladder section is shown in figure 3.5. Analysis yields its admittance parameter matrix as

$$\begin{bmatrix} I_1 \\ I_2 \end{bmatrix} = \begin{bmatrix} y_1 + y_2 - \dfrac{y_2^2}{y_2 + y_3 + y_4} & \dfrac{-y_2 y_4}{y_2 + y_3 + y_4} \\ \dfrac{-y_2 y_4}{y_2 + y_3 + y_4} & y_4 + y_5 - \dfrac{y_4^2}{y_2 + y_3 + y_4} \end{bmatrix} \begin{bmatrix} E_1 \\ E_2 \end{bmatrix} \qquad (3.4)$$

One notes that a lossless floating inductor with a grounded capacitor is realizable in the ladder of figure 3.5 for

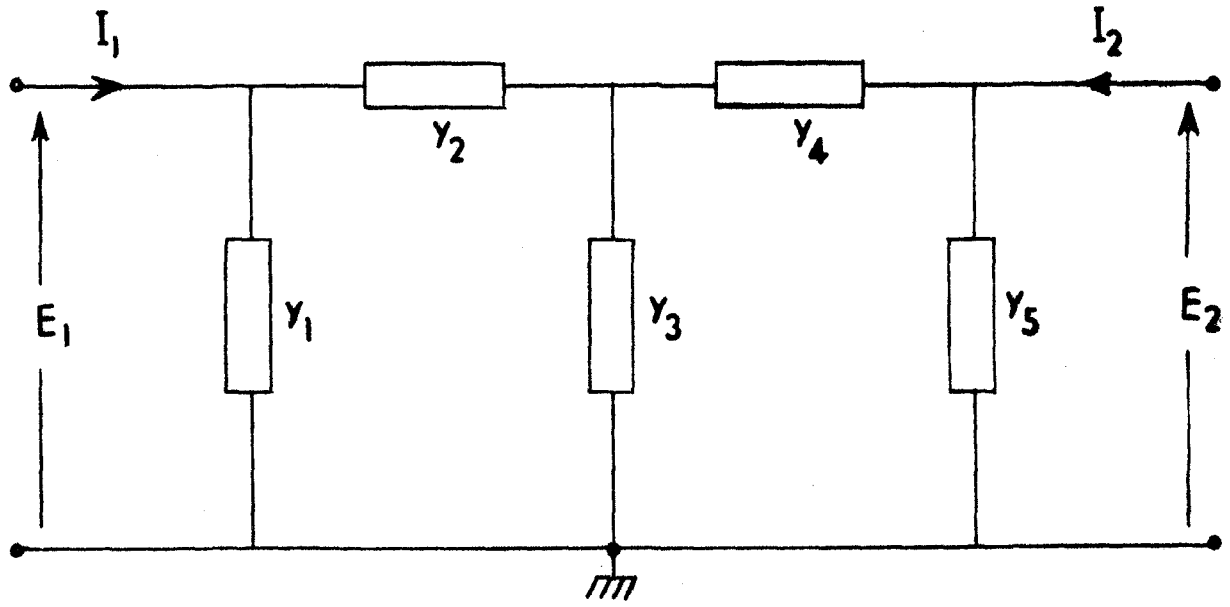

Fig.3.5 The five element ladder section

$$\text{(a)}\quad y_1 + y_2 = y_4 + y_5 = y_2 + y_4 = 0 \tag{3.5a}$$

$$\text{(b)}\quad y_2^2 = y_4^2 = y_2 y_4 \tag{3.5b}$$

and

$$\text{(c)}\quad y_3 = sC\ ;\quad y_j = g_j,\ (j \neq 3) \tag{3.5c}$$

along with the further conditions that all g_j's are identical and either y_2, y_3 and y_5 are negative or y_1, y_3 and y_4 are negative. With the above conditions the ladder network of figure 3.5 can be easily seen to be transformed to that of figure 3.2. From figure 3.2 similar steps lead to the final scheme of figure 3.4.

3.3 THE REALIZED INDUCTANCE

Either from the three port admittance matrix of equation (3.1) coupled with capacitor termination and transforming it into a two port form as discussed earlier or from the matrix of equation (3.4), the admittance parameter matrix of the ideal floating inductance is obtained as

$$\begin{bmatrix} Y_L \end{bmatrix} = \frac{g^2}{sC} \begin{bmatrix} 1 & -1 \\ -1 & 1 \end{bmatrix} \tag{3.6}$$

such that the realized ideal floating inductor is given as

$$L = \frac{C}{g^2} \tag{3.7}$$

3.4 NONIDEALITY OF INDUCTANCE DUE TO COMPONENT TOLERANCE

For nonunity gains of the INIC's and tolerance in the values of the conductances, the admittance matrix tends to become complicated However, the transmission matrix can be more easily derived from figure 3.3 in such a situation. If in figure 3.3, the INIC's from

right to left (port 2 to port 1) are considered to have gains k_1, k_2 and k_3 respectively, with k's as the ratios of the resistances r_1's and r_2's, and the conductances from the left to right (port 1 to port 2) are marked as g_1, g_2, g_3 and g_4, then the transmission matrix between ports 1 and 2 is easily obtained as

$$\left[A\right]_{12} = \begin{bmatrix} (1 + \frac{sC}{g_2})(1 - k_1 \frac{g_4}{g_3}) + \frac{1}{g_2}(k_1 k_2 g_4) & \frac{1}{g_3}(1 + \frac{sC}{g_2}) - \frac{k_2}{g_2} \\ \left\{g_1(1 + \frac{sC}{g_2}) - k_3 sC\right\} & (1 - k_1 \frac{g_4}{g_3}) + (\frac{g_1}{g_2} - k_3)\, k_1 k_2 g_4 \\ & \frac{1}{g_3}(g_1 + g_1 \frac{sC}{g_2} - k_3 sC) - (\frac{g_1}{g_2} - k_3)\, k_2 \end{bmatrix} \tag{3.8}$$

The realizability condition from equation (3.8) is now obtained as

$$g_1 = g_3 = k_3 g_2 = k_2 k_3 g_3 = k_1 k_2 k_3 g_4 \tag{3.9}$$

The inductance has a value

$$L = \frac{C}{g_2 g_3} \tag{3.10}$$

in such a situation.

Equation (3.9) shows that only two conductances need to be equal in value, the other two can be adjusted to compensate for the nonunity gains of the INIC's. This increases the design flexibility to a certain extent.

3.5 SENSITIVITY

In an ideal realization the sensitivity has to be calculated for $L = C/g^2$ only. This yields

$$S_C^L = \frac{1}{2} S_{1/g}^L = 1 \qquad (3.11)$$

indicating sufficiently low sensitivity figures. However, with equation (3.9) observed sensitivities from the parasitic consideration[9] may also be obtained. The floating impedance is

$$Z = \frac{sC}{g_2 g_3} + \frac{1}{g_3} - \frac{k_2}{g_2}$$

$$= \frac{sC}{g_2 g_3} + \frac{\pm \epsilon}{g_2 g_3} \qquad (3.12)$$

where ϵ is the parasitic $g_2 \sim k_2 g_3$. The sensitivity of Z is given by

$$MS_{\epsilon}^{Z(\epsilon)} \simeq \frac{\epsilon}{\omega C} \qquad (3.13)$$

where M stands for 'magnitude of'. In obtaining equation (3.13) second order of ϵ has been neglected. It appears from equation (3.13) that at very low frequencies $MS_{\epsilon}^{Z(\epsilon)}$ may be quite large unless ϵ is of the order of ppm. As a parasitic however ϵ is usually not larger than that, hence the sensitivity always tends to be quite low.

3.6 CIRCUIT STABILITY

The circuit stability in this context means the stability of the INIC's. It is simple to stabilize this circuit by properly choosing the input terminals of the operational amplifiers[10]. With

$r_1 > r_2$, the connections in the operational amplifiers with the indicated polarity as in figure 3.4 are proper for stability.

3.7 EXPERIMENTAL RESULTS

Experimental studies have confirmed the theoretical analysis. The circuit of figure 3.4 was then actually used to design a low pass filter[11] using low tolerance (1%) passive components and operational amplifiers with 1 MHz gain band width with an attempt for proper stop band trimming, the filter function being

$$\frac{e_o}{e_1} = \frac{1 + hs^2}{a_3 s^3 + a_2 s^2 + a_1 s + a_o} \qquad (3.14)$$

where

$$h = LC$$

$$a_3 = LR_1(CC_1 + CC_2 + C_1C_2)$$

$$a_2 = L(C + C_2)$$

$$a_1 = R_1(C_1 + C_2)$$

$$a_o = 1$$

The cut-off frequency obtained is at 10.8 kHz. Deviation of the experimental result was less than 5% from the calculated values. The experimental filter scheme is shown in figure 3.6, and the theoretical response curve along with the experimental plot are shown in figure 3.7.

3.8 CONCLUSION

Two systematic approaches for floating inductor realization through a grounded capacitor three operational amplifier scheme

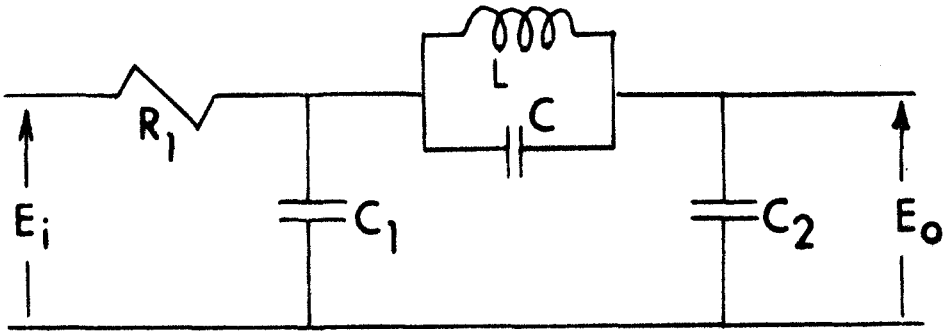

Fig.3.6. The Low-pass filter

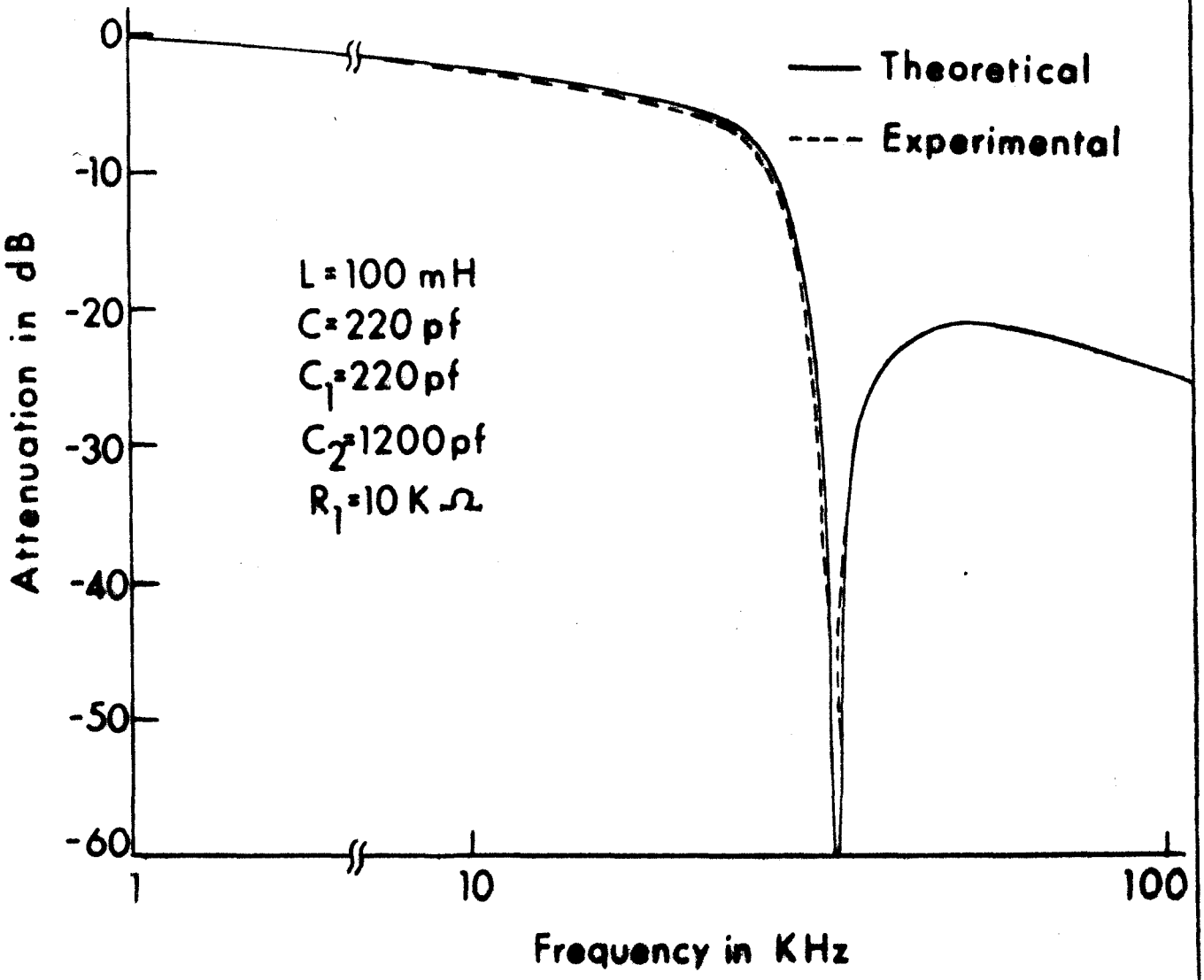

Fig.3.7. The LP filter responce

are presented in this chapter. Although two different approaches have been shown in Section 3.2, the basic structure obtained through them come out to be the same. A grounded capacitor scheme has been considered because of convenience in integrability. Of the many schemes, now known, the presented method has comparatively less cancellation constraints. A low-pass filter has been designed using the developed prescribed method of realization and it has been shown that the realization approaches the ideal values very well with 1% tolerance components.

The realized inductors can be used to design filters of desired response characteristics. The values of realized inductor and their Q-factor may be called to determine the frequency range and the filter selectivity and it is not difficult to have the filter operating at low frequency as required in instrumentation system. However inductorless filters may directly be designed with active RC elements only. In such situations inductors are inherently provided in the system. In the following chapter a generalized approach is presented to obtain such a scheme in which all types of response can be shown to be obtained by minor changes in the passive RC networks. The basic realization approach however, remains unchanged by these changes.

REFERENCES

1. Rollett,J.M. : 'Circulator capacitor networks'; Electron. Lett., Vol.4, pp.599-601, 1968.

2. Reddy,M.A. : 'Some new operational amplifier circuits for realization of the lossless floating inductance'; IEEE Trans. Circuits and Systems, Vol.CAS-23, No.3, pp.171-173, March 1976.

3. Hilberman,D. : 'Input and ground as complements in active filters'; IEEE Trans. Circuit Theory, Vol.CT-20, No.9, pp.540-547, Sept.1973.

4. Sewell,J.I. : 'Active circulator systems'; Int.J.Electron., Vol.33, No.6, pp.677-679, 1972.

5. Holt,A.G.J. and Taylor,J. : 'Method of replacing ungrounded inductors by grounded gyrators'; Electron.Lett., Vol.1, No.4, p.105, June 1965.

6. Deboo,G.J. : 'Application of gyrator type circuit to realize ungrounded inductors'; IEEE Trans. Circuit Theory, Vol.CT-14, No.1, pp.101-102, March 1967.

*7. Patranabis,D. Tripathi,M.P. and Roy,S.B. : 'A new approach for lossless floating inductor realization; IEEE Trans. Circuits and Systems, Vol.CAS-26, No.10, pp.892-893, Oct.1979.

8. Sewell,J.I. : 'A simple method for producing floating inductors'; Proc. IEEE, Vol.57, No.12, pp.2155-2156, Dec.1969.

9. Moschytz,G.S. : 'On the analysis of sensitivity of parasitic effects'; Electron. Circuits and Systems, Vol.13, pp.232-238, 1979.

10. Huelsman,L.P. : 'Theory and Design of Active RC Circuits'; New York : McGraw-Hill, 1968, pp.143-144.

11. Everitt,W.L. and Anner,G.E. : 'Communication Engineering'; New York : McGraw - Hill, 1956, p.268.

---

* Chapter-III is based mainly on this publication.

CHAPTER-IV

INDUCTORLESS FILTER REALIZATION SCHEME : A GENERAL APPROACH

4.1 INTRODUCTION

In the preceding chapter a floating inductor realization scheme and also its application in filter design has been demonstrated. The ideal floating inductor requires quite a few resistors and active blocks making the final filter topology sufficiently elaborate. Instead integrated development of inductorless filters through active RC form yields economic structures. In this direction individual schemes or particular forms have been produced[1-3] with success. This chapter presents a generalized appreach to realize inductorless filter schemes with a stress on allpass response characteristics. Allpass filters have large scale applications in the areas of communication and control systems. A typical example of its use is as a delay network in a communication channel or in a control loop where a time delay may be required to be introduced without reduction in the signal strength. The presented scheme uses interconnection of one three terminal network with another four terminal one, constrained by a single operational amplifier (OA). The scheme is sufficiently general in the sense that it can realize allpass, low, high and bandpass and also band elimination filter functions. It obtains these functions with complex poles such that high-Q realization is implied. As pointed out, the method starts with an approach to generalize the active RC-allpass schemes with a single OA.

4.2 THE GENERALIZATION OF THIS ALL-PASS FILTER[4*]

For obtaining a complete generalization scheme of the active RC allpass networks[5-16] with a single differential input operational amplifier, a 5-terminal RC network constrained by an operational amplifier as shown in figure 4.1 would be required. The terminal 4 and 5 are the output terminals and 1 is the input terminal. Employing only the constraints (a) $E_2 = E_3$, (b) $I_2 = I_3 = 0$ and (c) I_4 being arbitrary, dictated by the ideal OA to the admittance matrix of this 5-terminal network, it is possible to realize the voltage transmission matrix as

$$\left[t\right] = \left[t_{41}, t_{51}\right] \qquad (4.1)$$

This generalization covers almost the entire class of single OA allpass realization schemes. However, the constraints (a) to (c) can reduce the admittance matrix order from 5x5 to 4x3 at the most, but as such this reduction offers little advantage in evaluating the matrix $\left[t\right]$. Furthermore, if the OA has a finite gain A, constraint (a) changes to (á) $(E_2 - E_3)A = E_4$. Many of the above schemes[3-6, 11-15] have, however, used a 4-terminal constrained network to realize an all pass transmission function t_{41} In fact, the constraint provided by the OA, both for finite and infinite gain configurations, in a 4-terminal network make the evaluation of t_{41} considerably easier. The other schemes[7-10] have also used a 4-terminal (including a grounded one) network, but terminal 2 has been grounded in these, and the output has been obtained at 5 realizing t_{51}. The latter schemes were further simplified by making $y_{13} = y_{31} = g_{31}$ and the realization then

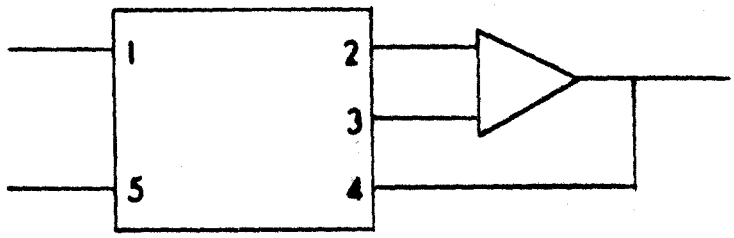

Fig. 4.1 The 5-Terminal network scheme

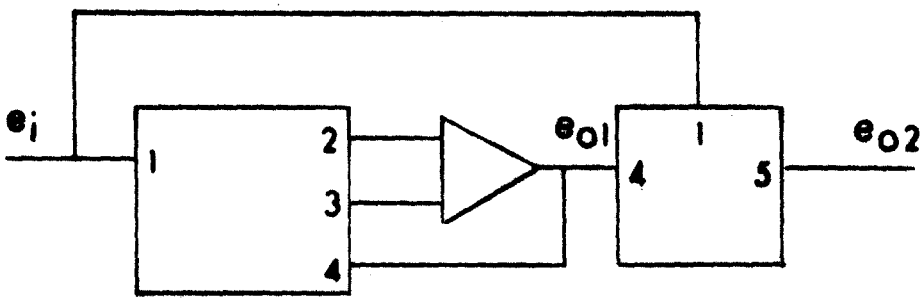

Fig. 4.2 The proposed scheme of generalisation

actually involves the synthesis of 3-terminal ladder or parallel ladder network. Combining the above two schemes, therefore, a generalized scheme can be attempted where the simplicity of analysis and synthesis of both the schemes can be retained. In the following, such a scheme, interconnecting a 3-terminal network with a 4-terminal network constrained by a differential input OA is presented. The evaluation of the overall transfer function in this network is considerably simplified. The proposed generalization scheme is shown in figure 4.2 where the voltages at the input (terminal 1), first output terminal (terminal 4) and second output terminal (terminal 5) are denoted by e_i, e_{01} and e_{02} respectively. The voltage transfer function t_{51} as defined earlier would now have a changed significance as indicated in figure 4.2. So, for brevity, t_{41} and t_{51} of equation (4.1) are replaced by t_{01} and t_{02} respectively, which are defined in equations (4.4) and (4.6) below. Applying the constraints (a) and (b) to the admittance matrix of the 4-terminal network one easily obtains

$$\begin{bmatrix} \frac{I_1}{y_{11}} \\ 0 \\ 0 \\ \frac{I_4}{y_{44}} \end{bmatrix} = \begin{bmatrix} 1 & \frac{1}{y_{11}A}(y_{12} - y_{13} + Ay_{14}) \\ \frac{y_{21}}{y_{22}} & \frac{1}{y_{22}A}(y_{22} - y_{23} + Ay_{24}) \\ \frac{y_{31}}{y_{33}} & \frac{1}{y_{33}A}(y_{32} - y_{33} + Ay_{34}) \\ \frac{y_{41}}{y_{44}} & \frac{1}{y_{44}A}(y_{42} - y_{43} + Ay_{44}) \end{bmatrix} \begin{bmatrix} e_i \\ e_{01} \end{bmatrix} \qquad (4.2)$$

from which the voltage transfer function $\frac{e_{01}}{e_i}$ is obtained as

$$\frac{e_{01}}{e_i} = \frac{A\left(\frac{y_{31}}{y_{33}} - \frac{y_{21}}{y_{22}}\right)}{A\left(\frac{y_{24}}{y_{22}} - \frac{y_{34}}{y_{33}}\right) - \left(\frac{y_{33}}{y_{22}} + \frac{y_{32}}{y_{33}} - 2\right)} \tag{4.3}$$

For the infinite gain OA realization, as is mostly the case, equation (4.3) simplifies to

$$t_{01} = \frac{e_{01}}{e_i}\Bigg|_{A \to \infty} = \frac{\frac{y_{31}}{y_{33}} - \frac{y_{21}}{y_{22}}}{\frac{y_{24}}{y_{22}} - \frac{y_{34}}{y_{33}}} \tag{4.4}$$

For obtaining t_{02} , we define for the 3-terminal network

$$t_{51} = \frac{e_{02} - e_{01}}{e_i - e_{01}} \tag{4.5}$$

and hence from figure 4.2

$$t_{02} = \frac{e_{02}}{e_i}\Bigg|_{A \to \infty} = t_{01} + t_{51}\,(1 - t_{01}) \tag{4.6}$$

The transmittance t_{51} can be written as the ratio of two second-order cofactors of the admittance matrix of the 3-terminal network.

$$\left[y_3\right] = \begin{bmatrix} y_{11} & y_{14} & y_{15} \\ y_{41} & y_{44} & y_{45} \\ y_{51} & y_{54} & y_{55} \end{bmatrix} \tag{4.7}$$

following the usual definition[17], and is given as

$$t_{51} = \frac{y_{54}^{14}}{y_{14}} \tag{4.8}$$

t_{02} can also be obtained from t_{54}, given as

$$t_{54} = \frac{e_{02} - e_i}{e_{01} - e_i} = \frac{y_{51}^{41}}{y_{41}} \tag{4.9}$$

when

$$t_{02} = 1 + t_{54}\,(t_{01} - 1) \tag{4.10}$$

t_{01} becomes identical with t_{02} if $t_{51} = 0$ or $t_{54} = 1$, which from equation (4.5) or (4.9) implies $e_{02} = e_{01}$.

Following equation (4.6) or (4.10) almost all the allpass networks are obtainable from figure 4.2 with the proper choice of y_{ij}'s in equation (4.4) and y_{mn}^{ki}'s (which are, again, y_{pq}'s only) in equation (4.8) or (4.9). We choose equation (4.6) and show by way of example how some of the important allpass realization schemes are derived from it.

The circuit of Dutta Roy[6] is easily obtained if

$$y_{34} = 0$$

$$\frac{y_{21}}{y_{22}} = \frac{1/R_1}{1/R_1 + 1/R_2} = \frac{\lambda}{1+\lambda}$$

and

$$y_{24} = y_{22} - y_{21}$$

$$t_{51} = 0$$

These give

$$t_{(DR)} = \frac{y_{31}(1 + \lambda) - y_{33}\lambda}{y_{33}} \qquad (4.11)$$

The Deliyannis[11] circuit is obtained for

$$y_{34} = 0$$

$$\frac{y_{31}}{y_{33}} = \frac{g_a}{g_a + g_b} = \frac{1}{1 + k}$$

$$y_{22} = y_{21} + y'_{22}$$

and

$$t_{51} = 0$$

The transfer function is given as

$$t_{(D)} = \frac{y'_{22} - ky_{21}}{(1+k)y_{24}} \qquad (4.12)$$

The circuits of Schoonaert and Kretzschmar[7] and that of Patranabis[1(
requires the component arrangement such that

$y_{22} = \alpha$; $y_{34} = g_{34}$; $y_{31} = g_{31}$; $y_{33} = g_{31} + g_{34}$; $m = \frac{g_{31}}{g_{34}}$

and $t_{51} = \beta_o$ (s, R, C) giving

$$t_{(P)} \text{ or } t_{(SK)} = \beta_o (1 - m) + m \qquad (4.13)$$

β_o must be synthesised in the ladder or parallel ladder form[10].
In an earlier generalization scheme[18], which required one 3-termina

network less than the Liberatore generalization[19], the Holt and Gray circuit was not realizable. In the present scheme this also is possible with the following identification

$$y_{31} = s + 1 \; ; \quad y_{21} = y_{24} = y \text{ (say)}; \; y_{34} = \frac{2s}{s+1}$$

$$y_{33} = s + 1 + \frac{2s}{s+1} + \frac{s}{s+1}$$

$$y_{22} = 2y \text{ and } t_{51} = 0$$

This gives

$$t_{(HG)} = \frac{1 - s + s^2}{1 + s + s^2} \qquad (4.14)$$

Most of the other circuits are only special cases of the above schemes and can similarly be shown to be realizable by this scheme including a circuit[17] with a finite gain OA.

The generalization has thus been shown to cover the allpass realization scheme almost fully, except perhaps the cases where the OA is used as a voltage-controlled current source[20]. It would further be noted that this structure with appropriate choice of the passive network could be adapted to realize any arbitrary transfer functions besides the allpass ones already discussed.

4.3 HIGH, LOW, BAND-PASS AND NOTCH FILTER REALIZATION

Some examples from second order, high, low, band-pass and notch filters are given below for confirming the generalization of the second scheme.

4.3.1 HIGH-PASS FILTER REALIZATION

From equation (4.4) and (4.10) for $t_{54} = 1$, we get

$$t_{02} = \frac{\frac{y_{31}}{y_{33}} - \frac{y_{21}}{y_{22}}}{\frac{y_{24}}{y_{22}} - \frac{y_{34}}{y_{33}}} \qquad (4.15)$$

Letting now,

$$y_{21} = s + 1 \; ; \quad y_{24} = s + 3 \; ; \quad y_{22} = 3s + 4$$

$$y_{31} = s + 2 \; ; \quad y_{34} = \tfrac{1}{2}(s+1); \quad y_{33} = 2s + 8$$

equation (4.15) yields

$$t_{02} = \frac{2s^2}{s^2 + 18s + 40} \qquad (4.16)$$

This is the transfer function of a High-pass filter with real poles.

However for highpass filters with complex poles the following selections are made

$$y_{21} = s + 1 \; ; \quad y_{24} = s + 3 \; ; \quad y_{22} = 3s + 4$$

$$y_{31} = s + 2 \; ; \quad y_{34} = \tfrac{1}{2} \quad ; \quad y_{33} = 2s + 8$$

The transfer function is then obtained as

$$t_{02} = \frac{2s^2}{4s^2 + 25s + 44} \qquad (4.17)$$

4.3.2 BAND-PASS FILTER REALIZATION

In equation (4.15) assuming

$$y_{21} = s + 1 \; ; \quad y_{24} = 2s + 1 \; ; \quad y_{22} = 3s + 2$$

$$y_{31} = s + 2 \; ; \quad y_{34} = s + 1 \; ; \quad y_{33} = 3s + 4$$

the band-pass filter transfer function with real poles is obtained as

$$t_{02} = \frac{s}{3s^2 + 6s + 2} \tag{4.18}$$

If however one identifies,

$$y_{21} = y_{24} = s + 1 \; ; \quad y_{22} = 3s + 2$$

$$y_{31} = s + 2 \; ; \quad y_{34} = 1 \; ; \quad y_{33} = 3s + 4$$

a band-pass filter with complex poles is obtained,

$$t_{02} = \frac{s}{3s^2 + 4s + 2} \tag{4.19}$$

4.3.3 LOW-PASS FILTER REALIZATION

A real pole second order filter can be easily synthesised with appropriate choice of y_{ij}'s. An example of complex pole second order filter is given below with

$$y_{21} = s + 5 \; ; \quad y_{24} = 3s + 11 \; ; \quad y_{22} = 4s + 16$$

$$y_{31} = s + 3 \; ; \quad y_{34} = 2s + 3 \; ; \quad y_{33} = 4s + 8$$

These yield

$$t_{02} = \frac{2}{s^2 + 6s + 10} \tag{4.20}$$

4.3.4 NOTCH FILTER REALIZATION

If one makes $t_{51} = \frac{1}{2}$ instead of 0 in the Holt and Gray realization procedure given above, then from equation (4.6)

$$t_N(s) = \frac{s^2 + 1}{s^2 + s + 1} \tag{4.21}$$

indicating that a notch network function is realizable by the scheme.

4.4 CONSIDERATION OF THE FINITE GAIN-BANDWIDTH PRODUCT OF THE OPERATIONAL AMPLIFIER

Since the constraints of infinite gain was not used in the beginning for obtaining the voltage transfer function from the 4-terminal network, equation (4.2) can be conveniently used to evaluate the effect of the finite gain-bandwidth product of the OA in the realization schemes. It may be shown that a simple-pole model of the OA introduces an additional pole in all these realizations with t_{01} now given as

$$t_{01f} = \frac{\frac{y_{31}}{y_{33}} - \frac{y_{21}}{y_{22}}}{\frac{y_{24}}{y_{22}} - \frac{y_{34}}{y_{33}} - \frac{s}{\omega_B}\left(\frac{y_{23}}{y_{22}} + \frac{y_{32}}{y_{33}} - 2\right)} \tag{4.22}$$

where ω_B is the unity gain-bandwidth of the amplifier.

4.5 CONCLUSION

The generalization scheme of active RC filters with a single operational amplifier has been described in this chapter. The scheme may be used as a single stock of active RC filter function realization schemes.

In Chapter-II a simulated inductor has been shown to generate sinusoidal oscillations. High, low and band-pass filters realized through integrated approach can be equally effective in producing harmonic generation. Further through a suitable choice, single element frequency controllability of such oscillators is easily obtained. This is borne out in the next chapter with associated details and applications.

REFERENCES

1. Patranabis,D. : 'An all-pass realization using a null network'; Int.J.Electron., Vol.28, No.4, pp.399-400, 1970.

2. Patranabis,D. : 'An RC all-pass filter'; Int.J.Electron., Vol.30, No.1, pp.91-94, 1971.

3. Patranabis,D. and Tripathi,M.P. : 'An active RC all-pass filter'; Int.J.Electron., Vol.39, No.6, pp.647-651, 1975.

*4. Patranabis,D. Roy,S.B. and Tripathi,M.P. : 'Generalization of active RC all-pass schemes'; Proc.IEEE, Vol.66, No.3, March 1978.

5. Khera,R. : 'Another realization of an all-pass transfer function using an operational amplifier'; Proc.IEEE, Vol.57, No.8, pp.1337-1338, Aug. 1969.

6. Dutta Roy,S.C. : 'RC active all-pass networks using a differential input operational amplifier'; Proc.IEEE, Vol.57, No.11, pp.2055-2056, Nov.1969.

7. Schoonaert,D.H. and Kretzschmar,J. : 'Realization of operational amplifier all-pass networks'; Proc.IEEE, Vol.58, No.6, pp.953-955, June 1970.

8. Genin,R. : 'Realization of an all-pass transfer function using operational amplifiers'; Proc.IEEE, Vol.56, No.10, pp.1746-1747, Oct.1968.

9. Bhattacharyya,B.B. : 'Realization of an all-pass transfer function'; Proc.IEEE, Vol.57, No.11, pp.2092-2093, Nov.1969.

10. Patranabis,D. : 'Synthesis of RC all-pass networks'; Int.J. Electron., Vol.27, No.4, pp.337-347, 1969.

11. Deliyannis,T. : 'RC active all-pass sections'; Electron. Lett., Vol.5, pp.59-60, Feb.1969.

12. Das,S.K. and Das,G. : 'Realization of all-pass transfer function using a differential amplifier'; IEEE. Trans. Circuit Theory, Vol.CT-20, pp.326-327, May 1973.

13. Aronhime,P. and Budak,A. : 'An operational amplifier all pass network'; Proc. IEEE, Vol.57, No.9, pp.1677-1678, Sept.1969.

14. Inigo,R.M. : 'Comments on realization of an all-pass transfer function'; Proc. IEEE, Vol.58, No.6, pp.944-946, June 1970.

15. Macdiarmid,I.F. : 'Active all-pass filter using a differential amplifier'; Electron-Lett., Vol.2, p.186, May 1966.

16. Holt,A.G.J., and Gray,J.P. : 'Active all-pass Sections'; Proc. IEEE, Vol.114, pp.1871-1872, Dec.1967.

17. Moschytz,G.S. : 'Linear Integrated Network : Fundamentals'; New York : Van Nostrand Reinhold,1974, ch.3, pp.116-141.

18. Patranabis,D. and Tripathi,M.P. : 'Additional generalization Scheme of active RC all-pass filters'; Electron.Lett., Vol.13, pp.167-168, March 1977.

19. Liberatore,A. : 'Additional considerations about William's circuit for all-pass networks'; Electron. Lett., Vol.7, pp.77-78, Feb.1971.

20. Dutta Roy,S.C. : 'Active all-pass filter using a differential input operational amplifier'; Proc. IEEE, Vol.57, No.9, pp.1687-1688, Sept.1969.

---

* Chapter-IV is based mainly on this publication.

CHAPTER-V

SINGLE ELEMENT CONTROL SINEWAVE OSCILLATOR

5.1 INTRODUCTION

In chapters II and III simulation of inductor both grounded and floating have been considered. Such a circuit component has been known to be useful in the synthesis of low frequency analogue signal processing network (filters) and in the design of sinewave oscillators. However filter design is of more importance with such simulations[1-3] and since literature abounds is such studies[4-5] only a generalized approach of realizing inductorless filter scheme with a single operational amplifier has been presented in the preceeding chapter.

Another important active RC system (i.e. the oscillator) generated from the filters for application in instrumentation and communication is considered in this chapter. In the subsequent chapters other types of oscillators have been discussed. All these oscillators are not identical in design, performance and utility. Mode of oscillations varying from harmonic to relaxation have been considered using two kinds of active devices. Continuing the use of operational amplifier, the present chapter is devoted to discuss a special type sinewave oscillator which is single element controllable[6*]. This control element should be resistive for convenience. Some types of this class of oscillator can be easily adopted to generate voltage controlled oscillation, which is very much useful in signal processing in instrumentation and communication areas. With suitable transducers these oscillators can also be used for measurement and control of industrial parameters.

In recent years studies on many different types of sinewave oscillators[7-10] whose frequency is controllable with a single variable resistor have been reported. Of the various circuits or class of circuits providing such oscillations, those of Sun[9] and Holt and Lee[10] have special merits, in so far as a few of these circuits use minimum RC elements, and only two amplifiers of appropriate gain conditions. Sun's approach in the design of these oscillators is by combining the feedback in a low/high/bandpass structure with that in a bandpass one, while Holt and Lee start with a paraphase amplifier. Here an alternative new approach of generating a class of such oscillators with direct feedback in an active RC high/low/bandpass filter or biquad in cascade with an amplifier is presented. A single such case was described earlier[11] in a piecemeal fashion. The analysis of the oscillation stability of the circuits presented, is also made and followed - through the generalized open loop transfer function, and Loeb's criteria for limit cycle stability are applied. Sensitivity of frequency to temperature and effect of finite gain bandwidth product of the operational amplifiers used have also been discussed. Results of experimental studies of a typical circuit have been given in graphs.

5.2 BASIC THEORY

The transfer function of an active RC filter with a cascaded amplifier of gain K_a may be written as

$$T(s) = \frac{K_a F(s)}{s^2 + s\frac{\omega_d}{Q_d} + \omega_d^2} \qquad (5.1)$$

where Q_d = pole Q-factor, ω_d = pole resonance frequency and K_a = a gain parameter. For generalized analysis, the function F(s) may be defined as

$$F(s) = as^2 + bs + c \tag{5.2}$$

such that when the feedback loop is completed, the condition of oscillation is derived as

$$K_a b = \frac{\omega_d}{Q_d} \tag{5.3}$$

and the frequency of oscillation is

$$\omega_o = \left(\frac{\omega_d^2 - K_a c}{1 - K_a a}\right)^{\frac{1}{2}} \tag{5.4}$$

$K_a b$ determines the condition of oscillation in relation to $\frac{\omega_d}{Q_d}$ and for independent control of frequency it is necessary that a and/or c should be a function of the controlling parameter which usually is the gain parameter of the filter amplifier. It may be observed further from equations (5.3) and (5.4) that for such an independent single element frequency control both a and c in F(s) should not be simultaneously zero when $b \neq 0$, meaning that a bandpass structure with a single zero at the origin is not permitted. Further when $b = 0$ and either a or c is zero i.e. for low and high pass filters $1/Q_d$ can and should be usually made zero making Q_d a function of the gain parameter of the filter amplifier when K_a can be adjusted for frequency control only. Table-5.1 summarizes the constraints, condition and tuning parameters.

TABLE-5.1

OSCILLATOR CONSTRAINTS CONDITION AND TUNING PARAMETERS

Cases	Zeros of F(s) allowed at	Oscillation condition	Frequency tuning by
1	$-\infty$	$\frac{1}{Q_d} = 0$	K_a
2	$0_+ , 0_-$	$\frac{1}{Q_d} = 0$	K_a
3	$-\frac{c}{b}$	$K_a = \frac{\omega_d}{bQ_d}$	c
4	$0, -\frac{b}{a}$	$K_a = \frac{\omega_d}{bQ_d}$	a
5	$\frac{-b \pm \sqrt{b^2 - 4ac}}{2a}$	$K_a = \frac{\omega_d}{bQ_d}$	a, c

5.3 THE CIRCUITS

Four filter circuits with the cascaded amplifier are shown in figures 5.1 and 5.2. Basically two circuit schemes are depicted and each of these schemes has two variations with the interchance of the RC elements. Figure 5.1(a), (b) show a low and a high pass structure respectively and figures 5.2(a), (b) are bandpass structures. Table 5.2 gives the condition of oscillation, frequency of oscillation and the limits of the product of the amplifier gains for the above four cases. It may be observed from Table 5.2 that

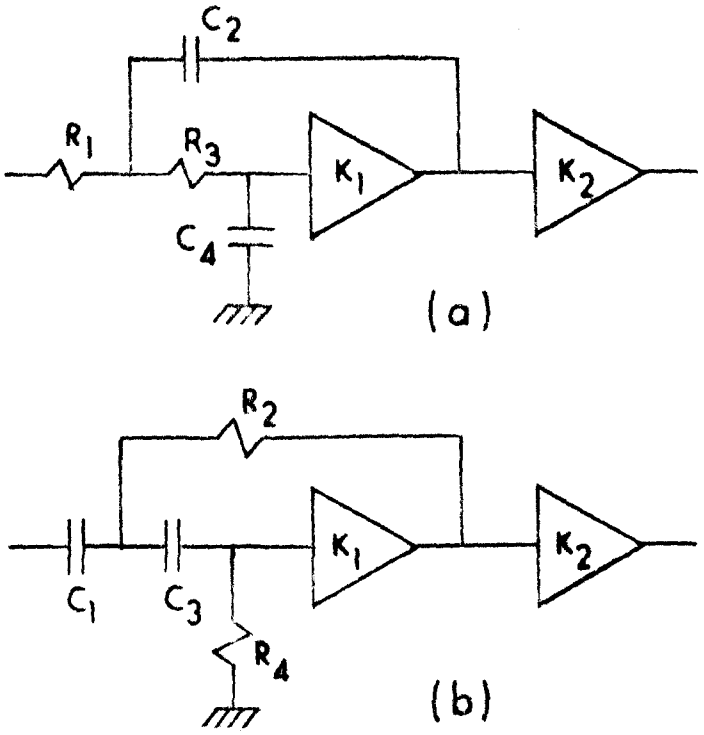

Fig.5.1 (a) (b) An active RC filter with a cascaded voltage amplifier stage

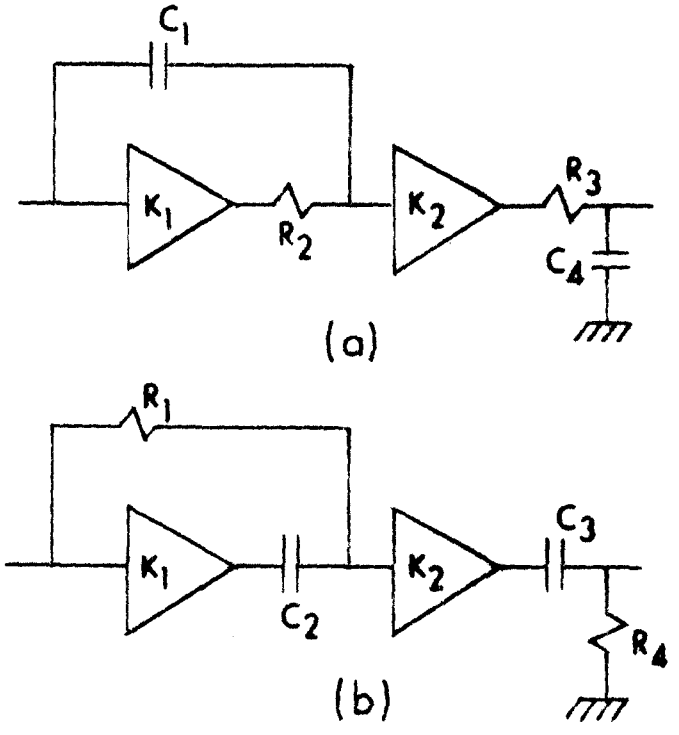

Fig.5.2 (a) (b) An active RC filter with a cascaded voltage amplifier stage

both negative and positive gains are permitted in the frequency setting amplifier. The limits of the tuning gain, gain conditions and normalized frequencies are tabulated in Table-5.3 for equal C's and R's.

TABLE-5.2

CONDITION, FREQUENCY AND GAIN LIMITS IN OSCILLATOR CIRCUITS

Figure Reference	Condition of Oscillation	ω_o	Limits of K_1K_2
5.1(a)	$K_1 = 1 + \frac{C_4}{C_2} + \frac{C_4R_3}{C_2R_1}$	$\left[\frac{1 - K_1K_2}{C_2C_4R_1R_3}\right]^{\frac{1}{2}}$	$-\infty < K_1K_2 < 1$
5.1(b)	$K_1 = 1 + \frac{R_2}{R_4} + \frac{C_1R_2}{C_3R_4}$	$\left[\frac{1}{C_1C_3R_2R_4(1-K_1K_2)}\right]^{\frac{1}{2}}$	$-\infty < K_1K_2 < 1$
5.2(a)	$K_2 = 1 + \frac{C_4R_3}{C_1R_2}$	$\left[\frac{1 - K_1K_2}{C_1C_4R_2R_3}\right]^{\frac{1}{2}}$	$-\infty < K_1K_2 < 1$
5.2(b)	$K_2 = 1 + \frac{C_2R_1}{C_3R_4}$	$\left[\frac{1}{C_2C_3R_1R_4(1-K_1K_2)}\right]^{\frac{1}{2}}$	$-\infty < K_1K_2 < 1$

TABLE-5.3

GAIN AND FREQUENCY LIMITS

Circuit shown in figure	Limits of K_i $(i = 1,2)$	Limits of K_j $(j = 1,2)$	$\omega_N = \frac{\omega_o}{\omega_d}$
5.1(a)	$-\infty \lesssim K_2 \lesssim \frac{1}{3}$	$K_1 = 3$	$\infty \gtrsim \omega_N \gtrsim 0$
5.1(b)	$-\infty \lesssim K_2 \lesssim \frac{1}{3}$	$K_1 = 3$	$0 \lesssim \omega_N \lesssim \infty$
5.2(a)	$-\infty \lesssim K_1 \lesssim \frac{1}{2}$	$K_2 = 2$	$\infty \gtrsim \omega_N \gtrsim 0$
5.2(b)	$-\infty \lesssim K_1 \lesssim \frac{1}{2}$	$K_2 = 2$	$0 \lesssim \omega_N \lesssim \infty$

It will be seen that the amplifier of gain K_2 in figures 5.2(a) and 5.2(b) is in fact the cascaded stage. Its position after the passive differentiator or the integrator increases its required value and the range of K_1.

5.4 STABILITY AND SENSITIVITY

It can be seen from the circuit configurations that all the circuits should have good operational stability. However, amplitude stabilization is controlled by the saturation characteristics of the amplifiers and it can be analysed with the help of the describing function technique to obtain stable limit cycle applying Loeb's criterion[12]. The analysis starts with the open loop transfer function T(s) of the loop shown in figure 5.3 where N(•) represents the single valued stabilizing saturation characteristic of the amplifier. For a stable sinusoidal oscillation $V = V_o \cos \omega_n t$ to exist in the closed loop system, the stability criterion, the oscillation conditions with the equation for evaluating the describing function[13]

$$D(V_o) = \frac{1}{\pi V_o} \int_0^{2\pi} N\,(V_o \cos x) \cos x \, dx \qquad (5.5)$$

are given respectively by

$$\frac{d\ I_m\ T(j\omega_n)}{d} \qquad \frac{dD\ (V_o)}{dV_o} \lessdot 0 \qquad (5.6)$$

$$I_m T\ (j\omega_n) = 0 \qquad (5.7)$$

and

$$1 + D(V_o)\ \mathrm{Re}\ T(j\omega_n) = 0 \qquad (5.8)$$

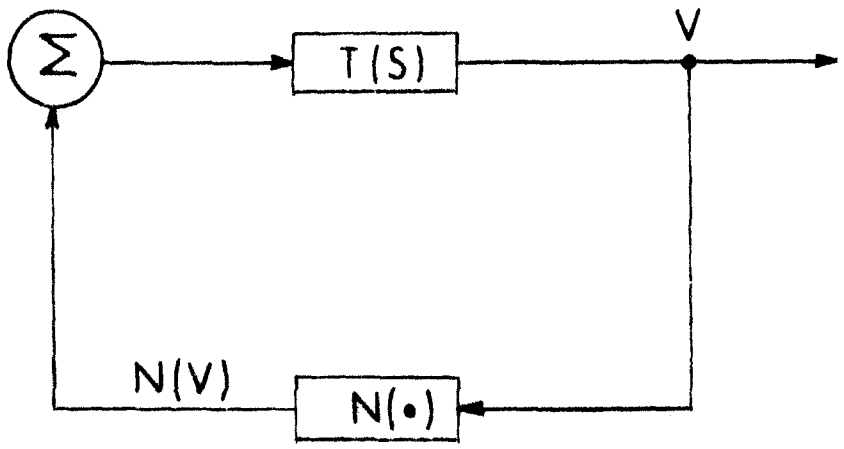

Fig.5.3 The representative autonomous system

where I_m and R_e stand for imaginary and real parts respectively.

Expressing T(s) as

$$T(s) = \frac{as^2 + bs + c}{\alpha s^2 + \beta s + \gamma} \tag{5.9}$$

one derives ω_n and $D(V_o)$ from equations (5.6), (5.7) and (5.8) as

$$\omega_n^2 = \frac{\gamma b - \beta c}{\alpha b - \beta a} \tag{5.10}$$

and

$$D(V_o) = -\frac{\beta}{b} \tag{5.11}$$

From equation (5.5), one derives

$$\frac{dD(V_o)}{dV_o} = \frac{1 + K_+ R_e T(j\omega_n)}{V_o R_e T(j\omega_n)} \tag{5.12}$$

where

$$K_+ = \frac{1}{\pi} \int_0^{2\pi} \frac{\partial_N}{\partial V} \cos x \, dx$$

and from equations (5.9) and (5.10), one gets

$$\frac{d\, I_m\, T(j\omega_n)}{d\omega} = \frac{2(a\beta - \alpha b)\omega_n^2}{(\gamma - \alpha\omega_n^2)^2 + \beta^2\omega_n^2} \tag{5.13}$$

Combining equations (5.5), (5.11) and (5.13), the criterion for stability of a biquadratic filter feedback oscillator is given by

$$\epsilon = \frac{2}{V_o}\left(K_+ + \frac{\beta}{b}\right) \frac{(a\beta - \alpha b)\omega_n^2}{(\gamma - \alpha\omega_n^2)^2 + \beta^2\omega_n^2} \ll 0 \tag{5.14}$$

Thus the value of ϵ for the different circuit configurations are given in Table-5.4.

TABLE-5.4

THE STABILITY CRITERION

Figure reference	ϵ
5.1(a)	0
5.1(b)	0
5.2(a)	$-(K_+ + 1)\frac{2\lambda}{CR}$
5.2(b)	$(K_+ + 1)\frac{2\lambda(2K_1 - 1)}{CR}$

Since

$$\lambda = \frac{2\omega_n^2}{V_o\left[(\gamma - \alpha\omega_n^2)^2 + \beta^2\omega_n^2\right]}$$

is always positive and K_+ is required to be positive always, the limit cycle stability criterion is satisfied for all the above four circuits. The suitability of this method for the generalized stability analysis for oscillators using saturation characteristics is further demonstrated by applying it into the circuit of figure 5.4, which although theoretically is quite amenable for use as single element-tuned sinewave oscillator, has in fact, stability incompatibility.

Working out condition (5.14) for this circuit one obtains

$$\epsilon = \frac{2\lambda}{CR}(K_+ + 1)$$

which is neither zero nor negative.

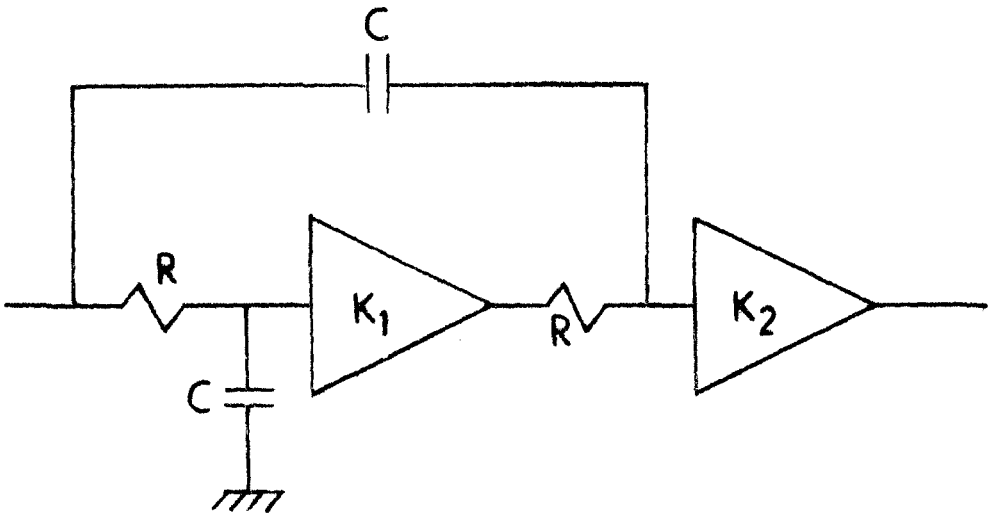

Fig. 5.4 An active RC filter for stability test

The frequency stability is likely to be affected by temperature variation. This can, however, be taken care of by proper choice of temperature co-efficients of resistors and capacitors used in the circuit, as is pointed out by Hribsek and Newcomb[14] following Moschytz[15]. In fact it is shown that if all capacitors and all resistors have the same temperature co-efficients, the relative change in frequency

$$\frac{\Delta \omega_o}{\omega_o} = -\left(\frac{\Delta R}{R} + \frac{\Delta C}{C}\right) \qquad (5.15)$$

is zero, if we choose

$$\frac{\Delta R}{R} = -\frac{\Delta C}{C} \qquad (5.16)$$

which is quite possible to realize in practice.

5.5 THE VCO'S AND THE EXPERIMENTAL RESULTS

For generation of voltage controlled oscillations, the frequency setting amplifiers are kept FET controlled where the FET is used as a voltage variable resistor. If R_F is the drain to source resistance of the FET and the gain-setting amplifier is used with a differential arrangement as shown in figure 5.5(a), gain K_i is given as

$$K_i = \frac{R_5 - \beta_o R_6 R_7 (V_p + V_{gs})}{R_5 + \beta_o R_5 R_6 (V_p + V_{gs})} \qquad (5.17a)$$

where V_p = FET pinch-off voltage, V_{gs} = applied gate to source voltage and β_o = a constant of the FET. For the amplifier providing the oscillation condition the general arrangement of the circuit

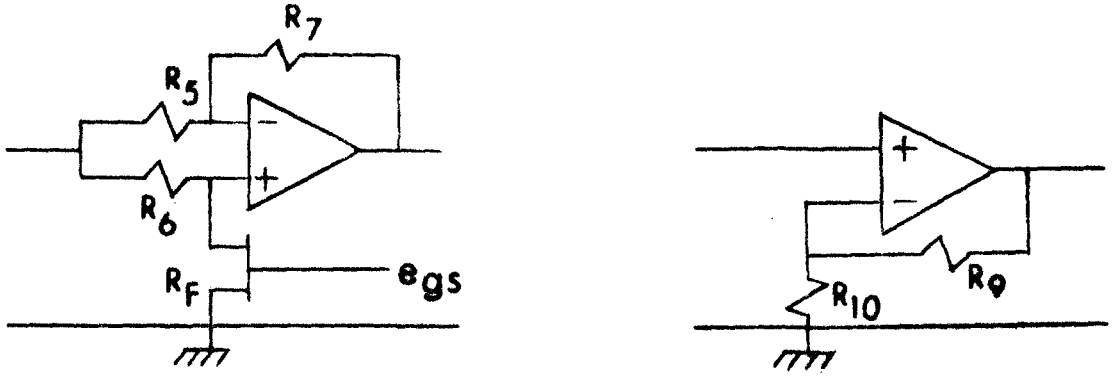

Fig. 5.5.(a) Amplifier stage with a FET and an operational amplifier. (b) Positive gain amplifier with an operational amplifier.

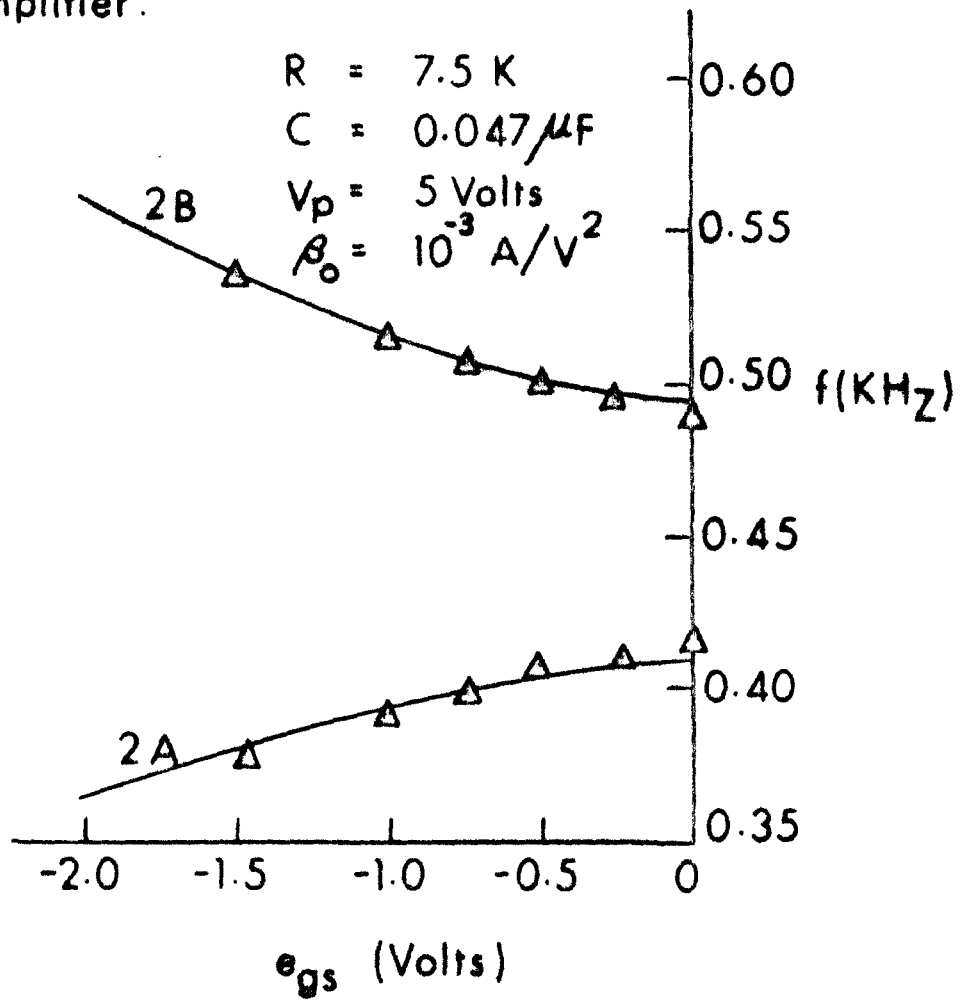

Fig. 5.6. Experimental results.

is shown in figure 5.5(b) where the gain K_j is calculated as

$$K_j = 1 + \frac{R_9}{R_{10}} \qquad (5.17b)$$

Results of the VCO's for Type-2 using amplifier circuits of figures 5.5(a) and 5.5(b) are shown in curves in figure 5.6. The triangles indicate the experimental values.

5.6 FREQUENCY LIMITING BY BANDWIDTH OF THE AMPLIFIERS

In the experimental set up operational amplifier μA741 has been used for designing the amplifiers. Its dominant pole design is accounted for, by writing the gain relation as

$$\frac{1}{A(s)} = \frac{s}{\omega_B} + \frac{1}{A_o} \qquad (5.18)$$

where ω_B represents the gain bandwidth.

The limitation this roll-off characteristic imposes on the high frequency operation can be discussed considering the individual amplifiers having finite gain K_i and K_j. Using equations (5.17) and (5.18) the effective gains for the circuits of figure 5.5(a) and 5.5(b) respectively are given as

$$K_i \text{ effective} \Big|_{A_o \to \infty} = \frac{\omega_B}{s(1 + \frac{R_7}{R_5}) + \omega_B} K_i \qquad (5.19)$$

and

$$K_j \text{ effective} \Big|_{A_o \to \infty} = \frac{s}{\omega_B} + K_j \qquad (5.20)$$

The highest frequency is thus limited by K_i more than by K_j.

5.7 CONCLUSION

Single resistive element-control sine-wave RC oscillators have been studied following a new approach of providing direct feed back in low/high/band pass filters. The design of the filters itself should be very carefully made so that the desired controllability can be achieved. The stability of oscillation has also been considered following Loeb's suggestions. This stability study is quite general and applicable to systems having lumped idealized active block like an operational amplifier. Often in practical applications fixed frequency sine wave oscillators with stability to temperature and supply voltage variation are necessary. Although operational amplifiers are inexpensive and easily available now, a cheaper and more readily available active device like a transistor appears to be a better choice for the design of such oscillators. A paired transistor block has in consequence been proposed to generate sine, harmonic and relaxation oscillations whose frequencies are however not necessarily fixed. For example a voltage controlled oscillator could be obtained in this group for application in measurement and telemetry systems. In the subsequent chapters these oscillators have been considered in details. In the next chapter emitter coupled differential pair is used to produce a high stability sinewave oscillator.

REFERENCES

1. Deboo,G.J. : 'Application of a gyrator type circuit to realize ungrounded inductors'; IEEE Trans. Circuit Theory, Vol. CT-14, No.1, pp.101-102, March 1967.

2. Yanagisawa,T. : 'Realization of lossless transistor gyrator'; Electron Lett., Vol.3, pp.167-168, April 1967.

3. Antoniou,A. : 'Gyrators using operational amplifiers'; Electron. Lett., Vol.3, pp.350-352, Aug. 1967.

4. Mitra,S.K. : 'Active Inductorless Filters'; New York : IEEE Press, 1971.

5. Heulsman,L.P.(Ed.) : 'Active Filters : Lumped, Distributed, Integrated, Digital and Parametric'; New York : McGraw-Hill, 1970.

*6. Tripathi,M.P., Roy,S.B. and Patranabis,D. : 'Some observations on single-element control sine-wave oscillators'; Int. J.Electron., Vol.43, No.5, pp.513-520, 1977.

7. Patranabis,D. and Sen,P.C. : 'A sine-wave oscillator' ; Int. J. Electron., Vol.29, No.5, pp.441-557, 1970.

8. Sidorowicz,R.S. : 'An abundance of sinusoidal RC oscillators'; Proc. IEE , Vol.119, No.3, pp.283-293,1972.

9. Sun,Y. : 'Generation of sinusoidal voltage (current) controlled oscillators for integrated circuits'; IEEE Trans. Circuit Theory, Vol.CT-19, No.2, pp.137-141, March 1972.

10. Holt,A.G.J., and Lee,M.R. : 'A class of RC oscillators' ; Proc.IEEE, Vol.55, pp.1119-1120, 1967.

11. Patranabis,D. : 'Sinusoidal oscillations in active RC filters'; Int.J.Electron, Vol.29, No.1, pp.93-99, 1970.

12. Murphy,G.J. : 'Basic Automatic Control Theory'; New York : Van Nostrand, 1966.

13. Gibson,J.E. : 'Nonlinear Automatic Control'; New York : McGraw-Hill, 1963.

14. Hribsek,M. and Newcomb,R.W. : 'VCO controlled by one variable resistor'; IEEE Trans. Circuits and systems, Vol.CAS-23, No.3, pp.166-169, March 1976.

15. Moschytz,G.S. : 'Gain-sensitivity product — a figure of merit for hybrid-integrated filters using operational amplifier'; IEEE J. Solid State Circuits, Vol.SC-6, No.3, pp.103-110, June 1971.

---

* Chapter-V is based mainly on this publication.

CHAPTER-VI

SINUSOIDAL OSCILLATION WITH AN EMITTER COUPLED DIFFERENTIAL PAIR

6.1 INTRODUCTION

In the previous chapter methods to obtain sinusoidal oscillations with single element control facility using two operational amplifiers (OA) have been described. OA's are available as chips making the commercial setting of the oscillators easy. However since every active RC circuits can now be fabricated as a whole in the chip form, a simpler oscillator circuit involving less number of transistors and other components would be economic. It is intended to present an RC oscillator circuit which is both simple and economic. In addition, a type of emitter coupling proposed here introduces an inherent tendency of self-compensation against changes of active circuit parameters and the frequency remains practically independent of temperature change even though germanium transistors are used.

Attempts to generate sinusoidal oscillations in conventional multivibrator circuit are thwarted to a large extend due to its inherently low selectivity, because of the use of load and interstage coupling elements as the frequency selecting part. This limitation can be avoided by (1) increasing the gain margin between the relaxation and the harmonic mode of operation by determining the optimum relationship of the load and coupling element and (2) eliminating the ppssibility of having real and positive roots of the characteristic equation of this oscillator using an amplitude defining mechanism with a differential circuit

arrangement. An emitter coupled differential stage proposed here is shown to accomplish these[1*].

The proposed circuit is analysed using the hybrid equivalent model of the transistor and other associated parameters. The rigour is followed till the stage it is necessary and based on the analysis, circuit components are selected for optimum operation. Condition and frequency of oscillation are also obtained through this analysis.

6.2 CIRCUIT DESCRIPTION

The emitter coupled differential amplifier with its output fed back to the input through a RC network is shown in figure 6.1. Circuits of this type are known to oscillate in relaxation mode, because of large system gain[2]. It is shown here that, it is possible to generate sinusoidal oscillation in such a system by maintaining near unity system gain by adjustment of the load and interstage coupling network.

The transistors Q_1 and Q_2 in figure 6.1 form a composite (CC-CB) pair having a current gain of $h_{fc}\, h_{fb}$[3]. Since such a pair does not introduce any phase shift, positive feed back is very easily derived by coupling the output of transistor Q_2 to the input of the transistor Q_1 with a capacitor C. The symmetrical limiting characteristic of the emitter coupled pair limits the oscillation amplitude and no other external limiter is necessary. The degenerative feed back introduced by the common emitter resistor R_E stabilizes the operating point and the gain of the amplifier against supply voltage and ambient temperature variation, thereby reducing the frequency drift of the oscillator.

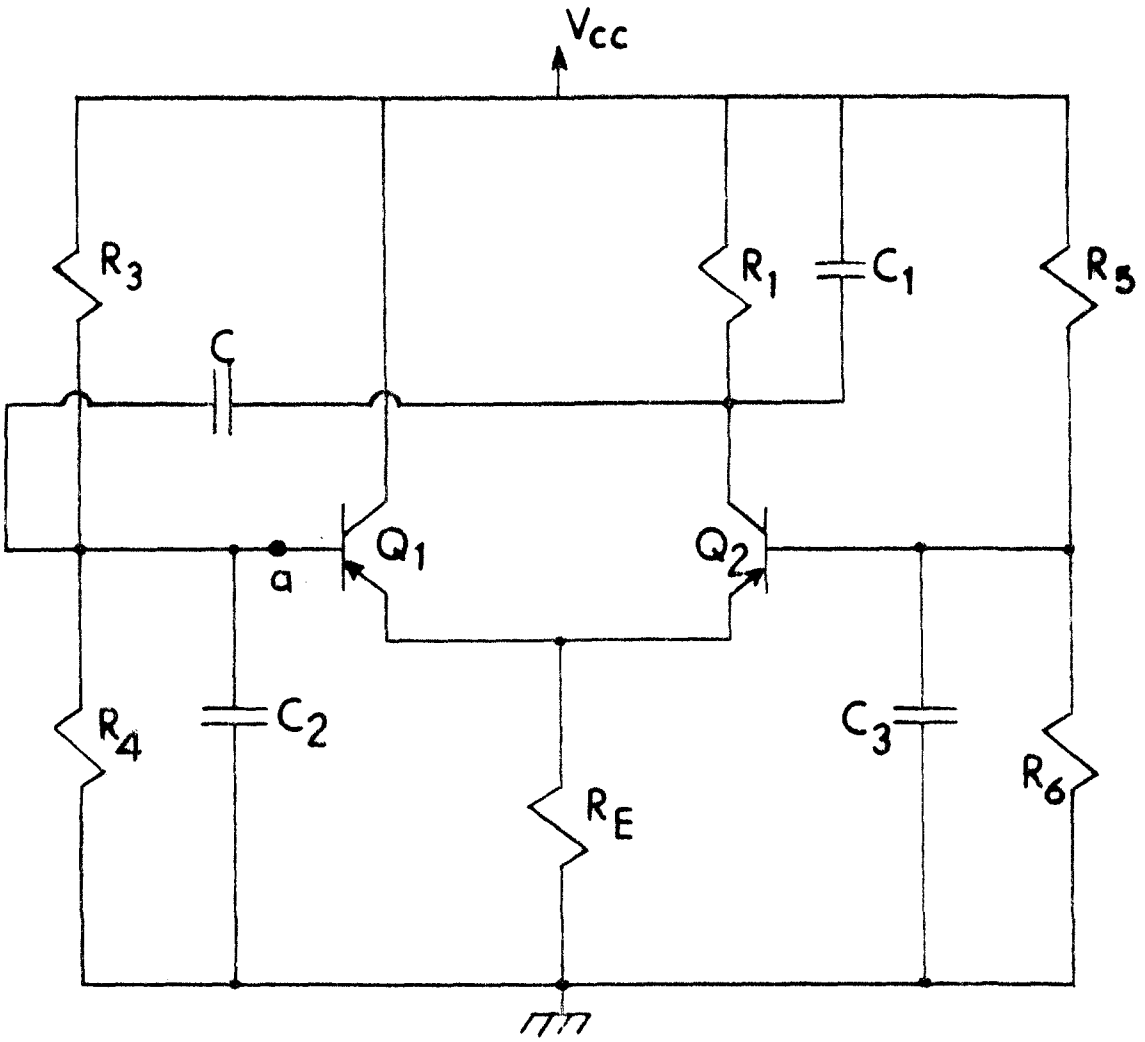

Fig. 6·1 Emitter coupled differential amplifier with the RC feedback network

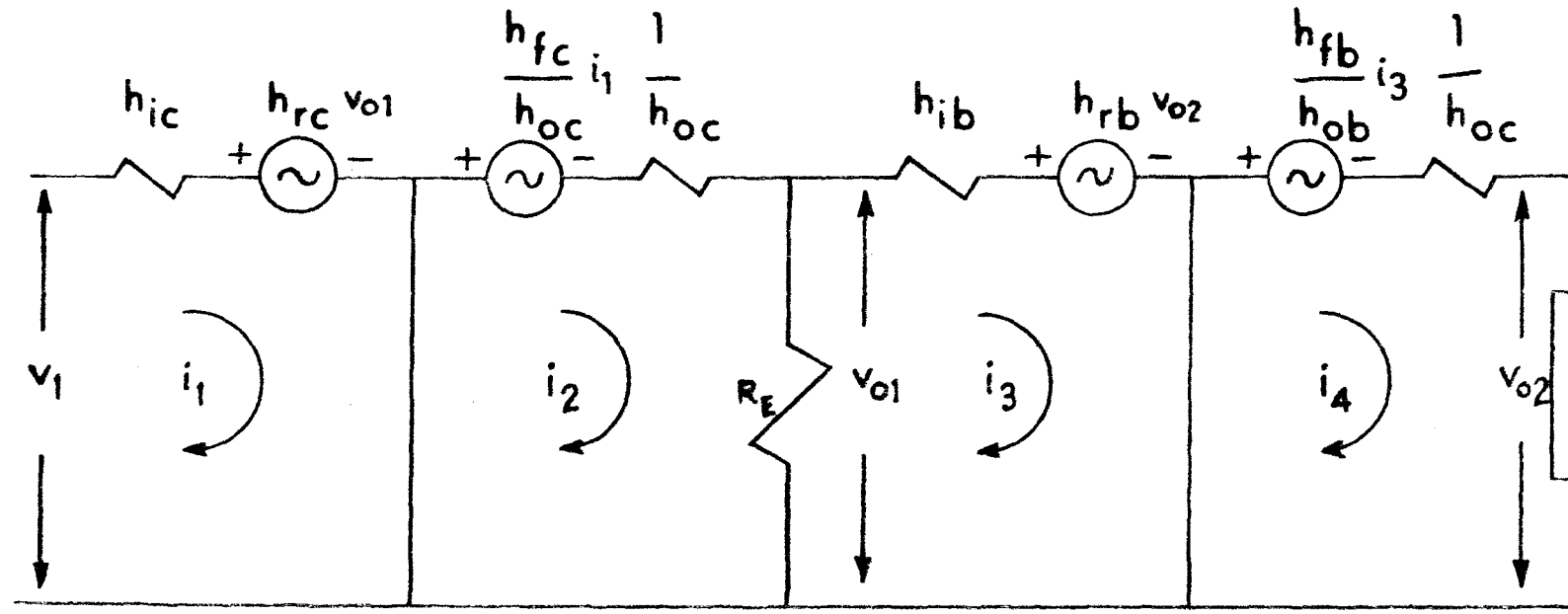

Fig.6.2. The modified hybrid equivalent circuit of Fig.6.1

The frequency determining elements are the collector load resistance R_1 of transistor Q_2 ; R_2 the parallel combination of R_3 and R_4 the biasing resistors of the transistor Q_1; the coupling capacitor C and the two shunt capacitors C_1 and C_2 which may be either lumped capacitors or the output and input capacitance of the amplifier. A large by-pass capacitor is connected between the base of Q_2 and ground in order to effectively ground the base of Q_2 particularly if the biaising resistors R_5 and R_6 are large.

6.3 CONDITION OF OSCILLATION AND FREQUENCY

The feed back loop is assumed to be opened at the point 'a' in figure 6.1 and a modified hybrid equivalent circuit of figure 6.1 is shown in figure 6.2 where the collector load of Q_2 is considered to be a complex load Z_L comprising of R_1, R_2, C, C_1 and C_2.

Let v_{02} be the output voltage across the complex load Z_L at the collector of Q_2 due to an applied input voltage v_1 at the base of Q_1 as shown in figure 6.2.

From the loop equations i_4 is obtained [see appendix 6.1, equation (A-6.2)] as

$$i_4 = \frac{v_1 \, h_{fb} \, h_{fc}}{\left\{h_{ib}\left(\Delta^{hc} + \frac{h_{ic}}{R_E}\right) + h_{ic}\right\} + \left\{\Delta^{hb}\left(\Delta^{hc} + \frac{h_{ic}}{R_E}\right) + h_{ic}\, h_{ob}\right\} Z_L} \qquad (6.1)$$

where [see appendix 6.1, equation (A-6.4)]

$$Z_L = \frac{\frac{1}{C} + j\omega R_2 \left(1 + \frac{C_2}{C}\right)}{\frac{1}{CR_1} - \omega^2 R_2\left(C_1 + C_2 + \frac{C_1C_2}{C}\right) + j\omega\left\{\frac{R_2}{R_1}\left(1 + \frac{C_2}{C}\right) + \left(1 + \frac{C_1}{C}\right)\right\}} \tag{6.2a}$$

and

$$\Delta^h = h_i h_o - h_f h_r \tag{6.2b}$$

The current i_6 flowing through Z_3 [see appendix 6.1, figure A-6.2; and equation (A-6.5)] provides the feed back voltage e_o at the base of transistor Q_1 when the loop is closed. Thus [see appendix 6.1, equation (A-6.5)]

$$i_6 = i_4 \frac{j\omega(1 + j\omega C_2 R_2)}{\frac{1}{CR_1} - \omega^2 R_2\left(C_1 + C_2 + \frac{C_1C_2}{C}\right) + j\omega\left\{\frac{R_2}{R_1}\left(1 + \frac{C_2}{C}\right) + \left(1 + \frac{C_1}{C}\right)\right\}} \tag{6.3}$$

and hence

$$e_o = i_6 \frac{R_2}{1 + j\omega C_2 R_2} \tag{6.4}$$

Combining equations (6.1) through (6.4) and writing $n_1 = \frac{C_1}{C}$; $n_2 = \frac{C_2}{C}$ and $m = \frac{R_2}{R_1}$ one obtains

$$e_o = \frac{j\omega h_{fb} h_{fc} R_2 v_1}{j\omega\left[\left\{m(1+n_2) + (1+n_1)\right\}\left\{h_{ib}\left(\Delta^{hc} + \frac{h_{ic}}{R_E}\right) + h_{ic}\right\} + R_2(1+n_2)\right.}$$

$$\left.\frac{}{\left\{\Delta^{hb}\left(\Delta^{hc} + \frac{h_{ic}}{R_E}\right) + h_{ic}h_{ob}\right\}\right] \frac{1}{C}\left\{\Delta^{hb}\left(\Delta^{hc} + \frac{h_{ic}}{R_E}\right) + h_{ic}h_{ob}\right\} +}$$

$$\frac{}{\left\{\frac{1}{CR_1} - \omega^2 R_2\left(C_1 + C_2 + \frac{C_1C_2}{C}\right)\right\}\left\{h_{ib}\left(\Delta^{hc} + \frac{h_{ic}}{R_E}\right) + h_{ic}\right\}} \tag{6.5}$$

Since for oscillation e_o must be equal to v_1, the condition of maintenance of oscillation is obtained from equation (6.5) as

$$\frac{h_{fb}h_{fc}}{h_{ib}\left(\Delta^{hc} + \frac{h_{ic}}{R_E}\right) + h_{ic}} + (1+n_2)\frac{h_{fb}\,h_{rb}}{h_{ib} + \frac{h_{ic}}{\Delta^{hc} + \frac{h_{ic}}{R_E}}} - (1+n_2)h_{ob}$$

$$= \frac{1}{R_2}\left\{m(1+n_2) + (1+n_1)\right\} \qquad (6.6)$$

and corresponding frequency of oscillation as

$$f = \frac{1}{2\pi C}\sqrt{\frac{1}{R_1R_2(n_1+n_2+n_1n_2)}\left[1 + R_1\left\{h_{ob} - \frac{h_{fb}h_{rb}}{h_{ib} + \frac{h_{ic}}{\Delta^{hc} + \frac{h_{ic}}{R_E}}}\right\}\right]} \qquad (6.7)$$

Writing $n = n_1+n_2+n_1n_2$ and $R_2 = mR_1 = mR$ equation (6.7) simplifies to

$$f = \frac{1}{2\pi CR\sqrt{mn}}\left[1 + R_1\left\{h_{ob} - \frac{h_{fb}h_{rb}}{h_{ib} + \frac{h_{ic}}{\Delta^{hc} + \frac{h_{ic}}{R_E}}}\right\}\right]^{\frac{1}{2}} \qquad (6.8)$$

6.4 CHOICE OF THE CIRCUIT ELEMENTS

6.4.1 CHOICE OF THE TRANSISTORS

The transistors should have high cut-off frequency and the common collector current gain $h_{fc}(\approx \beta)$ should be sufficiently large to satisfy the gain requirement with low value of R_1. The

two transistors should be matched[4], have low leakage and preferably be in the same header so that temperature variation affect both equally and full advantage of large common mode rejection properties of emitter coupled differential pair (ECDP) is easily realized. However to show the inherent stabilizing property of ECDP configuration, two independent but matched pair germanium transistors (OC 45) were used.

6.4.2 CHOICE OF FREQUENCY DETERMINING ELEMENTS

The choice of components for the oscillator circuit is primarily guided by the condition of maintenance as given by equation (6.6). The second and third term in the right hand side of this equation may be shown to have negligible contribution for almost all the present day small signal transistor even though n_2 may be quite large, such that equation (6.6) simplifies to

$$\left[\frac{h_{fb}h_{fc}}{h_{ib}\left(\Delta^{hc} + \frac{h_{ic}}{R_E}\right) + h_{ic}}\right] R_2 = m\,(1+n_2) + (1+n_1) \qquad (6.10)$$

The capacitors C_1 and C_2 act as harmonic filtering elements and C is the coupling element. For large harmonic rejection the capacitors C_1 and C_2 should be much larger than C i.e. n_1 and n_2 should be much larger than unity. For convenience the ratio $\frac{R_1}{R_2} = m$ is chosen to be unity and $n_1 = n_2 \gg 1$, the equation (6.10) further reduces to

$$\frac{h_{fb}h_{fc}}{h_{ib}\left(\Delta^{hc} + \frac{h_{ic}}{R_E}\right) + h_{ic}}\, mR_1 = n_1 + n_2 \qquad (6.11)$$

Thus R_1 may be calculated from equation (6.11) by assuming reasonable values of n_1 and n_2. The value R_2 is then easily obtained from the condition m = 1.

The value of the capacitor C may be obtained from the desired frequency of oscillation (equation 6.7). The values of C_1 and C_2 are then calculated from the assumed values of n_1 and n_2.

6.4.3 CHOICE OF COMMON EMITTER RESISTOR

A high common mode rejection ratio in the differential pair is ascertained when R_E is chosen following[4]

$$R_E \gg h_{ib} + R_g (1 + h_{fb}) \qquad (6.12)$$

where R_g is the common-mode signal generator impedance. It must be remembered that R_E should also be made variable to obtain proper biasing level as the biaising chain resistors cannot be changed from the chosen value for a given m.

6.4.4 CHOICE OF OTHER CIRCUIT COMPONENTS

The biaising resistors R_5 and R_6 for the transistor Q_2 are chosen to be equal to R_3 and R_4 for making the two stages electrically almost identical under quiescent operating condition.

A capacitor C_3 is connected in order to effectively ground the base of the transistor Q_2 under oscillatory condition. The value of C_3 is chosen such that the reactance of C_3 at the oscillation frequency is negligibly small in comparison to the effective resistance of the biasing chain.

6.5 THE EXPERIMENTAL CIRCUIT AND RESULTS

The frequency determining elements were chosen assuming $n_1 = 1$ and $m = 1$. The capacitor C_2 was omitted in order to avoid the possibility of operating point shift due to d.c. voltage build-up on C_2 through a rectifying circuit formed by the base-emitter diode of the transistor Q_1, C_2 and R_2. However C_2 cannot be made zero due to the input and stray capacitance. Thus $n_2 \ll 1$ and may be assumed to be zero for low frequency oscillator circuits. Thus the condition of maintenance of oscillation given by equation (6.10) and frequency of oscillation given by equation (6.7) reduces to

$$\frac{h_{fb}h_{fc}}{h_{ib}\left(\Delta^{hc} + \frac{h_{ic}}{R_E}\right) + h_{ic}} R_1 = 3 \qquad (6.13)$$

and

$$f = \frac{1}{2\pi CR_1\sqrt{mn_1}} \left[1+R_1\left\{h_{ob} - \frac{h_{fb}h_{rb}}{h_{ib} + \frac{h_{ic}}{\Delta^{hc} + \frac{h_{ic}}{R_E}}}\right\}\right]^{\frac{1}{2}} \qquad (6.14)$$

Based upon the above assumptions and analysis, an oscillator was set-up with a matched pair of OC 45 transistors. The passive parameter values chosen were

$R_1 = 190$ ohms; $R_3 = R_5 = 680$ ohms, $R_4 = R_6 = 250$ ohms

$R_2 = R_3 \parallel R_4 = 184$ ohms

$C = 1.05\,\mu F$; $C_1 = 1.02\,\mu F$; C_2 is negligible

R_E = 400 ohms; C_3 = 10μF, and V_{CC} = - 4.5 volts. The calculated and measured frequency are given in Table-6.1

TABLE-6.1

FREQUENCY OF OSCILLATION

Calculated Frequency Hz	Experimental Frequency Hz	Measured Distortion dB
820	802	- 35

6.6 CONCLUSION

A comprehensive linear analysis of an oscillator circuit with an emitter coupled differential pair of transistors has been presented in this chapter. It has been demonstrated that by optimising the load and coupling element and introducing an amplitude defining mechanism of emitter coupling, generation of temperature stable sinusoidal oscillation of good wave form purity is possible. Due to the high common mode rejection characteristics and inherent stabilizing property of an ECDP transistor amplifier, the effect of ambient temperature variation on oscillation frequency is minimised. Experimental study has shown about 0.1 percent frequency variation for an ambient temperature change from 24°C to 55°C without the use of any thermal stabilizing element in the circuit; indicating a very low dependance of oscillation frequency on the active circuit parameters - a criteria not very common is simple RC oscillator circuits.

It is well known that the amplitude stabilizing mechanism cannot be explained by linear analysis and for this circuit the oscillation amplitude stabilization is due to the antisymmetric limiting characteristic of the emitter coupled pair. Moreover since the circuit is basically like that of an emitter coupled multivibrator but by optimised load and coupling element it is used to generate sinusoidal oscillation, it would be of interest to study the circuit taking into account the non-linear amplitude defining mechanism and possibility of generation of harmonic to relaxation mode of oscillation. This has been taken up in the next chapter with the view to predict the behaviour and adjust the mode of operation in the desired range and/or zone.

APPENDIX-6.1

From the figure 6.2 the four loop equations may be written as

$$\left.\begin{aligned} v_1 &= i_1 h_{ic} + i_2 R_E h_{rc} - i_3 R_E h_{rc} + i_4 . 0 \\ 0 &= i_1 \frac{h_{fc}}{h_{oc}} + i_2 \left(R_E + \frac{1}{h_{oc}}\right) - i_3 R_E + i_4 . 0 \\ 0 &= i_1 . 0 - i_2 R_E + i_3 (h_{ib} + R_E) + i_4 Z_L h_{rb} \\ 0 &= i_1 . 0 + i_2 . 0 + i_3 \frac{h_{fb}}{h_{ob}} + i_4 \left(Z_L + \frac{1}{h_{ob}}\right) \end{aligned}\right\} \quad \text{(A-6.1)}$$

where Z_L is the complex load seen by the transistor Q_2.

From equation (A-6.1) the fourth loop current i_4 is easily evaluated as

$$i_4 = \frac{v_1 h_{fb} h_{fc}}{\left\{h_{ib}\left(\Delta^{hc} + \frac{h_{ic}}{R_E}\right) + h_{ic}\right\} + \left\{\Delta^{hb}\left(\Delta^{hc} + \frac{h_{ic}}{R_E}\right) + h_{ic} h_{ob}\right\} Z_L} \quad \text{(A-6.2)}$$

The complex load Z_L comprises of the frequency determining network as shown in figure A-6.1.

$$\text{where} \quad Z_1 = \frac{R_1}{1 + j\omega C_1 R_1} \quad \text{(A6.3a)}$$

$$Z_2 = \frac{1}{j\omega C} \quad \text{(A-6.3b)}$$

$$Z_3 = \frac{R_2}{1 + j\omega C_2 R_2}$$

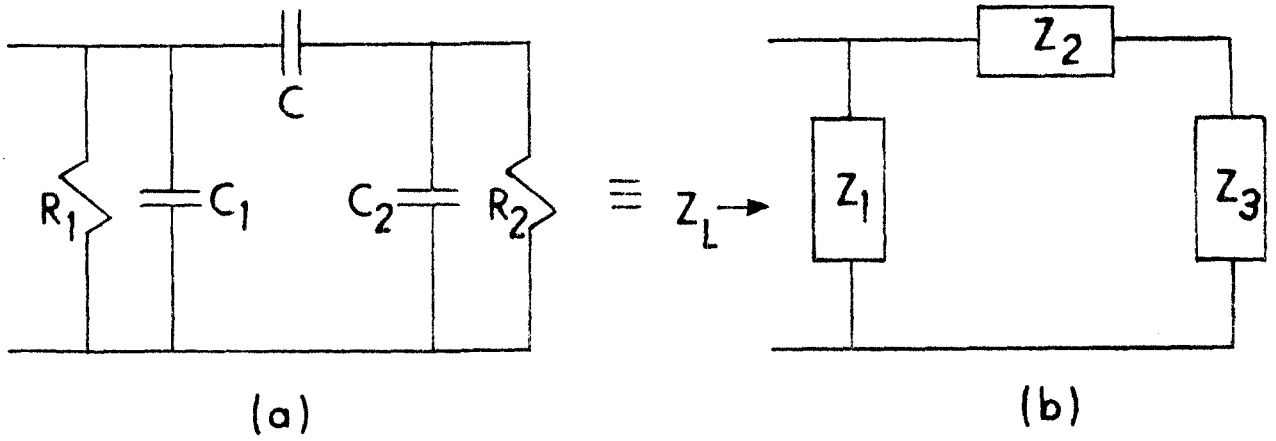

Fig. A-6.1 The complex load Z_L

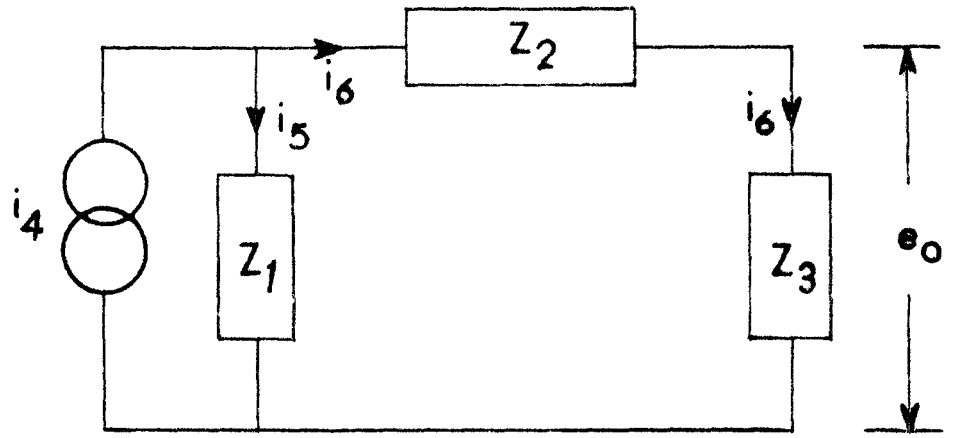

Fig. A-6.2 Currents in the branches of the complex load

$$Z_L = \frac{Z_1(Z_2 + Z_3)}{Z_1 + Z_2 + Z_3}$$

Therefore

$$Z_L = \frac{\frac{1}{C} + j\omega R_2 \left(1 + \frac{C_2}{C}\right)}{\frac{1}{CR_1} - \omega^2 R_2\left(C_1 + C_2 + \frac{C_1 C_2}{C}\right) + j\omega\left\{\frac{R_2}{R_1}\left(1 + \frac{C_2}{C}\right) + \left(1 + \frac{C_1}{C}\right)\right\}} \quad \text{(A-6.4)}$$

The current i_4 feeds the complex load as shown in figure A-6.2 and divides into two parts i_5 and i_6 as shown. Thus current i_6 is evaluated as

$$i_6 = i_4 \frac{Z_1}{Z_1 + Z_2 + Z_3}$$

Therefore

$$i_6 = i_4 \frac{j\omega(1 + j\omega C_2 R_2)}{\left\{\frac{1}{CR_1} - \omega^2 R_2\left(C_1 + C_2 + \frac{C_1 C_2}{C}\right)\right\} + j\omega\left\{\frac{R_2}{R_1}\left(1 + \frac{C_2}{C}\right) + \left(1 + \frac{C_1}{C}\right)\right\}}$$

(A-6.5)

REFERENCES

*1. Kundu,P. and Roy,S.B. : 'A temperature-stable RC transistor oscillator'; Proc. IEEE, Vol.57, No.3, pp.356-357, March 1969.

2. Littauer,R. : 'Pulse Electronics'; New York : McGraw-Hill, 1965, p.427.

3. Cattermole,K.W. : 'Transistor Circuits'; London : Heywood, 1959, pp.98-99.

4. Cutler,P. : 'Semiconductor Circuit Analysis'; New York : McGraw-Hill, 1964, pp.365-379.

---

* Chapter-VI is based mainly on this publication

CHAPTER-VII

NON-LINEAR OSCILLATIONS USING ANTISYMMETRIC TRANSFER CHARACTERISTICS OF A DIFFERENTIAL PAIR

7.1 INTRODUCTION

Oscillations in a regenerative circuit may be either in harmonic or relaxation mode, generating sinusoidal or non-sinusoidal waveforms respectively. The previous chapter has been devoted on a practical temperature and supply voltage insensitive sinewave oscillator using the self saturating characteristics of a transistor differential pair. The same circuit can be used to generate quasilinear and relaxation oscillations. Van der Pol[1] predicted that it is impracticable to obtain stable harmonic oscillation as well as relaxation oscillation from the same system as relaxation mode of operation is characterised by high degree of non-linearity and low order of selectivity and as such has requirement contrary to harmonic mode operation. Accordingly oscillators were partitioned into two distinct classes and treated separately. This precluded the possibility of having an unified analysis based on which the performance of a regenerative system could be predicted over the entire range from harmonic to relaxation mode and the parameters identified for adjustment for a particular mode of operation and wave form generation.

Adjustment from relaxation mode to stable harmonic mode of oscillation is, however, possible with a low-gain margin if proper modification is introduced with the optimized values of load and coupling elements together with the non-linearity of the antisymmetric transfer characteristic of a differential pair whereby the

output approaches the limiting value asymptotically. The non-linearity of the self-saturating characteristics is assumed to be a transcendental function of hyperbolic tangent type. An inverse tangent approximation of the amplifier function[2] was earlier proposed with limited success in predicting the practical oscillation waveform when operated at large amplitude. The anti-symmetric transfer characteristics introduces an instantaneous amplitude defining mechanism with reduced second harmonic distortion and makes the system self-compensating as regards parameter variation due to the change in ambient temperature and supply voltage variation[3], and much less critical for continuous control of operation from highly relaxed to harmonic mode. Realization of such an oscillator is interesting as it has a wide scope of control of its frequency and waveform making it useful as a test signal generator in various areas.

In this Chapter a comprehensive analytical approach to such a regenerative system with a particular type of non-linearity of the active circuit is presented[4*]. Through this approach its performance can be predicted over the entire range of operation and its operation can be controlled in a desired manner.

7.2 THE SYSTEM EQUATION

Instead of single parameter non-linear equation of van der Pol a more generalised equation of a non-linear oscillator has been derived here. This equation accounts more closely for the sharp rise and fall of the output voltage having a semi-exponential decay in between the relaxation, which cannot be obtained by the

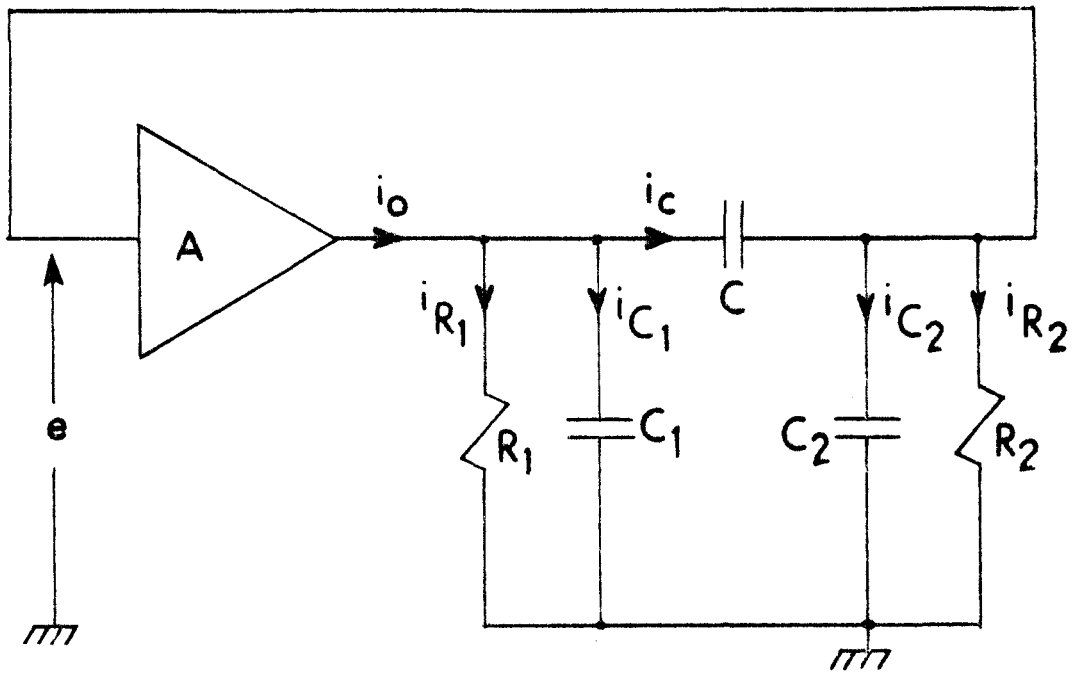

Fig. 7.1 Schematic of the oscillator

solution of the van der Pol equation in which the decay shows a convex nature. For a wide range of operation the non-linearity no longer remains restricted to a cubic function and probably this gives rise to the anomaly. It is now possible to suggest how the relative values of the two parameters may be changed to adjust the oscillation in a particular mode and generate a specific type of waveform.

Consider the oscillator shown in figure 7.1. The circuit equation is

$$\frac{1}{R_1}\left\{e + \frac{1}{C}\int\left(\frac{e}{R_2} + C_2\frac{de}{dt}\right)dt\right\} + C_1\left\{\frac{de}{dt} + \frac{1}{C}\left(\frac{e}{R_2} + C_2\frac{de}{dt}\right)\right\} + \frac{e}{R_2} + C_2\frac{de}{dt} = i_o \qquad (7.1)$$

Since the non-linearity of the self-saturating characteristic of the amplifier is utilized, the output current i_o will be a non-linear function of the input voltage e. Writing

$$i_o = a \tanh (be) \qquad (7.2)$$

as assumed and substituting equation (7.2) in equation (7.1) and differentiating equation (7.1) with respect to time and with the following substitutions :

(a) $R_2 = mR_1 = mR$

(b) $C_1 = n_1C$

(c) $C_2 = n_2C$

$$\left.\begin{aligned} &(d)\quad n = n_1 + n_2 + n_1 n_2 \\ &(e)\quad G = \frac{1}{mR}\,(1 + m + n_1 + mn_2) \\ &(f)\quad \omega_o^2 = \frac{1}{mnC^2R^2} \end{aligned}\right\} \qquad (7.3).$$

equation (7.1) reduces to

$$\frac{1}{\omega_o^2}\,\frac{d^2e}{dt^2} + (G - ab\,\mathrm{sech}^2 be)\,\frac{1}{\omega_o^2\,nC}\,\frac{de}{dt} + e = 0 \qquad (7.4)$$

Using the normalized parameter $\tau = \omega_o t$ equation (7.4) changes to

$$\frac{d^2e}{d\tau^2} - (ab - G)\,R\sqrt{\frac{m}{n}}\,\left(1 - \frac{ab}{ab - G}\,\tanh^2 be\right)\frac{de}{d\tau} + e = 0 \qquad (7.5)$$

The two parameters ϵ and β are defined as

$$\epsilon = (ab - G)\,R\sqrt{\frac{m}{n}} \qquad (7.6a)$$

$$\beta = \frac{ab}{ab - G} \qquad (7.6b)$$

Normalizing the parameter $e = \frac{V}{b}$, equation (7.5) now leads to the generalized expression of the non-linear differential equation for the regenerative system as

$$\frac{d^2V}{d\tau^2} - \epsilon\,(1 - \beta\tanh^2 V)\,\frac{dV}{d\tau} + V = 0 \qquad (7.7)$$

Since equation (7.7) is a trancendental equation, a closed form solution is not possible, except for the sinusoidal case when

$\epsilon = 0$. The numerical solution of the equation for non-sinusoidal wave is obtained with the help of a computer for different values of ϵ and β.

7.3 LIMITS OF PARAMETER VALUES

The parameters involved in constituting ϵ and β are R, m, n, G and ab, of which R, m, n and G are obtained from the passive parameter values and the factor ab is the slope of the normalized non-linear self-saturating transfer characteristics at the origin. Any values of the above parameters are not permissible and therefore it is necessary to set the limits of ϵ and β values. It can be seen from the following sections that ϵ and β cannot take-up any arbitrary value but must bear a relationship amongst themselves.

7.3.1 RATIO OF THE RESISTANCE m

Ideally $0 < m < \infty$, but for least component spread and brevity, m is assumed unity. Hence from equation (7.3a)

$$R_1 = R_2 = R \tag{7.8}$$

7.3.2 RATIO OF THE CAPACITORS n_1 and n_2

Parameters n_1 and n_2 may have any positive value. It is evident from equation (7.3d) that n will have different values for various choices of n_1 and n_2.

It can be easily shown that

$$n_{max} = n_1 (2 + n_1) \text{ when } n_1 = n_2 \tag{7.9a}$$

and

$$\left.\begin{aligned} n_{min} &= n_1 \quad \text{when } n_2 = 0 \\ &= n_2 \quad \text{when } n_1 = 0 \end{aligned}\right\} \tag{7.9b}$$

Rigorous analysis do not permit either n_1 or n_2 to take up a zero value as C_1 or C_2 can never be zero, because even if lumped capacitors are absent the output, input and stray capacitances will contribute to C_1 and C_2, even though n_1 and n_2 may be very small.

For simplicity n_2 has been assumed zero whenever necessary and a finite positive value has been assigned to n_1. This could also be reversed without affecting the results so long as m is assumed unity [cf. equations (7.3d) and (7.3e)].

7.3.3 THE CIRCUIT CONDUCTANCE G

From equations (7.3e) and (7.8)

The parameter G is defined as

$$G = \frac{1}{R}(2 + n_1 + n_2) \tag{7.10a}$$

or

$$n_1 + n_2 = GR - 2 \tag{7.10b}$$

Thus for $n_1 + n_2$ = constant, G can have only one value larger than $\frac{2}{R}$ as $n_1 + n_2 > 0$.

For $n_1 + n_2$ = constant, m = 1, conductance parameter G is also held constant. Accordingly the limits for β and ϵ are evaluated holding this constant.

7.3.4 THE PARAMETER β

From equation (7.6a)

$$\beta = \frac{ab}{ab - G} \tag{7.11}$$

where ab is the slope of the antisymmetric self-saturating characteristics at the origin, this is constant for a particular operating condition.

Under the assumed conditions it has been shown that G can have only one value, hence β will also have only one value.

7.3.5 THE PARAMETER ϵ

From equations (7.6a) and (7.8)

$$\epsilon = (ab - G)\, R\sqrt{\frac{1}{n}} \tag{7.12}$$

Under the assumed conditions the value of ϵ will only vary with n and lie within a range ϵ_{max} and ϵ_{min} dependent upon n_{min} and n_{max} respectively. Combining equations (7.11) and (7.12) the maximum and minimum values of ϵ are given by

$$\epsilon_{max} = \frac{abR}{\beta}\sqrt{\frac{1}{n_{min}}} \tag{7.13a}$$

$$\epsilon_{min} = \frac{abR}{\beta}\sqrt{\frac{1}{n_{max}}} \tag{7.13b}$$

From the expression of ϵ it is seen that there is another constraint on the value of G. The value of G cannot be more than ab, in which case ϵ would be negative.

The parameters ϵ and β are quite interlinked. However, the effect of increasing ϵ is to increase distortion or harmonic contents of the wave and the effect of increase in β has a more pronounced effect on amplitude. This is well corroborated by computer solution.

7.3.6 EFFECT OF CONTROL OF ϵ and/or β

Since a two-parameter equation has been derived for the oscillator system, it may be of interest to note the effect of

(a) Changing ϵ keeping β constant,

(b) Changing β keeping ϵ constant,

and the conditions that are required to be met for such cases.

The first case has already been covered in subsection 7.3.5.

For the second case, from equation (7.13) one may write

$$\beta\sqrt{n} = \frac{K}{\epsilon} = \text{constant}, \text{ where } K = abR \qquad (7.14)$$

Since both β and n are dependent on n_1 and n_2 the range of values of these two quantities are to be found for which the product $\epsilon\beta\sqrt{n}$ will remain constant and equal to K. From equations (7.10) and (7.11)

$$\beta = \frac{abR}{(abR - 2)(n_1 + n_2)} \qquad (7.15)$$

The maximum and minimum values of β are therefore obtained by varying n_1 and n_2 as

$$\beta_{max} = \frac{abR}{(abR - 2) - n_1} \qquad \text{when } n_2 = 0 \qquad (7.16)$$

and

$$\beta_{min} = \frac{abR}{(abR - 2) - 2n_1} \qquad \text{when } n_1 = n_2 \qquad (7.17)$$

Obviously n_1 in equations (7.16) and (7.17) is not the same. Its values for the two cases can be evaluated from equations (7.14) and (7.15) involving ϵ besides a, b and R. Correspondingly β_{max} and β_{min} are then obtained as

$$\beta_{max} = \frac{abR}{(abR - 2) - \frac{\{2(abR-2) + \epsilon^2\} \pm \sqrt{4(abR-2)\epsilon^2 + \epsilon^4}}{2}} \qquad (7.18)$$

$$\beta_{min} = \frac{abR}{(abR - 2) - 2\left[\frac{\{2(abR-2)+\epsilon^2\} \pm \sqrt{4(abR-2)\epsilon^2+\epsilon^4+\epsilon^2(abR-2)^2}}{4 - \epsilon^2}\right]} \qquad (7.19)$$

7.4 THE SOLUTION OF THE DIFFERENTIAL EQUATION

The computerized solution of the differential equation [equation (7.7)] is based upon the modified Runge-Kutta method of numerical solution and its flow chart is given in figure 7.2.

7.5 COMPUTERIZED SOLUTION AND EXPERIMENTAL RESULTS

Three sets of computerized solutions and experimental results for verification were obtained for

(a) near sinusoidal oscillation
(b) near relaxation oscillation
(c) hard relaxation oscillation.

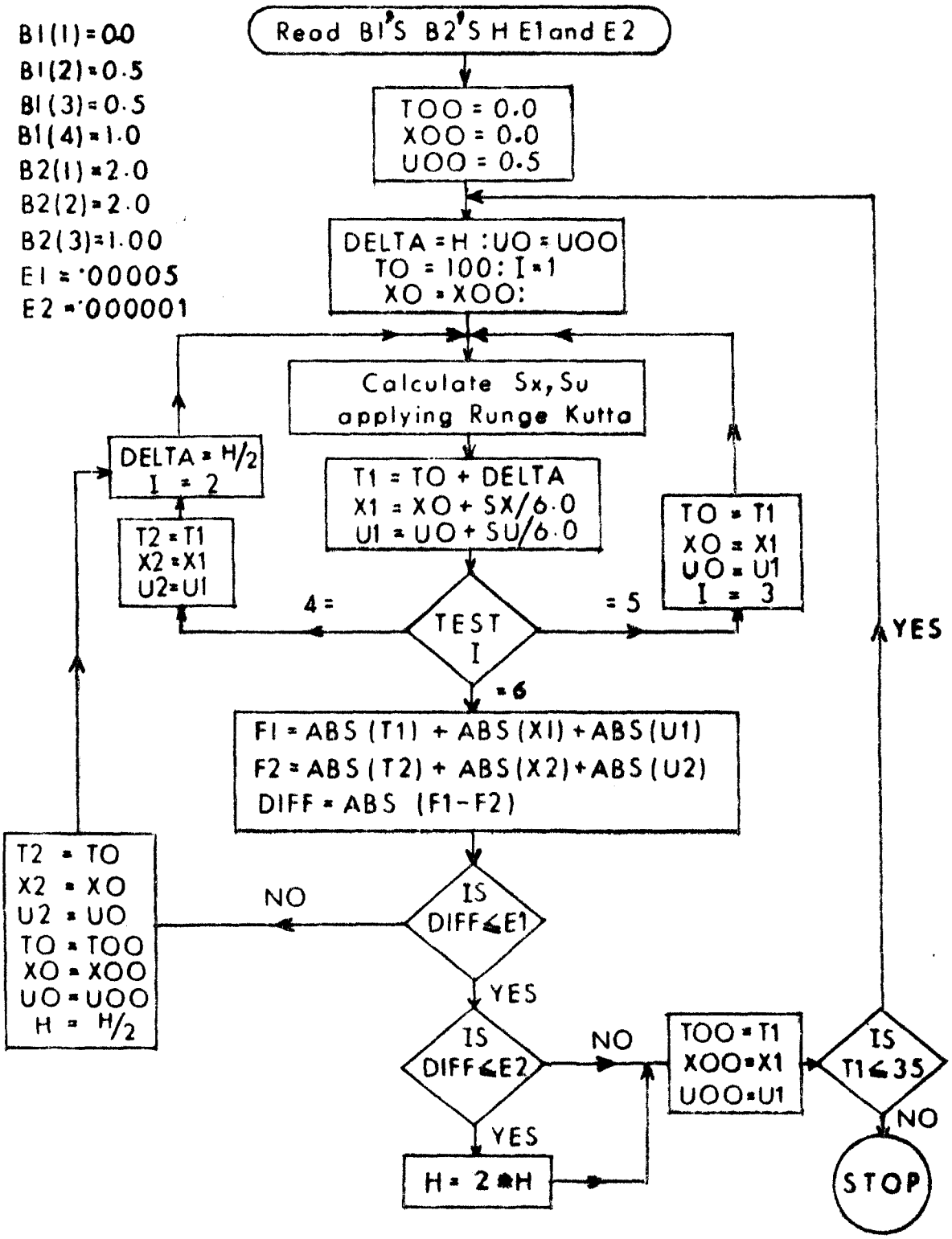

Fig.7.2. The programme flow chart. T and X in the chart correspond to τ and V in the text.

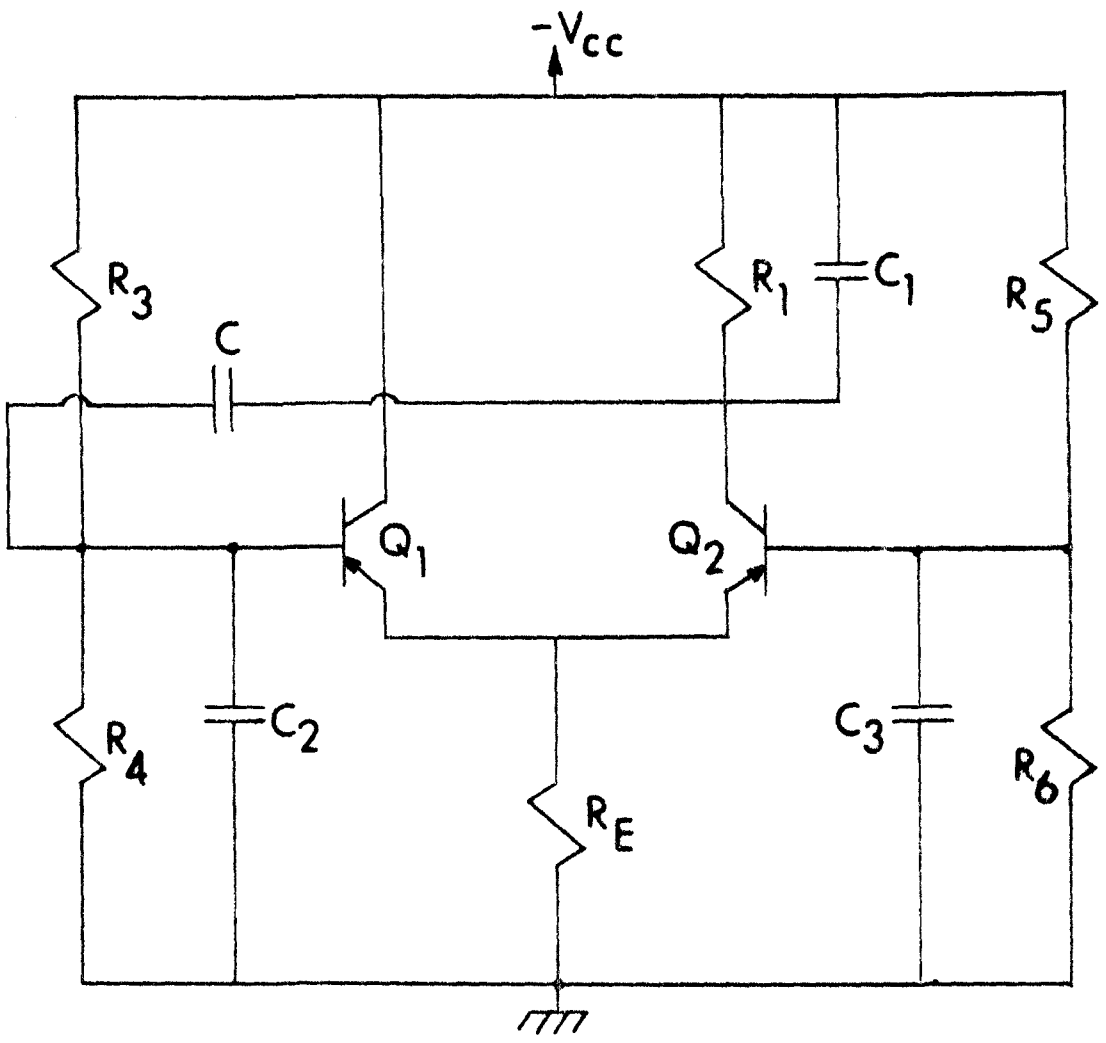

Fig. 7.3. The experimental circuit .

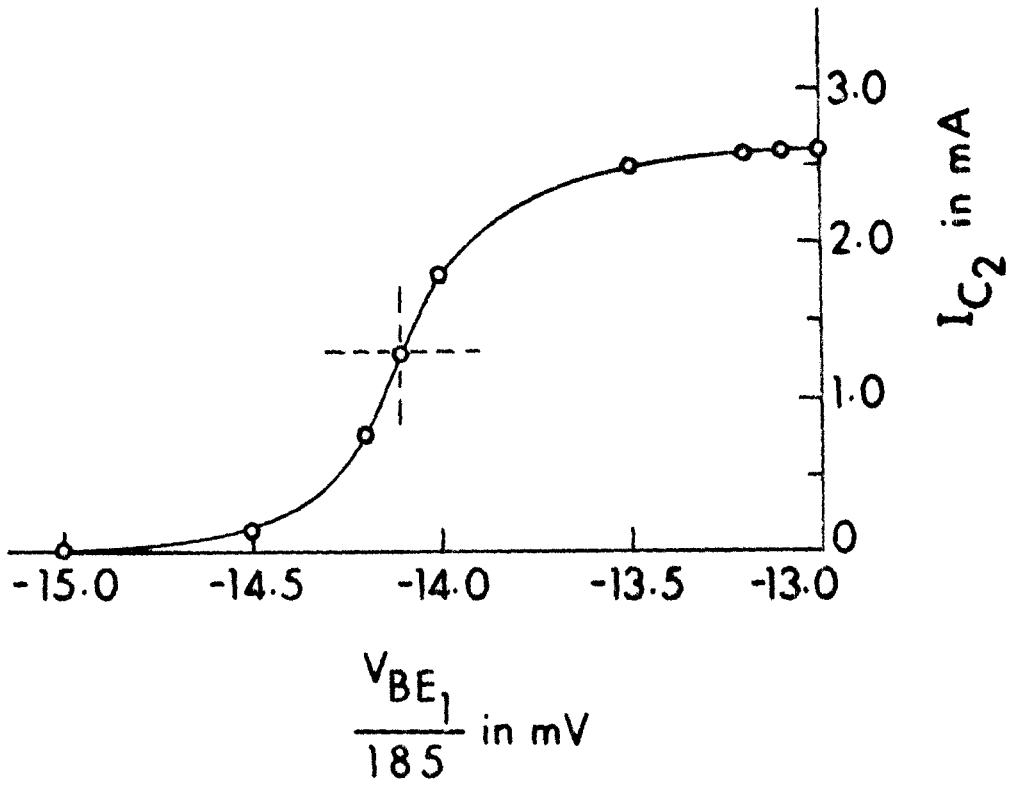

Fig.7.4. The antisymmetric self-saturating transfer characteristics of the differential pair.

The experimental circuit, as shown in figure 7.3 was initially adjusted for obtaining the slope ab, of the antisymmetric self-saturating characteristic of the differential pair shown in figure 7.4.

The different types of oscillation were obtained by changing the ratios of the capacitors i.e. n_1 and n_2 only, and the following parameters were kept constant at the denoted values for all the three cases.

R_1 = 1.35k ohms; m = 1; C = 0.011 μF and ab = 27.02 x 10^{-3} mhos.

TABLE-7.1

CONTROLLED PARAMETER AND DERIVED PARAMETER VALUES

Nature of Oscillation	Controlled Parameters		Derived Parameters			
	n_1	n_2	n	G	β	ϵ
Near Sinusoidal	10	10	120	16.30×10^{-3}	2.520	1.327
Near Relaxation	10	0.03	10	8.90×10^{-3}	1.490	7.740
Hard Relaxation	0.1	0.118	0.23	1.63×10^{-3}	1.069	74.600

Table-7.1 gives the controlled parameter and derived parameter values and Table-7.2 compares the calculated and experimental values of the frequency and amplitude of oscillation for the three cases.

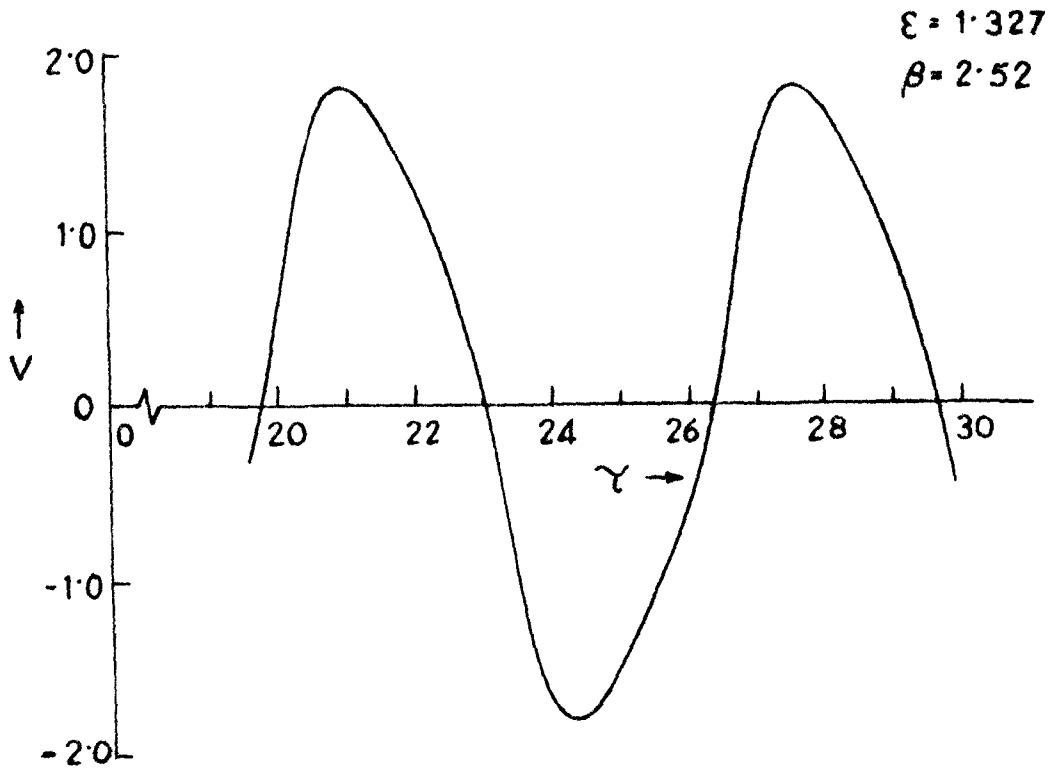

(a)

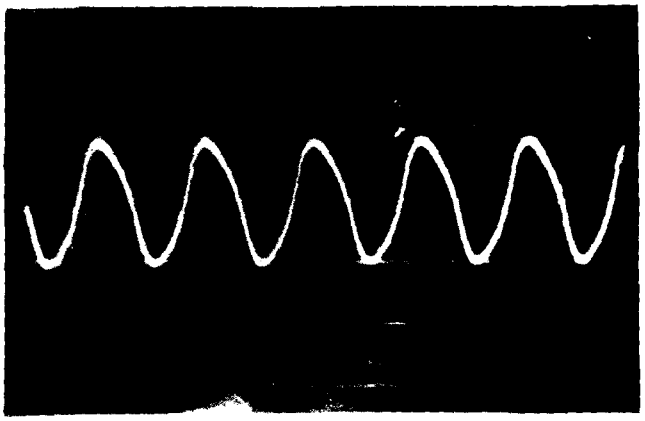

(b)

Fig.7.5. Waveforms for near sinusoidal oscillation. (a) Theoretical: (b) experimental: amplitude scale 100 mV per division.

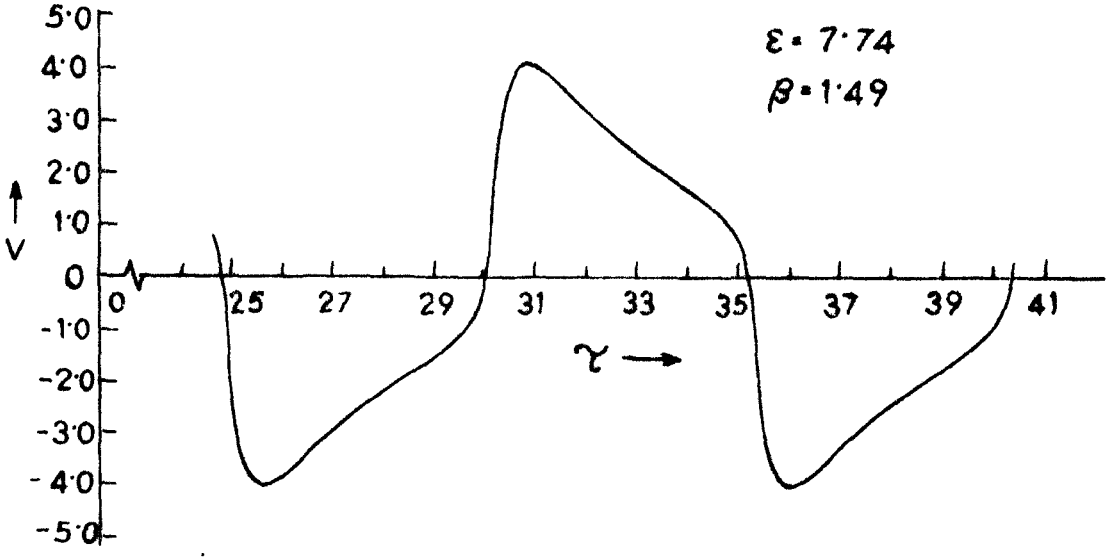

(a)

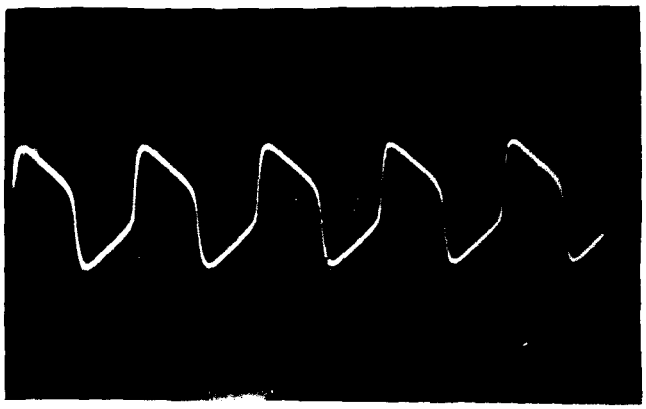

(b)

Fig. 7.6. Waveforms for near relaxation oscillation. (a) Theoretical: (b) experimental: amplitude scale 200 mV per division.

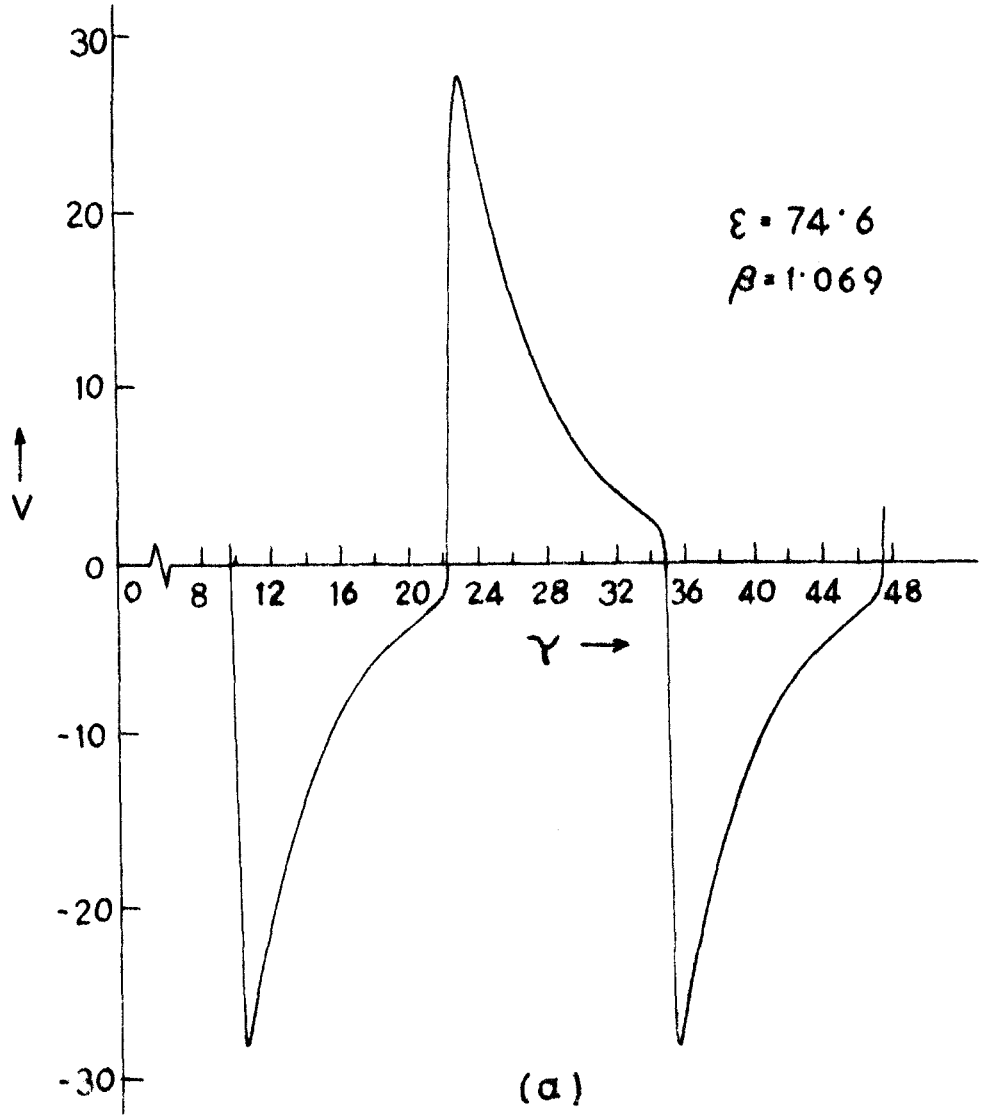

(a)

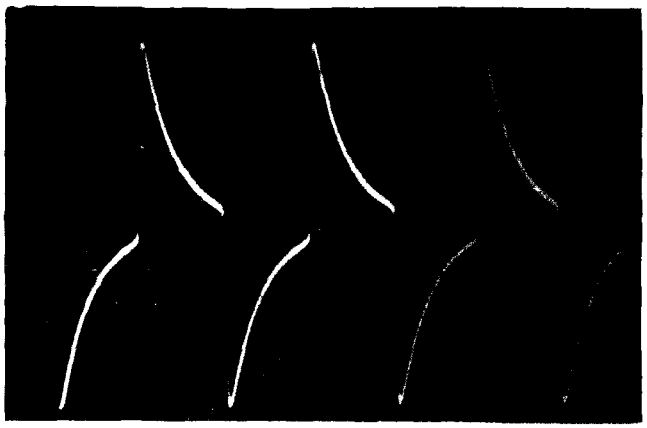

(b)

Fig.7.7. Waveforms for hard relaxation oscillation. (a) Theoretical; (b) experimental; amplitude scale 500 mV per division.

TABLE-7.2

CALCULATED AND EXPERIMENTAL VALUES OF FREQUENCY AND AMPLITUDE OF OSCILLATIONS

Nature of Oscillation	Amplitude of Oscillation Volts(Peak)		Frequency of Oscillation kHz	
	Calculated	Experimental	Calculated	Experimental*
Near Sinusoidal	0.087	0.095	0.935	0.980
Near Relaxation	0.197	0.200	2.050	2.150
Hard Relaxation	1.340	1.500	5.850	5.850

* Frequencies were measured with a counter

Though the assumed non-linearity gives a transcendental equation and a closed-form solution of equation (7.7) is not possible, from the results of Table-7.2, it is evident that the experimental results and theoretical numerical solution agree very well in all modes of oscillation, which is not so if the non-linearity is assumed to be of lesser complexity.

Figures 7.5(a), 7.5(b), 7.6(a), 7.6(b) and 7.7(a), 7.7(b) show the theoretical and experimental wave shapes for the three cases.

7.6 EFFECTS OF ϵ AND β ON DISTORTION AND AMPLITUDE

It has been stated that the effect of the parameter β has a predominant effect on amplitude and ϵ on distortion and this has been demonstrated in the curve of figures 7.8 and 7.9. Figures 7.8(a), 7.8(b) and 7.8(c) are plotted for constant β ($\beta = 8.14$)

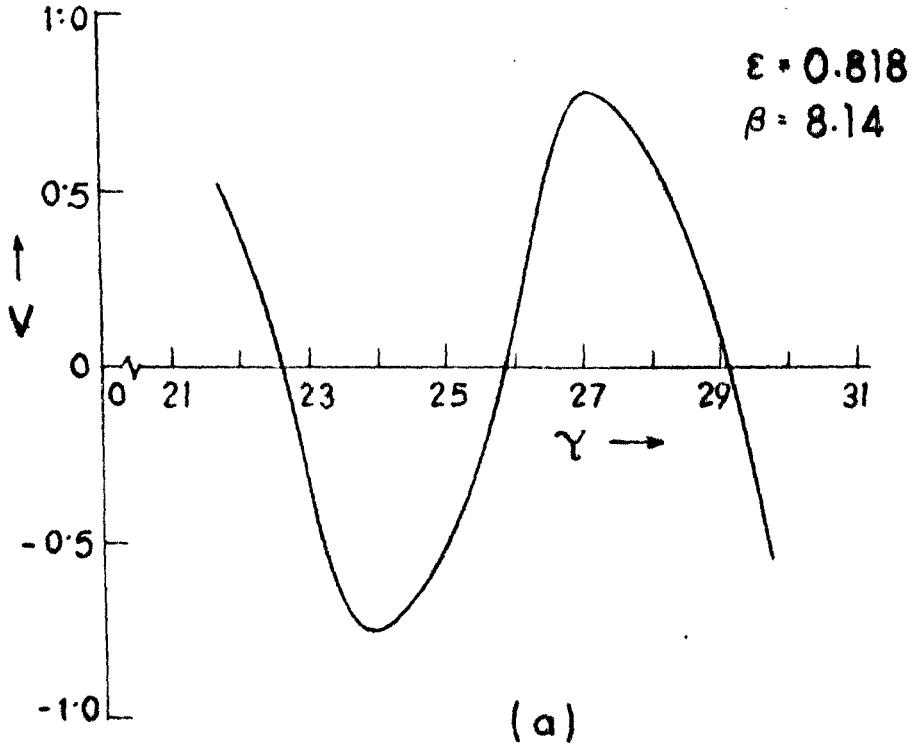

(a)

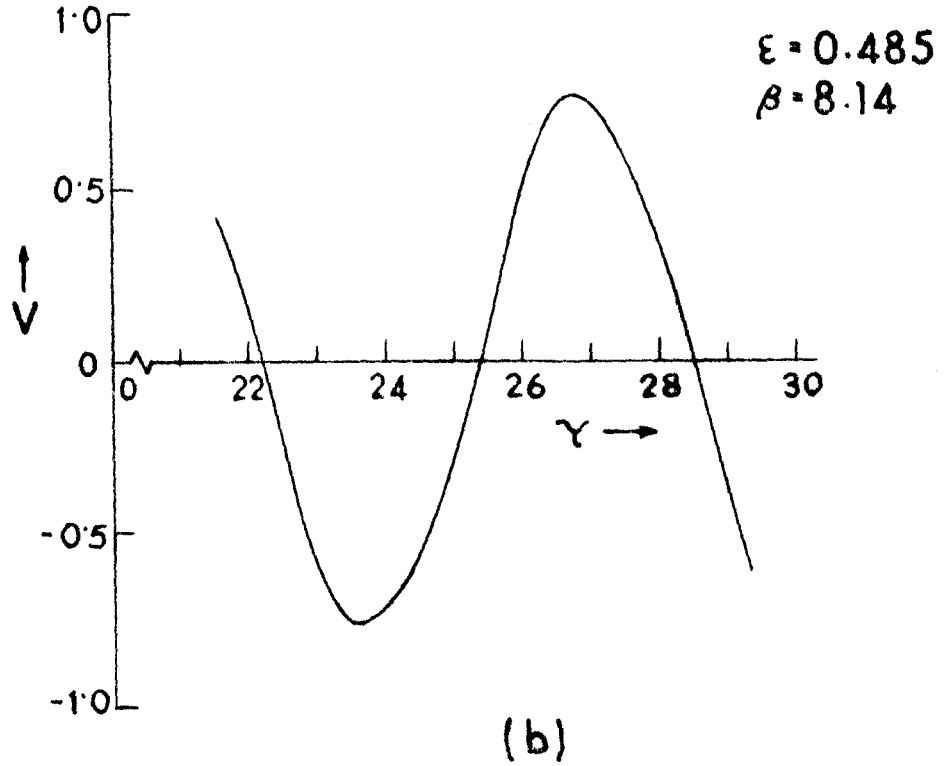

(b)

(continued over)

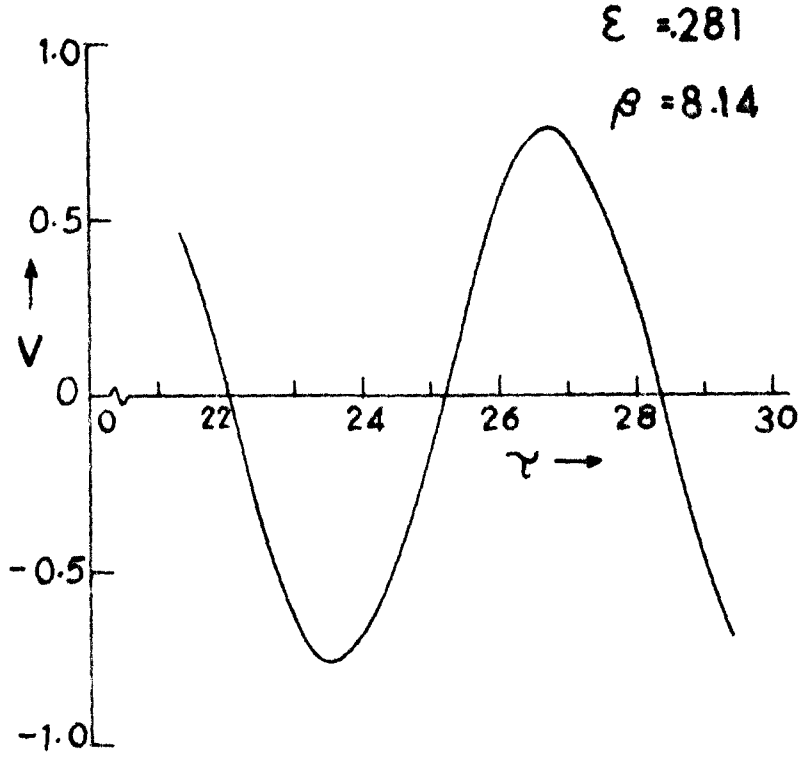

(c)

Fig. 7.8. Waveforms obtained for constant β ($\beta = 8.14$) and varying: (a) $\epsilon = 0.818$; (b) $\epsilon = 0.485$; (c) $\epsilon = 0.281$.

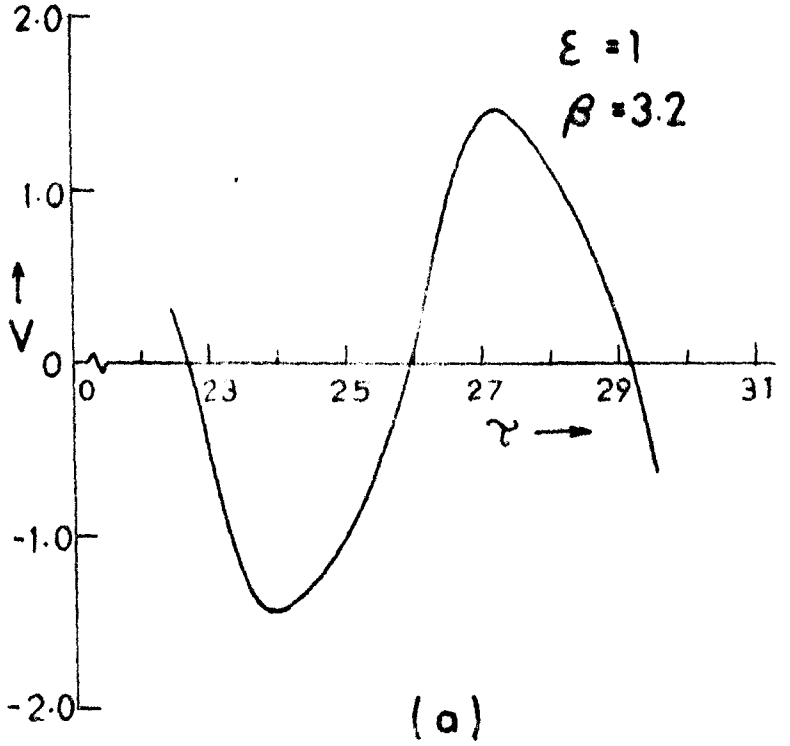

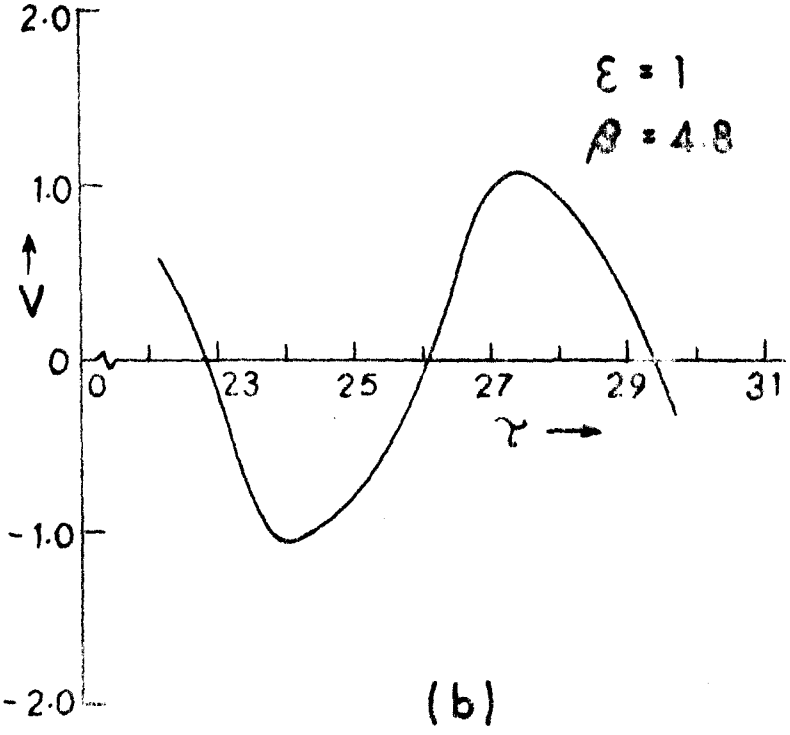

Fig. 7.9. Waveforms obtained for constant ϵ ($\epsilon = 1$) and varying: (a) $\beta = 3.2$: (b) $\beta = 4.8$.

and varying ϵ whose possible limits of variation are $0.818 \rangle \epsilon \rangle 0.281$. From the curves it is observed that the amplitude remains constant but the distortion increases slightly with increasing values of ϵ.

The next set of curves are plotted for constant ϵ ($\epsilon = 1$) and varying β over the possible limits $6.76 \rangle \beta \rangle 3.007$. Computerized solutions were obtained for $\epsilon = 1$ and $\beta = 3.2$ and $\beta = 4.8$ and have been plotted in figures 7.9(a) and 7.9(b). It is observed that the amplitude decreases with increase in the value of β.

7.7 THE VOLTAGE CONTROLLED OSCILLATOR[5*]

It has been shown so far, that oscillations in the system described may be controlled over harmonic to relaxation mode by controlling a passive parameter G obtained from the load and coupling elements. If G is held constant the mode of operation can still be controlled by varying the slope ab (at the origin) of the transfer characteristics. This slope can be varied quite simply by changing the operating bias voltage of one of the transistors of the differential pair and keeping that of the other constant. This in effect change the symmetric operation of the pair to asymmetric operation and the change in the average slope varies the parameter ϵ in equation (7.6a). This is effectively a voltage controlled oscillator (VCO) whose operation is gradually changed from harmonic mode to quasiharmonic mode, thereby changing the oscillation frequency due to harmonic depression[6]. However for a large frequency deviation, the distortion level still remains quite low and realization of a practical VCO is therefore envisaged.

The relation between the slope and the differential change in the bias voltage has been derived from the transfer characteristics [equation (7.2)] where e now represents the differential change in voltage and is replaced by u in subsequent discussion for clarity. Using this, a computerised solution of equation (7.7) is performed to obtain the frequency of VCO. The frequencies are also measured. The results are presented in Table-7.3 along with the results obtained by using the method of small parameters[6].

TABLE-7.3

RESULTS

[C = 1050pF, R = 2K, R_3 = 3.78K, R_4 = 2K, n = 9.476, m = 0.654, G = 8.509×10^{-3} mho, R_5 = 25Ω, h_{fe} = 500, I_{EE}=0.77mA; Ref.Fig.7.10(a)]

milli Volts	milli Siemen	Normalized frequency f/f_o^*			Measured distortion dB
		Computer Solution	Method of small parameter	Experimental	
1.78	10.240	0.9683	0.9483	0.9691	30
7.80	10.353	0.9579	0.9413	0.9527	28
13.90	10.591	0.9435	0.9252	0.9330	25
19.97	10.980	0.9241	0.8947	0.9034	22
26.06	11.527	0.9029	0.8428	0.8870	20

* f_o = Sinusoidal mode frequency at balanced operation [cf. equation (7.22)].

7.7.1 THE CIRCUIT AND THE ANALYSIS

The circuit using a matched pair of transistors (TD 101) and its partial equivalent for deriving the expression for the differential voltage in relation to the constant emitter current

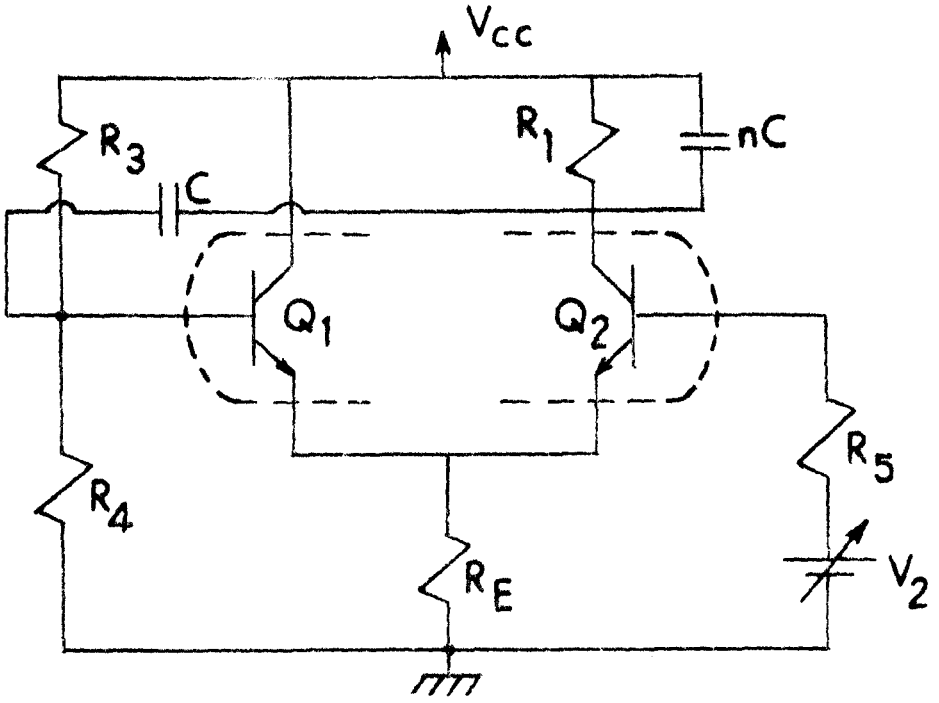

(a)

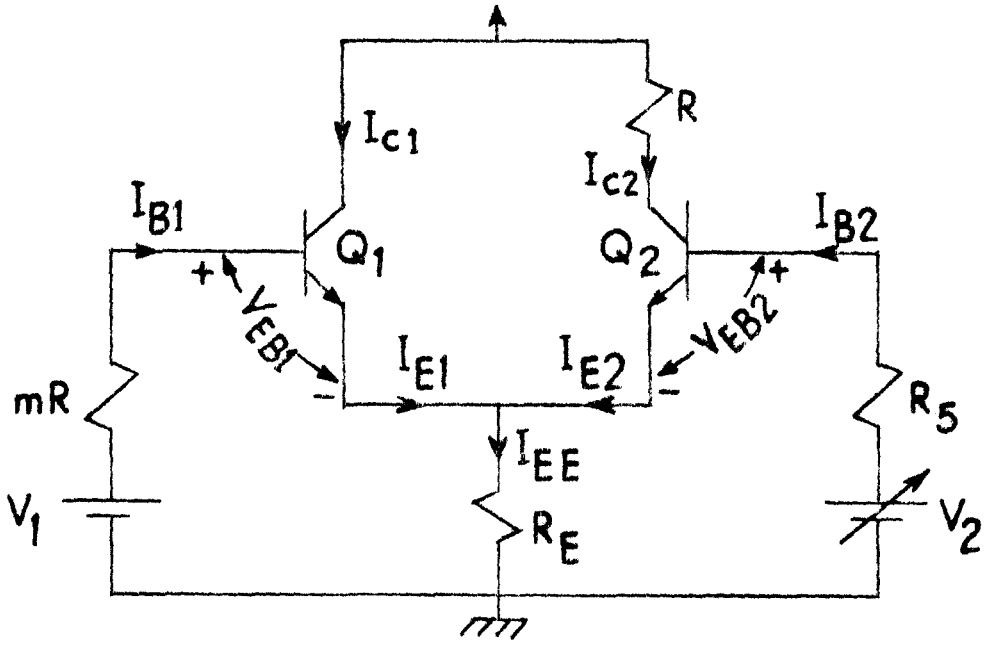

(b)

Fig.7.10 (a) VCO circuit

(b) Partial equivalent circuit of 7.10 (a)

and quiescent condition are shown in figures 7.10(a) and (b) respectively. The voltage source V_1 and resistance mR are the Thevenin generator and resistance as seen by the base of the transistor Q_1. The differential voltage is easily derived as (see appendix 7.1).

$$u = V_1 - V_2 + I_{c_2} \frac{mR + R5}{h_{fe}} - I_{EE} \frac{mR}{1 + h_{fe}} \qquad (7.20)$$

where h_{fe} is the common emitter current gain of the transistor.

From the logical development laid out above and from the transfer characteristics the desired relation is easily obtained as

$$g = ab = g_o \cosh^2 bu \qquad (7.21)$$

where g_o is the slope at the origin for balanced operation with given operating conditions. Combining equation (7.20) and (7.21), g can be obtained for different u, the corresponding ϵ and β are evaluated by using equation (7.6a) and (7.6b) and equation (7.7) is solved to obtain the frequencies. It should be remembered that every differential change in u produces a new asymmetric operating point with the changed value of g. Parameter g is obtained by considering average fixed value of b obtained from the balanced operating condition.

The asymmetric points may be obtained from the intersections of the graphs of equations (7.2) and (7.21). Presumably this shift in the operating points leads to distortion in waveform; however when the shift is kept small, sufficiently wide frequency variation

with low distortion is obtainable. With asymmetry thus limited the assumption of balanced operation shows good correlation between theoretical and experimental results as shown in Table-7.3.

Since operation is limited to the near harmonic mode, one is tempted to approximate equation (7.7) to classical van der Pol equation. In such cases one can have an approximate solution for frequency by using the method of small parameters[6], the frequency relation in which case is given by

$$f = f_o \left[1 - \frac{1}{16}\epsilon^2 + \ldots\right] \qquad (7.22)$$

where

$$f_o = \frac{1}{2\pi RC\sqrt{mn}}$$

The frequencies are calculated by using equation (7.7) for different values of u. Table-7.3 shows the results along with the measured distortion figures. For the variation of frequencies with respect to u given in Table-7.3 the distortion level is seen to be quite low. Further, it may be noted that the results are same, irrespective of the direction of change of u.

7.7.2 PRACTICAL SCHEME

As a practical utilization scheme to telemeter process data the variable voltage V_2 is replaced by a data-to-voltage source. The partial scheme is shown in figure 7.11. Test results have shown the same accuracy as obtained in Table-7.3.

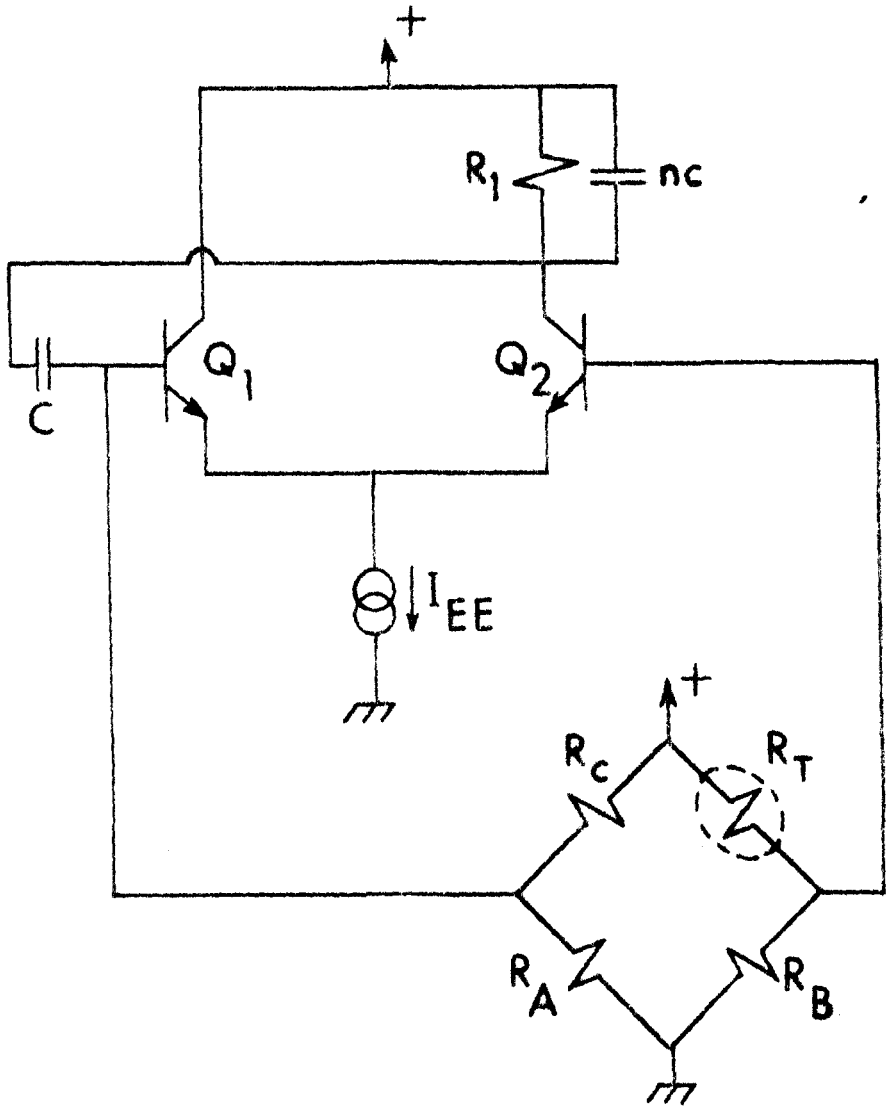

Fig.7.11. Scheme of a VCO using Resistance Thermometer for temperature telemetering $R_A = R_B$; $R_C = R_{Tn}$ is the resistance of the thermometer at reference temperature

7.7.3 DISCUSSIONS

Transistor base leakage currents have not been considered in deriving equation (7.20); this is quite justified for the silicon planar transistor used (TD 101). Results obtained with a pair of germanium transistors (2N483) show that, when leakage current is not negligible and the transistors have a low value of h_{fe}, a wider and a more linear frequency variation is obtainable for the same level of distortion with a larger variation of u. However, the analysis in this case becomes quite involved and as the leakage currents have to be accurately known, no attempt has been made to accommodate these in equation (7.20).

7.8 CONCLUSION

A nonlinear oscillatory system using the self-saturating antisymmetric transfer characteristic (ASTC) of an emitter coupled differential pair has been presented with a comprehensive analysis showing adjustability from sinusoidal to hard relaxation mode by two-parameter control, unlike the existing types of van der Pol oscillators where a single-parameter control is used. This approach completely explains the mode, frequency and waveform, and furnishes information as to selection ranges of the parameter values.

It should however be noticed that the two-parameter control can be effected by the variation of n_1 and n_2 the capacitor ratios, or ab the slope of the ASTC or by m the ratio of the resistors alone. Table-7.1 shows that even n_2 alone could change the mode from near sinusoidal to near relaxation oscillation. This implies the adaptability of such an oscillator to instrumentation system

with C_2 replaced by a capacitive transducer[7] to monitor a process variable. Differential capacitive transducer[7] could as well be used in place of C_1 and C and/or C_2 and C as each of the pair has a common terminal. The change in both frequency or amplitude could be a measure of the variable. The utility of this type of a generator is more as a waveform generator, as the change in waveform may not be quite acceptable for the signal processing purpose . Interestingly however if the operating slope ab is changed by changing the bias voltage of one of the transistors a wide frequency variation is obtained with very little waveform distortion and gives rise to a VCO with this differential pair. Such a VCO has also been studied and the results are given in Table-7.3. A partial practical scheme to replace the control bias source by a data-to-voltage source has also been shown indicating a practical utilization scheme of the VCO to telemeter process data and test results have shown the same accuracy as obtained in Table-7.3.

It is interesting to note that the hard relaxation mode only, can be analysed with an approximation that derives the frequency analytically within 5 to 10% tolerance and such an approximate analysis is discussed in the next chapter.

APPENDIX-7.1

From figure 7.10(b) the loop equations for loop 1 and loop 2 are

$$V_{EB1} + I_{EE}R_E - V_1 + I_{B1}\,mR = 0 \qquad \text{(A-7.1)}$$

$$V_{EB2} + I_{EE}R_E - V_2 + I_{B2}\,R_5 = 0 \qquad \text{(A-7.2)}$$

Subtracting equation (A-7.2) from equation (A-7.1) the differential base voltage u is obtained as

$$u = V_{EB1} - V_{EB2} = V_1 - V_2 + I_{B2}R_5 - I_{B1}mR \qquad \text{(A-7.3)}$$

The two transistors Q_1 and Q_2 being matched the common emitter current gain $\beta_1 = \beta_2 = \beta$, hence equation (A-7.3) is written as

$$u = V_1 - V_2 + \frac{1}{\beta}\,(I_{C2}R_5 - I_{C1}\,mR) \qquad \text{(A-7.3)}$$

For an emitter coupled differential transistor pair

$$I_{EE} = I_{E1} + I_{E2} \qquad \text{(A-7.4)}$$

or

$$I_{C1} = \alpha I_{EE} - I_{C2} \qquad \text{(A-7.5)}$$

where α is the common base current gain.

From equation (A-7.5) and equation (A-7.3)

$$u = V_1 - V_2 + \frac{1}{\beta}\left[I_{C2}\,(R_5 + mR) - \alpha I_{EE}\,mR\right]$$

$$= V_1 - V_2 + I_{C2}\,\frac{R_5 + mR}{h_{fe}} - I_{EE}\,\frac{mR}{1 + h_{fe}} \qquad \text{(A-7.6)}$$

where $\alpha = \dfrac{\beta}{\beta + 1}$ and $\beta = h_{fe}$.

REFERENCES

1. van der Pol,B. : 'The nonlinear theory of electric oscillation'; Proc. IRE, Vol.22, No.9, pp.1051-1082, Sept.1934.

2. Scott,P.R. : 'Large amplitude operation of the nonlinear oscillator'; Proc. IEEE, Vol.56, No.12, pp.2182-2183, December 1968.

3. Kundu,P. and Roy,S.B. : 'A temperature-stable RC transistor oscillator'; Proc. IEEE, Vol.57, No.3, pp.356-357, March 1969.

*4. Roy,S.B. and Patranabis,D. : 'Non-linear oscillations using antisymmetric transfer characteristics of a differential pair'; Int. J. Electron., Vol.42, No.1, pp.19-32, 1977.

*5. Roy,S.B. and Patranabis,D. : 'Voltage-controlled oscillator using an emitter-coupled differential pair'; Electron. Lett., Vol.13, No.19, pp.590-591, Sept. 1977.

6. Groszkowski,J. : 'Frequency of Self-Oscillations'; Oxford : Pergamon Press, 1964, pp.181-184.

7. Patranabis,D. : 'Principles of Industrial Instrumentation'; New Delhi : Tata McGraw-Hill, 1976, pp.60-62.

---

* Chapter-VII is based mainly on these two publications.

CHAPTER-VIII

AN INSENSITIVE LINEAR SINGLE-ELEMENT-CONTROL PULSE GENERATOR

8.1 INTRODUCTION

Generation of harmonic to relaxation oscillation using the non-linearity of the antisymmetric self saturating transfer characteristics (ASTC) of an emitter coupled differential pair (ECDP) has been presented[1] in Chapter-VII. The ASTC had been approximated by a transcendental function of hyperbolic tangent type resulting in a two parameter non-linear differential equation and the mode of oscillation could be adjusted by the control of these two parameters. The two parameter control could be effected by changing the capacitor ratios or the resistance ratios in the frequency determining network or by changing the operating slope ab of the ASTC. Interestingly, the operating slope ab can be changed by bias voltage change of the ECDP and this was utilised to obtain a VCO[2] giving sinusoidal output. This has also been presented in Chapter-VII. However, the frequency range obtained was not very large. In practice, however, wide frequency-deviation ratio oscillators, basically, are of multivibrator type, providing pulse or square wave output. Using the ASTC of the proposed ECDP a linear wide range, variable frequency pulse generator can be designed. This pulse generator can be conveniently adapted to instrumentation system with the control element replaced by a suitable transducer to provide a process parameter to pulse period conversion facility.

Since no closed form solution of the two-parameter non-linear differential equation with a transcendental function is possible, an approximate analytical approach, to enumerate the design criteria and predict the behaviour of such a system in relaxation mode, to obtaining symmetric pulse waveform, has been presented in this chapter[3*]. The repetition rate of the generated pulse wave form is obtained through jump behaviour[4], while hyberbolic tangent non-linear characteristic[1] is used to obtain the shift in the operating point thereby correcting the repetition rate of the generator. The number of frequency determining parameters in such a system is reduced to a minimum with the provision for linearly varying the time period with a single resistive element.

The validity of the analytical approach has been tested experimentally and the repetition rate and the region of linearity of the controlled generator have been found to agree closely with the theoretical analysis. Conditions have also been derived under which the frequency sensitivity of the circuit can be minimized. The effects of temperature on both the active and passive parameters have been considered and it has been indicated how the effect of temperature on the frequency determining parameters may be utilized for compensation, offering a scope of improvement which may be best exploited in integrated circuit implementation of such generators.

Experimental results, covering several aspects of the proposed circuit with discrete components, for substantiating the theoretical analysis, are shown in tables and a graph.

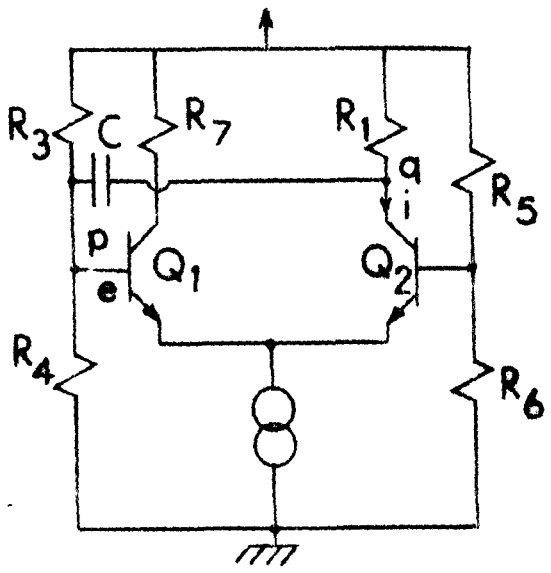

Fig.8·1 Circuit of the propsed generator

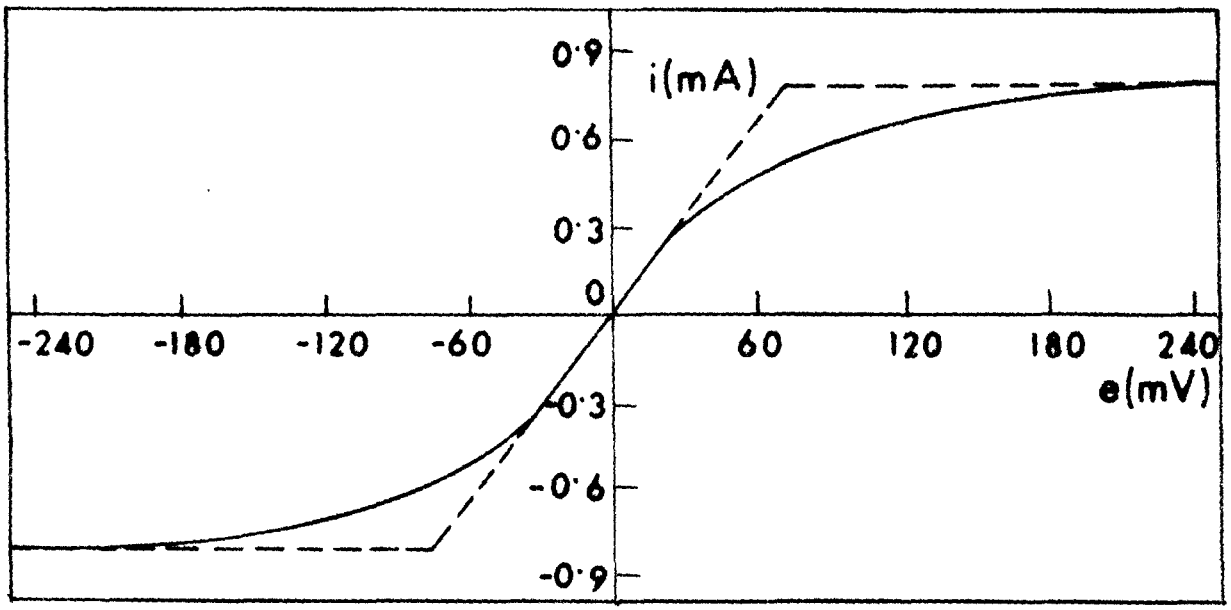

Fig.8·2 The normalized transfer characteristic of the ECDP

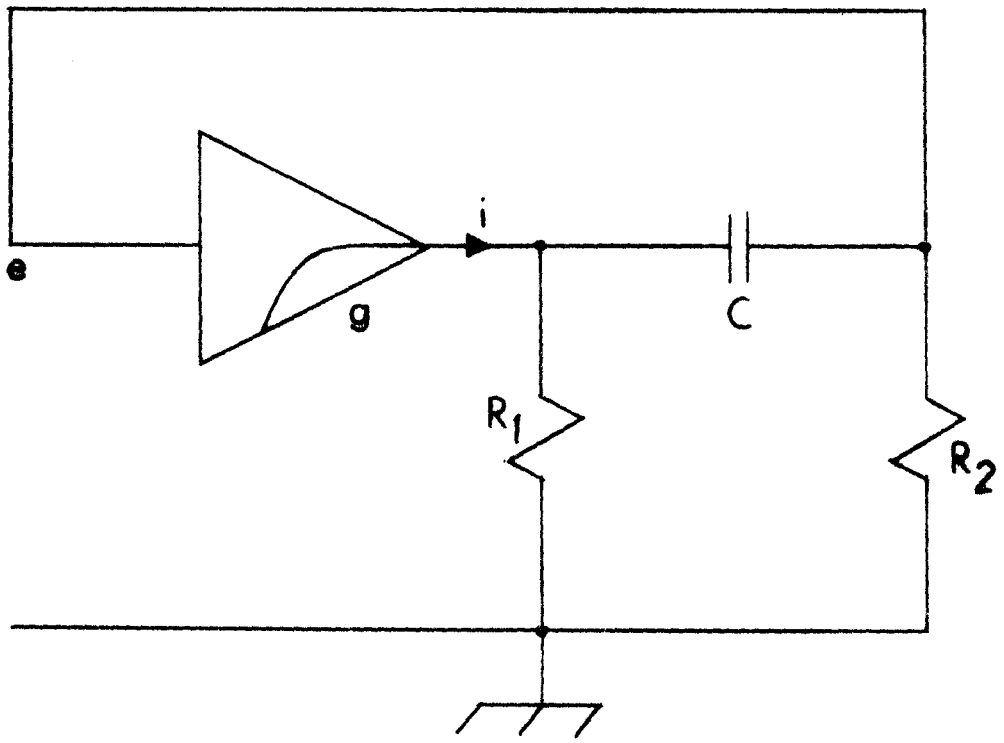

Fig. 8.3 Equivalent scheme of Fig. 8.1 .

8.2 THE SCHEME AND FREQUENCY OF OSCILLATION

The scheme of the proposed circuit is shown in figure 8.1. While the capacitor is open R_3, R_4, R_5 and R_6 are adjusted for balanced biasing and the differential pair acts as a transconductance element between the points 'p' and 'q' whose saturation transfer characteristic is shown in figure 8.2 and is assumed to be represented by the transcendental form[1]

$$i = a \tanh be \tag{8.1}$$

when the feedback path is closed through the capacitor, the positive feedback provided sets relaxation oscillation in the circuit which can be easily deduced from the equivalent circuit of figure 8.1 drawn in figure 8.3 where R_2 is $R_3 \parallel R_4$. The system differential equation[1]

$$CR_1R_2 \frac{de}{dt} \left[\left(\frac{1}{R_1} + \frac{1}{R_2} \right) - \frac{di}{de} \right] + e = 0 \tag{8.2}$$

represents the dynamic model of the oscillator. Considering the linearized saturation characteristic as shown by the dotted lines in figure 8.2 whose slope at the operating point is g and the fact that a jump would occur in the system voltage to double its value on just reaching the saturation level (because the coupling is by capacitor C only), one can obtain the repetition rate by integration of equation (8.2)[4] as

$$T = C(R_1 + R_2) \ln (2gR_1 - 1) \tag{8.3}$$

If R_1 is controlled for governing the repetition rate, while the operating point remains fixed, both the product terms vary

simultaneously giving a large variation in the repetition rate. The normalized rate of this is in fact given by

$$\rho = \frac{1}{C}\frac{dT}{dR_1} = \frac{2g(R_1 + R_2)}{2g\,R_1 - 1} + \ln\,(2gR_1 - 1) \qquad (8.4)$$

which is much larger than that in conventional design.

For linearity of the T-R_1 relationship, ln $(2gR_1 - 1)$ should not vary substantially with R_1. However, from equation (8.4), a range of values for R_1 can be obtained for which this is approximately true and an almost linear variation of T with respect to R_1 over this range is obtainable.

Differentiating equation (8.4) with respect to R_1

$$\frac{d\rho}{dR_1} = \frac{4g}{(2gR_1 - 1)^2}\left[g\,(R_1 - R_2) - 1\right] \qquad (8.5)$$

one observes that a near linear T-R_1 relationship is obtained for

$$g(R_1 - R_2) = 1 \qquad (8.6a)$$

From equation (3) one finds that the oscillation condition requires

$$R_1 > \frac{1}{2g} \qquad (8.6b)$$

Showing compatibility of equation (8.6).

For a given value of R_2, therefore, a range of values for R_1 is to be chosen following equations (8.6a) and (8.6b) such that ρ is nearly constant over that range. Deviation from linearity at

any value of T can be obtained from equations (8.4) and (8.6a) for the corresponding value $R_1 = R_{1x}$ (say)

$$\delta_L = \frac{\rho_x - \rho_o}{\rho_o} = \frac{1}{2 + \ln(2gR_2 + 1)} \left[\frac{2g(R_2 - R_{1x}) + 2}{2GR_{1x} - 1} + \ln \left(\frac{2gR_{1x} - 1}{2gR_2 + 1} \right) \right] \qquad (8.7)$$

where ρ_o is obtained by substituting equation (8.6a) in equation (8.4). For allowable δ_L, the limiting values of R_{1x} can now be evaluated from equation (8.7).

8.3 THE OPERATING POINT AND VALUE OF g

The value of g is obtained from the actual plot[1] for balanced bias conditions with compatible values of R_j's, j = 1,3,4,5,6 as dictated by equation (8.6b) and for better linearity in $T-R_1$, also by equation (8.6a). However, as oscillation sets in, the operating point of the transistor Q_1 (figure 8.1) shifts, thereby changing the value of g. This shift in the point is only graphically obtainable through complex analysis[5] for an arbitrary mode of oscillation. As only relaxation oscillation is considered here, this shift is maximum and is calculable from the non-linear saturation transfer characteristic. When shift occurs, the approximated linearized characteristic changes such that the slope g is also different. In fact this increases the value of g, as the constant current source (CCS) at the emitters decreases the saturation voltage in the ASTC of the differential pair, when the idealized and linearized model of this is considered. At hard relaxation the input e

(figure 8.1) via the base-emitter junction reduces the effective saturation voltage to half its balanced bias condition. Therefore, from equation (8.1) the effective value of g is calculated

$$g_e = g \cosh^2 be = g \cosh^2(0.5) = 1.27g \qquad (8.8)$$

This value of g_e is used in equation (8.3) for calculating the repetition rate as R_1 is controlled. As relaxation through jump phenomenon occurs, the waveform at the output point q is not a square-wave. The waveform undergoes a certain change, retaining however the pulse nature, because of the difference in voltage across Q_2 and R_1. The output waveform becomes nearly square when these voltages are very close. A square-wave can, however, easily be extracted by standard clipping techniques.

8.4 EFFECT OF NON-IDEAL CURRENT SOURCE

When the current source at the emitters is replaced by a simple resistor R_{EE} of correct value, the basic operation of the generator remains unaltered, but there is a marginal shift in the controlled frequency range. This occurs because the 'non-ideal' current source tends to shift the operating point in a different manner, producing a different linearized slope g_f, however close its value may be to g_e. In the balanced biased condition in this case, let I_{EQ} denote the balanced emitter operating currents on each side. In hard relaxation oscillation let this value be I_{ES}. Let E_{OB} be the amplitude of base drive at p (figure 8.1) due to this oscillation, then one can write the approximate equation during oscillation for transistor Q_1 as,

$$I_{ES} = I_{EQ} + \frac{E_{OB} - 2R_{EE}\,(I_{ES} - I_{EQ})}{h_{IE}}\,h_{FE} \tag{8.9}$$

where h_{IE} and h_{FE} have the usual significances. Equation (8.9) is simplified to

$$I_{ES} = I_{EQ}\left[1 + \frac{E_{OB}}{I_{EQ}\left(\frac{h_{IE}}{h_{FE}} + 2R_{EE}\right)}\right] \tag{8.10}$$

showing an increase in the saturation current. In fact when relaxation oscillation occurs, the amplitude at the base is fixed by the non-linearity of the slope of the characteristic and actual saturation occurs at a higher value of e, say E_{BSS}, but this apparently does not change the saturation current, I_{ESO}(say). The oscillation amplitude would, however, cause a change in the actual emitter current for the changed slope that occurs because of the shift in the operating point. This is calculated in equation (8.10) where E_{OB} is to be replaced by E_{BSS}, which in turn is calculated from equation (8.1) by assuming a linearized and idealized model of the enhanced-slope saturation characteristic with tanh be = 1, as saturation current is assumed constant. This gives

$$E_{OB} = E_{BSS} = \frac{1}{b}\tanh^{-1} 1 = E_{BSO}\tanh^{-1} 1 \tag{8.11}$$

The parameter b is obtained from the standard saturation model. From equations (8.10) and (8.11) I_{ES} is calculated and used to obtain

$$g_f = \frac{I_{ES}}{E_{BSO}} \tag{8.12}$$

which is the new value of g with the non-ideal constant current generator.

8.5 SENSITIVITY TO SUPPLY, TEMPERATURE AND PASSIVE PARAMETERS

It would be observed from equation (8.3) that in the proposed oscillator, the frequency changes when g is affected. As g is basically dependent on the emitter current, when an ideal constant current source supplies the emitters of the differential pair, g is not affected. Even when the supply voltage changes within prescribed limits, the current remains unaltered, and once relaxation oscillation sets in, g_e would not change its value from the one calculated from equation (8.8).

If however the 'approximate current source' obtained with a resistor between common emitters and ground is considered, I_{EE} would change as the supply voltage is varied. This can easily be seen from equations (8.9) and (8.10). In fact, if one assumes h_{IE} and h_{FE} do not change to the extent to warrant any consideration, I_{ES} changes directly with I_{EQ} as the supply changes. From equation (8.10) it can further be shown that if the supply varies by $\pm \triangle E_s$, $\pm \triangle I_{EQ}$ is given by

$$\pm \triangle I_{EQ} = \pm \frac{K \triangle E_s}{2R_{EE}} \qquad (8.13)$$

where K is a constant determined by the biasing chain. Frequency variation due to supply change is therefore dependent on K and R_{EE}. For CCS, $R_{EE} \rightarrow \infty$ giving no variation in frequency due to supply fluctuation. Table-8.1 gives these results both with ideal and non-ideal CCS for a $\pm$ 10% supply variation.

TABLE-8.1

EXPERIMENTAL SENSITIVITY FIGURES TO SUPPLY VARIATION

$\frac{\Delta E_s}{E_s}$ (%)	$\frac{\Delta T}{T}$ x 100 (%), with CCS	$\frac{\Delta T}{T}$ x 100 (%), with R_{EE}
- 10.0	- 0.440	- 5.60
- 7.5	- 0.300	- 4.20
- 5.0	- 0.200	- 2.80
- 2.5	- 0.100	- 1.40
0	0	0
2.5	0.095	1.50
5.0	0.180	2.70
7.5	0.280	4.20
10.0	0.390	5.50

Frequency shift due to temperature variation is more serious, particularly with the CCS design when the CCS is not individually compensated. The differential pair is self-compensated as regards temperature[6] but this degree of compensation is also important. A shift in the value of g occurs because of the bias unbalance resulting due to inequality in the temperature coefficient of V_{BE} of the pair. As the differential temperature coefficient is likely to be small for a matched pair mounted in the same header g varies almost linearly with it. From equation (8.3) neglecting higher order products of the differential quantities, one can easily derive the change in the repetition rate with changes in resistances, capacitances and the transconductance with temperature as

$$\frac{\Delta T}{T} = \frac{\Delta C}{C} + \frac{\Delta R}{R} + \frac{\ln\left[1 + (\Delta g/g) + (\Delta R/R)\right]}{\ln(2g\,R_1 - 1)} \qquad (8.14)$$

Where it has been assumed that

$$\frac{\Delta R_1}{R_1} = \frac{\Delta R_2}{R_2} = \frac{\Delta R}{R}$$

As can be seen from equation (8.14) $\Delta T/T$ can be made zero, if either

$$\frac{\Delta C}{C} = \frac{\Delta R}{R} = \frac{\Delta g}{g} = 0 \qquad (8.15a)$$

or

$$\frac{\Delta R}{R} = -\frac{\Delta C}{C} = -\frac{\Delta g}{g} \qquad (8.15b)$$

While equation (7.15a) is a little hypothetical, equation (8.15b) is more easily satisfied in practice particularly in integrated circuit forms. Actual values of $\Delta T/T$ would depend on the magnitudes and signs of $\Delta C/C$, $\Delta R/R$ and $\Delta g/g$, and thus a third probable alternative for $\Delta T/T = 0$ is

$$\frac{\Delta C}{C} + \frac{\Delta R}{R} = -\frac{\ln\left[1 + (\Delta g/g) + (\Delta R/R)\right]}{\ln\,(2gR_1 - 1)} \qquad (8.15c)$$

The wrost-case shift in T with the change in temperature is studied for the proposed circuit and it is shown that even when adequate compensation is not provided the change in repetition rate is within tolerable limits.

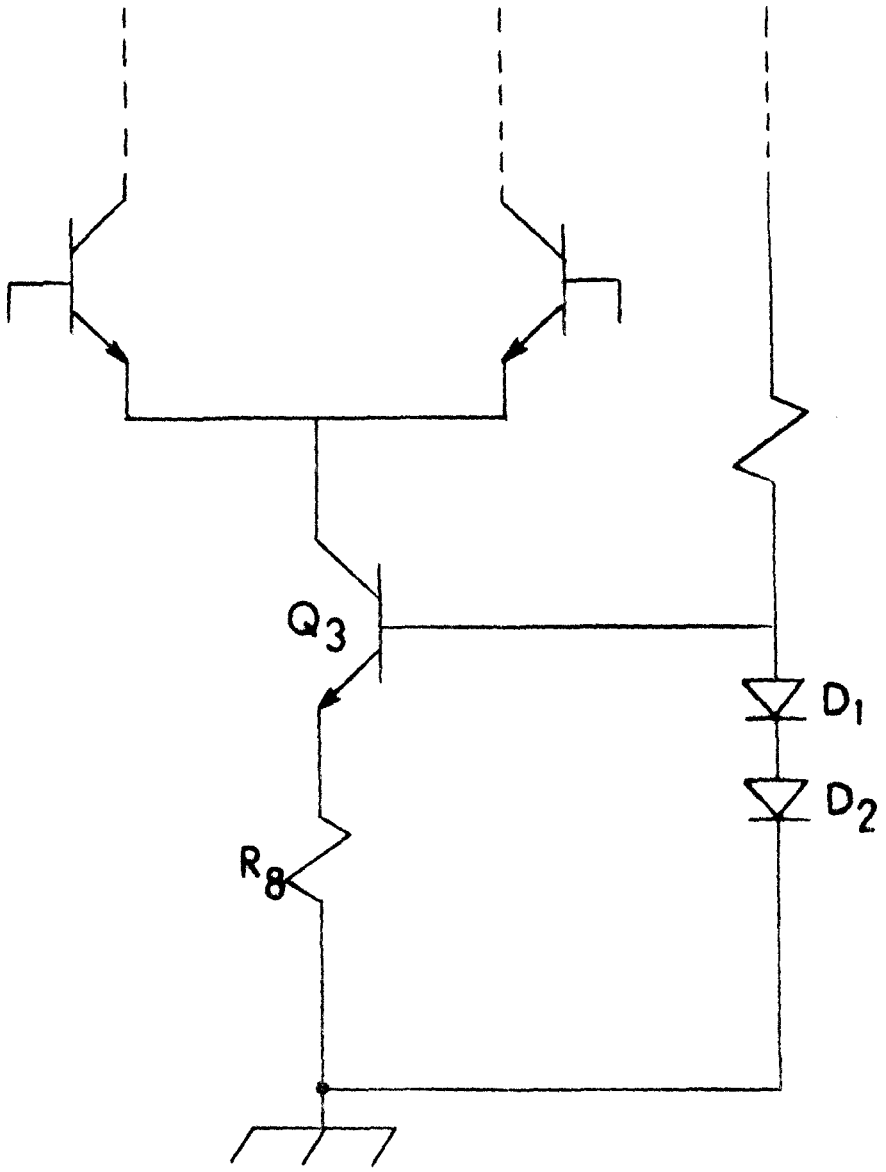

Fig. 8.4 Scheme of the CCS

The circuit of the CCS used is shown in figure 8.4. The temperature coefficient of the base-emitter junction diode of transistor Q_3 being equal to the temperature coefficient of the biasing diodes. With the rise in temperature, the base driving potential would decrease as the biasing chain contains two diodes, thus decreasing the transistor current and making $\Delta g/g$ negative. Since the change in the transistor current is linearly related to its base potential and the temperature coefficient of the diode is large, as shown subsequently, one derives

$$\left|\frac{\Delta g}{g}\right| > \left|\frac{\Delta R}{R}\right|$$

such that the last term in equation (8.14) is actually negative. The approximate value of $\Delta g/g$ can be calculated from the diode temperature coefficient ($\Delta E_d/°C$) and the temperature coefficient of the input offset voltage of the differential pair ($\Delta E_p/°C$).

The approximate relation is

$$\frac{\Delta g}{g} \approx \pm \frac{|\Delta E_p|}{E_{BB} \pm |\Delta E_p|} - \frac{|\Delta E_d|}{I_{EQ} R_e} \qquad (8.16)$$

Typical values of $|\Delta E_p|$ and $|\Delta E_d|$ are 6 μV/°C and 2.5 mV/°C respectively and for the proposed circuit E_{BB} = 2.117V, $I_{EQ} = 0.77 \times 10^{-3}$A, and R_e = 390 ohms, from which one can easily show that

$|\Delta E_p| / (E_{BB} \pm |\Delta E_p|) \ll \Delta E_d / I_{EQ} R_e$ such that, one can always write

$$\frac{\Delta g}{g} = -\frac{|\Delta E_d|}{I_{EQ} R_e}$$

Further $(\Delta R/R)/°C = 50$ p.p.m. and $(\Delta C/C)/°C = -150$ p.p.m. and using the above data $\Delta T/T$ can be calculated from equation (8.14).

If however, a non-ideal current source is considered the last term on the right-hand side of equation (8.16) is replaced by $\Delta R/R$ such that

$$\frac{\Delta g}{g} \approx \pm \frac{|\Delta E_p|}{E_{BB} \pm |\Delta E_p|} - \frac{\Delta R}{R} \qquad (8.17)$$

Evidently

$$\left|\frac{\Delta R}{R}\right| < \left|\frac{\Delta E_d}{I_{EQ} R_e}\right| \qquad (8.18)$$

so that, in general it is true that

$$\left|\frac{\Delta T}{T}\right|_{CCS} > \left|\frac{\Delta T}{T}\right|_{R_{EE}} \qquad (8.19)$$

Experimental results confirming the above are shown in Table-8.2. Equations (8.14) - (8.17) also confirm that it is possible to reduce the temperature sensitivity of T to a minimum by correct component choice and appropriate design of the CCS, and as such, temperature sensitivity should not pose any problem for the generator.

TABLE-8.2

TEMPERATURE SENSITIVITY; NOMINAL TEMPERATURE 30°C

Δt (°C)	$\frac{\Delta T}{T}$ with CCS, x 10^{-3}		$\frac{\Delta T}{T}$ with R_{EE}, x 10^{-3}	
	Theoretical	Experimental	Theoretical	Experimental
- 10	21.22	19.20	0.993	1.071
- 5	10.79	9.00	0.496	0.583
0	0	0	0	0
5	-11.36	- 9.20	-0.504	-0.620
10	-22.96	-19.90	-1.007	-1.980
15	-35.20	-28.70	-1.511	-2.330
20	-47.98	-39.80	-2.015	-2.850
25	-61.40	-47.70	-2.517	-3.420

One should also see how the repetition rate changes with the tolerance limits of the passive parameters R_1, R_2 and C. Using the definition of classical sensitivity one gets from equation (8.3).

$$S^T = \sum_{i=1,2} S^T_{Ri} = S^T_C = 2 + \frac{2gR_1}{(2gR_1-1)\ln(2gR_1-1)} \qquad (8.20)$$

Since $2gR_1 \gg 1$, S^T never tends to be very large.

8.6 RESULTS AND DISCUSSION

The circuit was tested with both a constant current source and a fixed emitter resistor R_{EE} = 1k ohm and with C = 0.06 μF, R_2 = 1.308k ohms. The experimental results with CCS are shown along with the theoretical curves, in figure 8.5. Results are seen to be

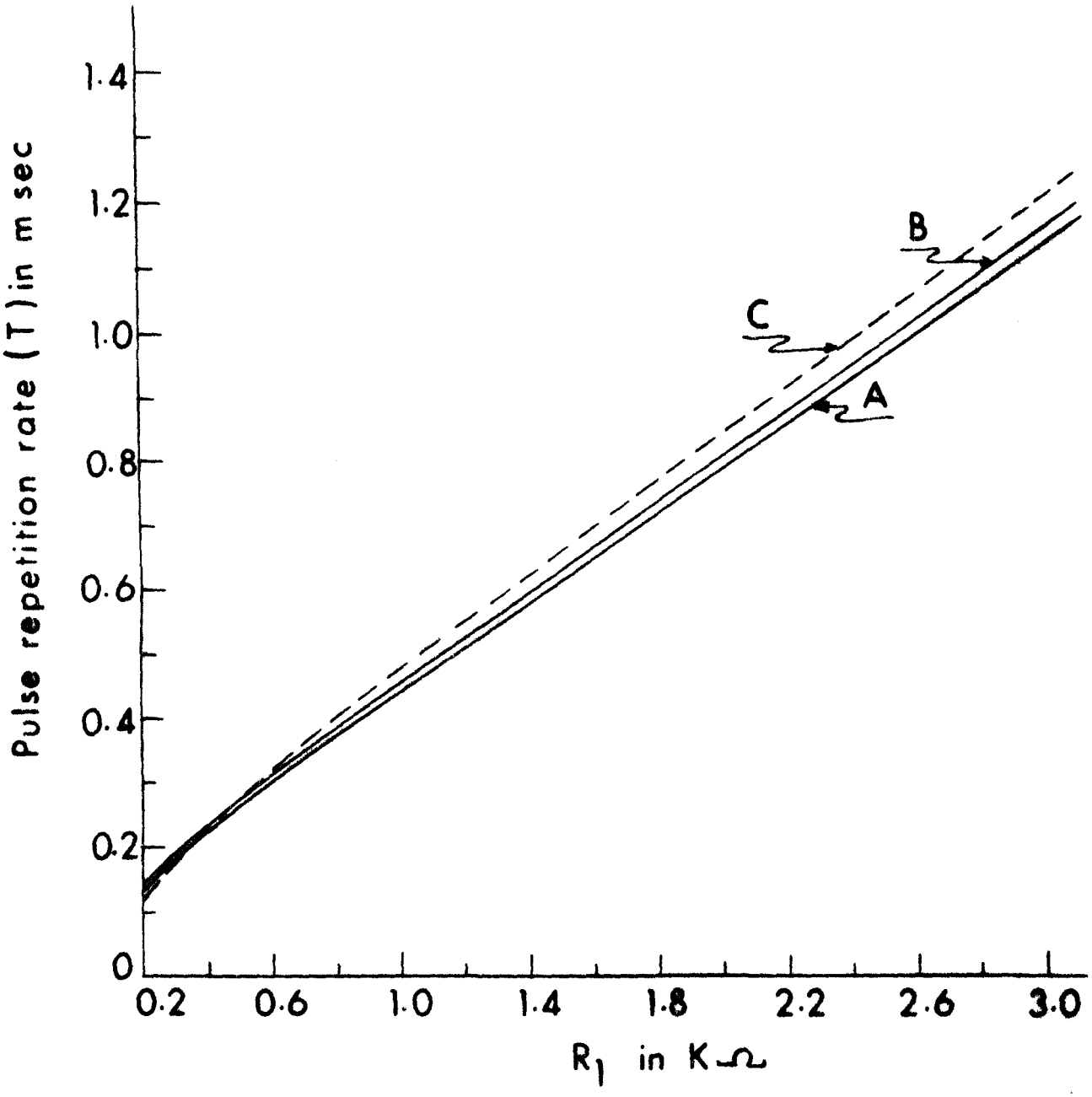

Fig.8.5. R_1 – T plot of the generator; R_2 = 1.308 KΩ, C = 0.06 μF

Curve A: Calculated with CCS (g_e = 13.06 m℧)

Curve B: Calculated with R_{EE} (g_f = 14.4 m ℧)

Curve C: Experimental with CCS

quite in agreement with the analysis. The results with a simple resistor have not been shown in figure 8.5 as they are almost coincident with those using the CCS. In both theoretical and experimental results, except for a small region of low R_1 the T-R_1 relationship is found to be almost linear. Using equation (8.7) it can be shown that the linearity of repetition rate is within $\pm$ 5% for a range of 0.36 ms to 1.12 ms, when R is varied from 750 ohms to 3k ohms. From figure 8.5, the practical figure for linearity is seen to be nearly the same in this range of R_1. However, if larger non-linearity is tolerable the range can be extended further.

For varying supply voltage the shifts in the repetition rate from a nominal value of 0.833 ms are shown in Table-8.1 for both cases. While the percentage variation obtained with the CCS is less than 0.45%, that with a simple resistor is as high as 5.6% when the supply is varied within $\pm$ 10%.

The theoretical and practical data for temperature sensitivity of the repetition rate at its nominal value of T_o = 0.833 ms are given in Table-8.2 with the CCS and R_{EE}. As predicted, this sensitivity is larger with the CCS. For a 25°C increase in temperature, T_o is shown to shift by about 6.14% with the CCS, while with R_{EE} the change is only about 0.3%. It is interesting to note that practical $\Delta T/Ts$ with the, CCS are less than the calculated values, while with R_{EE} the nature of the variation is the opposite. However, in both cases results are quite confirmatory. The discrepancy may be attributed to the fixed idealized data assumed in the calculations.

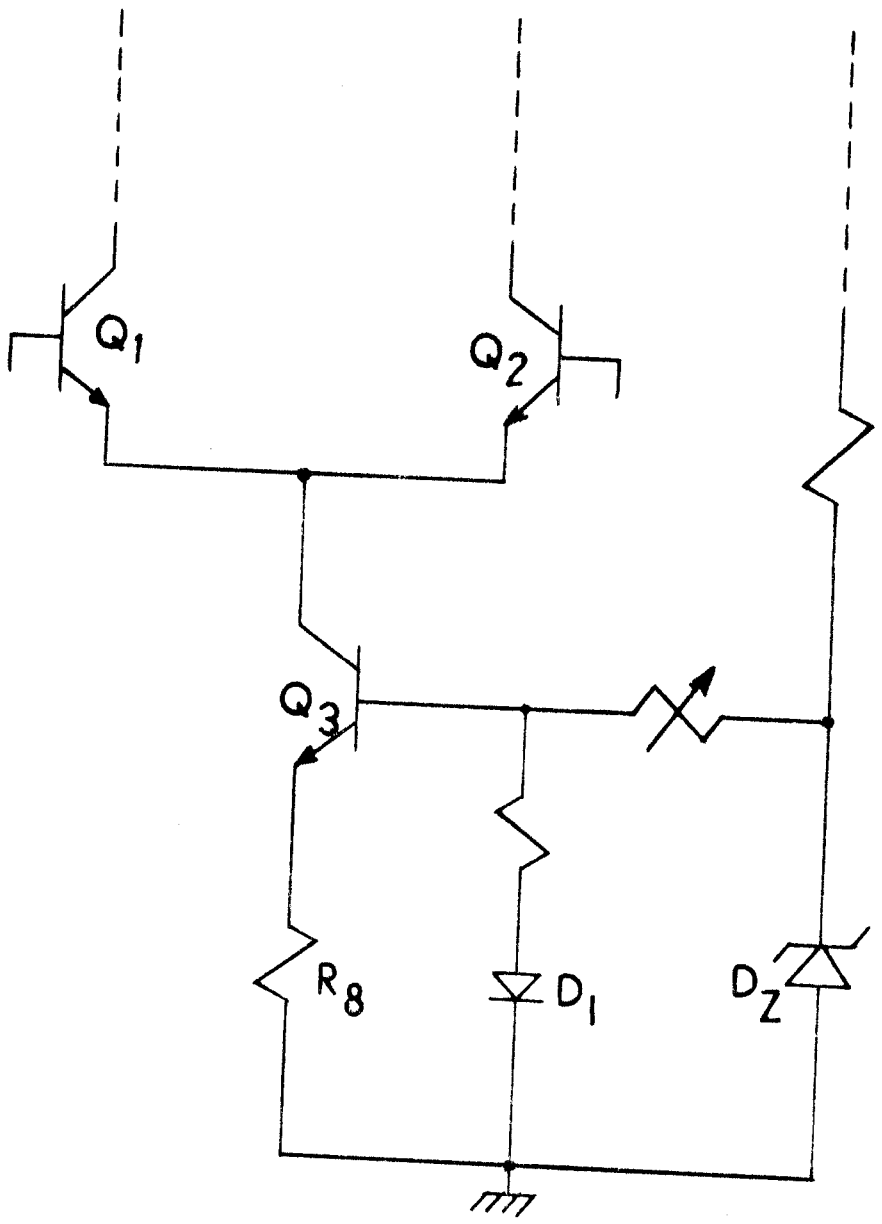

Fig.8.6 Circuit scheme of the compensated CCS

The temperature sensitivity is considerably improved with the CCS feeding the differential pair, if the CCS is individually compensated. A scheme of such a compensated CCS is shown figure 8.6. The Zener diode D_Z should have a zero temperature coefficient. The base drive potential here does not change with temperature as the variation in V_{EB} of the transistor Q_3 would tend to be compensated by an opposite change in diode D_1 voltage drop. Table-8.3 shows the theoretical and experimental sensitivity of time period with temperature.

TABLE-8.3

TEMPERATURE SENSITIVITY OF TIME PERIOD WITH A COMPENSATED CCS FEEDING THE DIFFERENTIAL PAIR; NOMINAL TEMPERATURE 30°C

Δt (°C)	$\frac{\Delta T}{T} \times 10^{-3}$	
	Theoretical	Experimental
- 10	0.993	1.00
- 5	0.496	0.46
0	0	0
5	-0.504	-0.57
10	-1.007	-1.37
15	-1.511	-1.80
20	-2.015	-2.37
25	-2.517	-2.93

The above results have been obtained using discrete components and a matched pair of transistors.

It may be shown that the contribution of the last term of equation (8.14) is negligible for the case when the coupled emitter is fed from a compensated CCS and the temperature sensitivity of the time period is predominantly dependent on the temperature coefficients of the passive parameters. Hence the temperature sensitivity of a fixed-frequency pulse generator can be made to approach zero by adopting hybrid integration techniques, where the passive components should be of the thin-film type[7].

However for a variable time period symmetric pulse generator, two of the frequency-determining elements R_1 and C [equation (8.3)] are externally controlled and the rest of the circuit may be integrated. In such a case the expression for the temperature sensitivity of T is obtained from equation (8.3), neglecting the higher order products of the differential quantities, as

$$\frac{\Delta T}{T} = \frac{\Delta C}{C} + \frac{\Delta R_1}{R_1 + R_2} + \frac{\Delta R_2}{R_1 + R_2} + \frac{\ln(1+(\Delta g/g)+(\Delta R_1/R_1))}{\ln(2gR_1 - 1)} \qquad (8.21)$$

In equation (8.21) the contribution due to the last term is still negligible such that equation (8.21) reduces to

$$\frac{\Delta T}{R} = \frac{\Delta C}{C} + \frac{\Delta R_1}{R_1 + R_2} + \frac{\Delta R_2}{R_1 + R_2} \qquad (8.22)$$

If, now, the frequency-determining passive elements are appropriately chosen ($\Delta R_1/R_1$ = + 100 p.p.m./°C, e.g. Nichrome potentiometer; $\Delta R_2/R_2$ = - 100 p.p.m./°C, thin-film integrated), $\Delta T/T$ is

easily shown to be essentially dependent on the thermal drift of the capacitor alone. If a high quality ceramic chip capacitor with a temperature coefficient of NPO ± 30 p.p.m./°C is used[7], the temperature sensitivity of the time period would tend to be of the same order, which is about one order lower than that obtained with discrete component design.

8.7 CONCLUSION

A pulse generator scheme with a single emitter-coupled differential transistor pair was studied and by means of an analytical approach it has been shown that by using a temperature-compensated constant current source feeding the coupled emitters, the generator can produce very stable oscillation. Experimental stability figures of ± 0.44% for ± 10% supply voltage change and less than 150 p.p.m./°C with temperature variation are easily obtained in the scheme. Conditions for further improving these figures, particularly the temperature sensitivity, have been obtained when this configuration is adopted in an integrated circuit, as can be seen from equation (8.22). Besides, the repetition rate has been shown to be linearly varying with a single resistive element and the experimental figures actually show a linear variation of ± 55% around 0.65 ms for a resistance variation of ± 62% around 1.6k ohms.

REFERENCES

1. Roy,S.B. and Patranabis,D. : 'Non-linear oscillations using antisymmetric transfer characteristics of a differential pair'; Int. J. Electron., Vol.42, No.1, pp.19-32, 1977.

2. Roy,S.B. and Patranabis,D. : 'Voltage-controlled oscillator using an emitter-coupled differential pair'; Electron. Lett., Vol.13, No.19, pp.590-591, Sept.1977.

*3. Roy,S.B. Patranabis,D. and Kundu,P. : 'An insensitive linear single-element-control pulse generator'; Int. J.Electron, Vol.46, No.3, pp.229-239, 1979.

4. Sen,P.C. and Patranabis,D. : 'Oscillations in a first order all-pass filter'; Int. J. Electron, Vol.29, No.1, pp.83-91, 1970.

5. Clarke,K.K. : 'Design of self-limiting transistor sinewave oscillator'; IEEE Trans. Circuit Theory, Vol.CT-13, No.1, pp.58-63, March 1966.

6. Kundu,P. and Roy,S.B. : 'A temperature-stable RC transistor oscillator'; Proc.IEEE, Vol.57, No.3, pp.356-357, March 1969.

7. Moschytz,G.S. : 'Linear Integrated Networks : Fundamental'; New York : Van Nostrand Reinhold, 1974, pp.367-407.

---

* Chapter-VIII is based mainly on this publication.

CHAPTER-IX

CONCLUSION

9.1 INTRODUCTION

The investigation was intended to realize certain active RC network for application in Instrumentation, Communication and Industrial Control Systems.

9.2 BRIEF OUTLINE OF THE WORK

In Process Instrumentation and Control, signal frequency makes excursion down to very low/small values such that filtering shaping and computation network can hardly use real inductors, whenever necessary. Replacement of real inductors with active RC simulated inductors started as early as sixties but newer schemes of simulation are still being added to the bulk of literatures already existing, on various counts of superiority. After a little relevant review of the state of the art, the present treatise opens with some new schemes[1,2] of such simulation of both grounded and floating inductors with RC parameters and standard Operational Amplifiers (OA). Most of these techniques have been aptly supported with application examples or suggestions thereof. The first one[1] of the series uses two capacitors and two OA's. The scheme however is versatile enough to produce linear, bilinear and ideal inductors by minor trimming. But the realized inductor is of grounded type. A sinewave generator has also been developed from this scheme. To have low component and high selectivity, analogue filters often require a floating lossless inductor. The second scheme[2]

provides this simulation through an altogether different but logical approach. A practical filter realization scheme has been appended to show the application of such a simulated inductor.

While the conventional filter can be synthesized using resistors, capacitors and simulated inductors, inductorless filters can also be obtained through a different synthetic approach using less components, particularly the active ones. The investigation towards such synthesis has been made[3] with emphasis on all-pass filters where the filter gain with frequency remains constant but the delay follows a specific law. The method has then been extended to other types of filters such as high-pass, band-pass, low-pass and band-rejection. The method uses a single OA and the approach is very general.

A very major function active RC networks are called upon to perform is to generate waveforms. Basically these systems are regenerative autonomous systems. From equipment testing to data telemetering, a variety of purpose is served by such systems. Investigations have been made to develop a number of such regenerative systems. Sinewave generation is a major area that has been receiving attention since long. However generation of very low frequency sinewave through a direct approach without using large RC parameters is of consequence in Process Instrumentation and Control Systems and is of late being investigated with considerable emphasis on practical footing. Investigation on generation of sinewave

using feedback in active RC filters have first been made[4]. A difference term co-efficient in the expression for frequency, either in the numerator or denominator makes generation of very low or very high frequency oscillations possible in such systems. All the proposed schemes are single resistive element tunable. For application in telemetering of process data the system has been converted to VCO's as well.

Operational amplifiers have been used in the investigations mentioned so far. The basic differential input stage of OA can itself form a kind of active block with certain special properties retaining the essential characteristics of the OA. This block can be called the Emitter Coupled Differential (Transistor) Pair (ECDP). Very stable sinewave has been generated[5] using this block. Such a system has been shown to be almost insensitive to temperature and supply variation. Such a block has other uses also. Following the van der Pol oscillator, waveforms starting from quasisinusoidal to hard relaxation mode have been generated in the proposed system[6]. Further the discrepancy in the earlier analysis to establish the point-to-point corroboration of the derived waveform has been explained by assuming a hyperbolic tangent type transfer characteristic of the differential pair. The system has been further extended to obtain a VCO by controlling the differential bias which effectively controls the slope of the transfer characteristic[7]. Finally the same scheme has been shown to obtain pulse train whose repetition rate is linearly related to a

single resistive element[8]. This linear pulse generator is also shown to be almost insensitive to temperature and supply variation and an approximate analysis corroborates the results remarkably well.

9.3 FINAL COMMENTS

The investigations carried out here provide a systematic approach to develop additional superior schemes of active RC circuits. Although this is not the only approach, it may be considered powerful in the sense that the proposed schemes use either Operational Amplifier as the active block or a part of the operational amplifier in its place making the schemes more simple and economic. A few of the circuits that have been developed are for low frequency applications, that are more relevant to Process Instrumentation and Control. In the realizations it has been attempted to use an unified active block, to derive low sensitivity and high performation as well as low count passive components with small spread in values, to make the system IC-compatible, to obtain independent single element controllability of the relevant response function and to extend the range in time or frequency in an efficient manner.

To a large extent these have been achieved in the investigations. These results in turn show some positive features and marked improvement in the design and synthesis of active RC circuits for applications in Instrumentation, Communication and Industrial Control. It is expected that these would be accepted without reservations.

REFERENCES

1. Patranabis,D. and Roy,S.B. : 'Active RC realization of bilinear and linear RL impedances'; Int.J.Electron., Vol.33, No.6, pp.681-687, 1972.

2. Patranabis,D. Tripathi,M.P. and Roy,S.B. : 'A new approach for lossless floating inductor realization'; IEEE Trans. Circuits and Systems, Vol.CAS-26, No.10, pp.892-893, Oct.1979.

3. Patranabis,D. Roy,S.B. and Tripathi,M.P. : 'Generalization of active RC all-pass schemes'; Proc.IEEE, Vol.66, No.3, pp.354-356, March 1978.

4. Tripathi,M.P., Roy,S.B. and Patranabis,D. : 'Some observations on single-element control sine-wave oscillators'; Int.J.Electron., Vol.43, No.5, pp.513-520, 1977.

5. Kundu,P. and Roy,S.B. : 'A temperature-stable RC transistor oscillator'; Proc.IEEE, Vol.57, No.3, pp.356-357, March 1969.

6. Roy,S.B. and Patranabis,D. : 'Non-linear oscillations using antisymmetric transfer characteristics of a differential pair'; Int.J.Electron., Vol.42, No.1, pp.19-32,1977.

7. Roy,S.B. and Patranabis,D. : 'Voltage-controlled oscillator using an emitter-coupled differential pair'; Electron. Lett., Vol.13, No.19, pp.590-591, Sept.1977.

8. Roy,S.B., Patranabis,D. and Kundu,P. : 'An insensitive linear single-element-control pulse generator'; Int.J.Electron., Vol.46, No.3, pp.229-239, 1979.